BUDAPEST UNIVERSITY OF TECHNOLOGY AND ECONOMICS

Economic and Controllability Analysis of Energy-Integrated Distillation Schemes

A dissertation submitted to the
Budapest University of Technology and Economics

For the degree of

Ph.D. in Chemical Engineering

by

Mansour Masoud Khalifa Emtir

under the supervision of

Professor Dr. Zsolt Fonyo

Department of Chemical Engineering
Budapest University of Technology and Economics

November 200

Declaration

The research work reported in this thesis has been carried out under the supervision of Prof. Dr. Zsolt Fonyo, Head of Chemical Engineering Department at Budapest University of Technology and Economics.

No portion of the work referred to in this thesis has been submitted in support of an application for another degree or qualification of this, or any other university, or other institution of learning.

Mansour Emtir

November 2002

Dedication

Dedicated to the enduring memory of my father

and to my beloved mother

Acknowledgements

I would like to express my sincere gratitude to my supervisor Prof. Dr. Zsolt Fonyo for his guidance during the course of this research. I am grateful for his encouragement and giving me an opportunity to use all the facilities available in the department for my research work.

I wish to express my sincere appreciation to Prof. Dr. Peter Mizsey and Dr. Endre Rev for their suggestions and practical experience during my research.

I am thankful to all the staff members of the department and students and secretaries for providing a friendly and stimulating environment. I wish to thank Dr. Istvan Kalmar, and my laboratory mate Szitkai Zsolt for their helps in various way.

I am very grateful to the Libyan ministry of education for the financial support during the course of this Ph.D. study.

I would like to express my gratitude to my mother for her enormous love, support and sacrifice. I would also like to express my thanks to my brother, and my sisters.

Last but not least, special thanks to my wife and my children for their love, understanding, patience, and companionship during my study.

Above all, I am very much grateful to God “Allah” almighty for giving me courage and good health for completing this venture.

Abstract

Distillation is the primary separation process used in the chemical processing industries (CPI). While this unit operation has many advantages, one drawback is its significant energy requirements. Conventional distillation schemes are well-known configurations for separation of ternary mixtures by distillation. Due to the higher cost of energy during the last decade, and environmental impacts, there is increasing interest in alternative methods. They include conventional heat-integrated distillation schemes, thermally coupled distillation columns, and complex distillation arrangements, which offer alternatives to conventional distillation columns, with the possibility of savings in both energy and capital costs. The design, optimization, and control of such energy-integrated distillation schemes require engineering experience and knowledge, which represent a challenge to the researchers. In practice, the economic potential of such energy-integrated schemes has already been recognised, but their control properties have not been studied to the same degree. Since dynamic behaviour and control of these energy-integrated schemes is also important recent efforts have contributed to the understanding of the dynamic properties of the energy-integrated schemes.

The primary goal of this Ph.D. study to explore the design and economic features of the energy-integrated distillation schemes for the separation of ternary mixture (ethanol, n-propanol, n-butanol) with high product purity of 99 %. Three different feed compositions are investigated (0.45/0.1/0.45), (0.33/0.33/0.33), and (0.1/0.8/0.1). The studied schemes are: conventional distillation schemes (direct and indirect separation sequence), conventional heat-integrated schemes (forward and backward heat integration), thermally coupled sloppy separation sequence (Petlyuk column), and heat-integrated sloppy separation sequence (forward and backward heat integration).

The secondary gaol is to investigate the controllability features of the distillation schemes that indicates better economic feature by determining their steady state control indices; Niederlinski index (NI), Morari resiliency index (MRI), relative gain

array (RGA), and condition number (CN). According to steady-state control indices results, open loop and closed-loop dynamic simulations have been carried out for the equimolar feed to investigate its dynamic behaviour. The time constants, controller settings, overshoots, and the settling times are determined to characterize the schemes. Finally, flue gas emissions of the optimum schemes are estimated for two different types of fuels (natural gas and petroleum oil).

The results of economic study show that Petlyuk column has a limited TAC saving in the range of 28 % to 33 % for all the three feed compositions and the Petlyuk column is winner only in the case of lower middle component composition (n-propanol = 0.1) with 33 % savings. In the case of equimolar feed composition, direct separation sequence with backward heat integration and sloppy separation sequence with forward and backward heat integration are the best schemes in TAC savings with 41 % and 36 % respectively. In the case of high middle component (n-propanol = 0.8), sloppy separation sequences with backward and forward heat integration are the winners with the highest TAC saving values of 53 % and 51 % respectively. This result indicates that the possibility of the heat integrated schemes to achieve higher saving in energy and TAC is increasing together with increasing middle component (n-propanol) concentration in the feed, because the heat requirement increases drastically with increasing concentration of the intermediate substance. Operating pressure plays an important role in TAC savings; schemes that operated at higher pressure are showing less TAC savings due to the use of high-pressure steam, which is costly, comparing to the schemes at lower pressure. The selection of theoretical fractional recovery β^* of the middle component as initial design parameter is very important in determining of the internal recycle streams in Petlyuk column and the optimum fractional recovery is found close to the theoretical fractional in most of the cases. This design parameter is applied for sloppy separation sequences and found to be valid also.

The controllability study shows the following results:

- Controllability study shows that energy-integrated schemes can be controlled with decentralized control structures.
- Steady state control indices of the equimolar feed (0.33/0.33/0.33), and high middle component feed (0.1/0.8/0.1) compositions are showing the best steady-state control indices compared to the case of lower middle component composition (0.45/ 0.1/0.45).
- Conventional heat-integrated schemes are showing advantages over the other investigated scheme (Petlyuk column, and sloppy separation sequence with forward and backward heat integration) by showing good steady-state control indices which give indications that less interactions among the control loops are expected in the case of the conventional heat-integrated schemes.
- Open loop dynamic behavior of the studied distillation schemes show similar order of magnitude for the time constants except for sloppy sequence with backward heat integration, which shows significantly slower dynamic behavior compared to the other schemes.
- Closed-loop dynamic behaviour proves that conventional heat-integrated schemes can be controlled easily and show similar controllability features to those of the base case (conventional scheme). The other energy-integrated schemes (Petlyuk column and sloppy separation sequence with forward and backward heat integration) show less controllability features. The dynamic behaviour of the sloppy sequence are different depending on the direction of heat integration, the forward integration sloppy scheme shows better controllability features than the backward one, which has a poor performance. Since they are similar in TAC savings the controllability features influence the selection.

Finally, the flue gas emissions results show that a significant reduction of the flue gas emissions can be achieved by the various energy-integrated schemes. The energy savings of the energy-integrated schemes are proportional to the flue gas emissions.

Table of Contents

Chapter 1: Introduction 1

1.1. Motivation 1

1.2. The aims of this work 2

1.3. Approach 3

1.4. The scope and contribution 4

1.5. Outline of the dissertation 6

Chapter 2: Literature review 8

2.1. Separation processes 8

2.2. Classification of separation process 8

2.3. Distillation unit 10

2.4. Distillation reversibility 11

2.5. Energy requirement of distillation unit 11

2.6. Methods of energy conservation in distillation system 13

2.6.1 Conventional distillation schemes 16

2.6.2. Conventional heat-integrated schemes 17

2.6.3. Thermo-coupling 20

2.6.4. Side rectifier column and side stripper column 21

2.6.5. The Petlyuk column and the divided wall column 21

2.6.6. The separation sloppy systems 24

2.7. Controllability considerations 27

2.7.1. Steady-state control indices 29

2.7.2. Design of control structure 31

2.8. Environmental considerations 33

2.8.1. Process waste 33

2.8.2. Utility waste 33

2.8.3. Waste treatment 34

Chapter 3: Rigorous simulation and optimization 35

3.1. Introduction 35

3.2. **Short-cut analysis** 36
3.3. **Rigorous case studies** 38
3.4. **Assumptions and techniques** 40
3.5. **Optimization procedure** 42
3.5.1. Optimization of conventional distillation schemes 43
3.5.2. Optimization of conventional heat-integrated schemes 46
3.5.3. Optimization of Petlyuk column 47
3.5.4. Optimization of sloppy heat-integrated schemes 48
3.6. **Optimal fractional recovery of the middle component** 49
3.7. **Results of conventional distillation schemes** 50
3.8. **Results of the energy-integrated schemes** 51
3.8.1. Results of Case 1 52
3.8.2. Results of Case 2 53
3.8.3. Results of Case 3 54
3.9. **Sensitivity of the TAC savings** 54
3.10. **Conclusions of the economic study** 56
Chapter 4: Controllability study of energy-integrated schemes 59
4.1. **Steady-state control analysis** 59
4.1.1. Studied schemes 59
4.1.2. Results of the steady-state control indices for feed composition 1 63
4.1.3. Conclusion of feed composition 1 65
4.1.4. Results of the steady-state control indices for feed composition 2 65
4.1.5. Conclusion of feed composition 2 68
4.1.6. Results of the steady-state control indices for feed composition 3 68
4.1.7. Conclusion of feed composition 3 71
4.1.8 Conclusions of the steady state control indices study 71
4.2. **Dynamic simulations** 72
4.2.1. Level control 72
4.2.2. Composition control 73
4.2.3. Controllers Tuning 73
4.2.4. The Biggest Log-modulus Tuning (BLT) 74

4.2.5. A case study 75
4.2.6. Steady state control indices of the case study 75
4.2.7. Open loop dynamic simulation 77
4.2.8. Results of open loop dynamic simulation 78
4.2.9. Closed-loop dynamic simulation 86
4.2.10. Results of closed-loop dynamic simulation 86
4.2.11. Conclusions of the dynamic simulations study 104
Chapter 5: Environmental consideration 105
5.1. Types of flue gas emissions 105
5.2. Estimation of the flue gas emissions 106
5.3. Flue gas emission by various energy-integrated schemes 108
5.4. Conclusions of the estimated flue gas emissions 109
Chapter 6: Conclusions and major new results 111
6.1. Conclusions of the economic study 111
6.2. Conclusions of the optimal fractional recovery of the middle component 113
6.3. Conclusions of the controllability study 114
6.3.1. Steady-state control indices study 114
6.3.2. Dynamic simulations case study 114
6.4. Conclusions of the estimated flue gas emissions 115
6.5. Major new results 117
References 119
Publications 124
Nomenclature 126
Appendix A: Activity model interaction parameters 130
Appendix B: Sizing and costing of distillation columns and heat exchangers 131
Appendix C: Optimization results of the rigorous cases 137
Appendix D: Simulation results of closed-loop dynamic behavior 143

List of Figures

Figure 2.1:	Classification of the main separation process	9
Figure 2.2:	Main approaches for energy conservation in distillation systems	14
Figure 2.3:	The conventional sequences for the separation of a ternary mixture	16
Figure 2.4:	Heat integrated sequences for separating a ternary mixture	17
Figure 2.5:	Thermally coupled systems	20
Figure 2.6:	Composition profile of the middle component in direct sequence	22
Figure 2.7:	Composition profile of the middle component in the Petlyuk column	23
Figure 2.8:	The sloppy separation systems	25
Figure 3.1:	Composition triangle	37
Figure 3.2:	Simplified representation of the optimizing procedure	42
Figure 3.3:	Comparison of TAC savings in optimized schemes for European utility prices	56
Figure 4.1:	Direct sequence with backward heat integration (**DQB**) indicating its manipulated variables	60
Figure 4.2:	Petlyuk column (**SP**) indicating its manipulated variables	60
Figure 4.3:	Sloppy sequence with forward heat integration (**SQF**) indicating its manipulated variables	61
Figure 4.4:	Sloppy sequence with backward heat integration (**SQB**) indicating its manipulated variables	61
Figure 4.5:	Open loop transient behavior of direct sequence (**D**) for feed rate disturbance	80
Figure 4.6:	Open loop transient behavior of direct sequence (**D**) for feed composition disturbance	80
Figure 4.7:	Open loop transient behavior of **DQB** scheme for feed rate disturbance	81
Figure 4.8:	Open loop transient behavior of **DQB** scheme for feed composition disturbance	81

Figure 4.9: Open loop transient behaviour of **DQF** scheme for feed rate disturbance 82

Figure 4.10: Open loop transient behaviour of **DQF** scheme for feed composition disturbance 82

Figure 4.11: Open loop transient behavior of Petlyuk column (**SP**) for feed rate disturbance 83

Figure 4.12: Open loop transient behavior of Petlyuk column (**SP**) for feed composition disturbance 83

Figure 4.13: Open loop transient behavior of **SQF** scheme for feed rate disturbance 84

Figure 4.14: Open loop transient behavior of **SQF** scheme for feed composition disturbance 84

Figure 4.15: Open loop transient behavior of **SQB** scheme for feed rate disturbance 85

Figure 4.16: Open loop transient behavior of **SQB** scheme for feed composition disturbance 85

Figure 4.17: Closed-loop transient behavior of direct sequence (**D**) for feed rate disturbance using (D_1-L_2-B_2) manipulated variables 89

Figure 4.18: Closed-loop transient behavior of direct sequence (**D**) for feed composition disturbance using (D_1-L_2-B_2) manipulated variables 89

Figure 4.19: Closed loop transient behavior of direct sequence (**D**) for feed rate disturbance using (L_1-D_2-B_2) manipulated variables 90

Figure 4.20: Closed-loop transient behavior of direct sequence (**D**) for feed composition disturbance using (L_1-D_2-B_2) manipulated variables 90

Figure 4.21: Closed-loop transient behavior of **DQB** scheme for feed rate disturbance using (D_1-L_2-B_2) manipulated variables 91

Figure 4.22: Closed-loop transient behavior of **DQB** scheme for feed composition disturbance using (D_1-L_2-B_2) manipulated variables 91

Figure 4.23: Closed-loop transient behavior of **DQB** scheme for feed rate disturbance using (L_1-D_2-B_2) manipulated variables 92

Figure 4.24: Closed-loop transient behavior of **DQB** scheme for feed composition disturbance using (L_1-D_2-B_2) manipulated variables 92

Figure 4.25: Closed-loop transient behavior of **DQB** scheme for feed rate disturbance using (L_1-D_2-Q_2) manipulated variables 93
Figure 4.26: Closed-loop transient behavior of **DQB** scheme for feed composition disturbance using (L_1-D_2-Q_2) manipulated variables 93
Figure 4.27: Closed-loop transient behavior of **DQF** scheme for feed rate disturbance using (D_1-L_2-B_2) manipulated variables 94
Figure 4.28: Closed-loop transient behavior of **DQF** scheme for feed composition disturbance using (D_1-L_2-B_2) manipulated variables 94
Figure 4.29: Closed-loop transient behavior of **DQF** scheme for feed rate disturbance using (L_1-D_2-B_2) manipulated variables 95
Figure 4.30: Closed-loop transient behavior of **DQF** scheme for feed composition disturbance using (L_1-D_2-B_2) manipulated variables 95
Figure 4.31: Closed-loop transient behavior of **DQF** scheme for feed rate disturbance using (L_1-D_2-Q_2) manipulated variables 96
Figure 4.32: Closed-loop transient behavior of **DQF** scheme for feed composition disturbance using (L_1-D_2-Q_2) manipulated variables 96
Figure 4.33: Closed-loop transient behavior of Petlyuk column (**SP**) for feed rate disturbance using (D-S-Q) manipulated variables 97
Figure 4.34: Closed-loop transient behavior of Petlyuk column (**SP**) for feed composition disturbance using (D-S-Q) manipulated variables 97
Figure 4.35: Closed-loop transient behavior of Petlyuk column (**SP**) for feed rate disturbance using (L-S-B) manipulated variables 98
Figure 4.36: Closed-loop transient behavior of Petlyuk column (**SP**) for feed composition disturbance using (L-S-B) manipulated variables 98
Figure 4.37: Closed-loop transient behavior of **SQF** scheme for feed rate disturbance using (D-S-Q) manipulated variables 99
Figure 4.38: Closed-loop transient behavior of **SQF** scheme for feed composition disturbance using (D-S-Q) manipulated variables 99
Figure 4.39: Closed-loop transient behavior of **SQF** scheme for feed rate disturbance using (L-S-B) manipulated variables 100
Figure 4.40: Closed-loop transient behavior of **SQF** scheme for feed composition disturbance using (L-S-B) manipulated variables 100

Figure 4.41: Closed-loop transient behavior of **SQF** scheme for feed rate disturbance using (D-S-Q) manipulated variables 101
Figure 4.42: Closed-loop transient behavior of **SQF** scheme for feed composition disturbance using (D-S-Q) manipulated variables 101
Figure 4.43: Closed-loop transient behavior of **SQB** scheme for feed rate disturbance using (L-S-B) manipulated variables 102
Figure 4.44: Closed-loop transient behavior of **SQB** scheme for feed composition disturbance using (L-S-B) manipulated variables 102
Figure 4.45: Closed-loop transient behavior of **SQB** scheme for feed rate disturbance using (D-S-Q) manipulated variables 103
Figure 4.46: Closed-loop transient behavior of **SQB** scheme for feed composition disturbance using (D-S-Q) manipulated variables 103

List of Tables

Table 2.1:	Parameters for selecting the best heat-integrated sequence	19
Table 3.1:	Relative volatility and separation index for Rigorous Cases	38
Table 3.2:	Feed and product specifications for Rigorous Case 1	39
Table 3.3:	Feed and product specifications for Rigorous Case 2	39
Table 3.4:	Feed and product specifications for Rigorous Case 3	39
Table 3.5:	Utilities cost data	40
Table 3.6:	Data exported from HYSYS to Excel for each column	45
Table 3.7:	Optimization results of **DQB** scheme for feed composition (0.333/0.333/0.333), using European utility prices	47
Table 3.8:	Comparison between theoretical and optimal fractional recovery of the middle component	50
Table 3.9:	Optimization results of direct scheme	51
Table 3.10:	Optimization results of indirect scheme, BC in liquid phase	51
Table 3.11:	Optimization results of indirect scheme, BC in vapour phase	51
Table 3.12:	Winning schemes in Case 1 (10 % middle component)	52
Table 3.13:	Winning schemes in Case 2 (equimolar feed)	53
Table 3.14:	Winning schemes in Case 3 (80 % middle component)	54
Table 3.15:	TAC savings (%) for 10 years project life, Europe utility prices and (M & S index = 1056.8)	55
Table 3.16:	TAC savings (%) for 10 years project life, Europe utility prices and (M & S index = 1093.9)	55
Table 3.17:	TAC savings (%) for 5 years project life, Europe utility prices and (M & S index = 1056.8)	55
Table 4.1a:	Steady state control indices for feed composition 1, **DQB** scheme	63

Table 4.2a:	Steady state control indices for feed composition 1, Petlyuk column (**SP**)	64
Table 4.3a:	Steady state control indices for feed composition 1, **SQF** scheme	64
Table 4.4a:	Steady state control indices for feed composition 1, **SQB** scheme	65
Table 4.1b:	Steady state control indices for feed composition 2, **DQB** scheme	66
Table 4.2b:	Steady state control indices for feed composition 2, Petlyuk column (**SP**)	67
Table 4.3b:	Steady state control indices for feed composition 2, **SQF** scheme	67
Table 4.4b:	Steady state control indices for feed composition 2, **SQB** scheme	68
Table 4.1c:	Steady state control indices for feed composition 3, **DQB** scheme	69
Table 4.2c:	Steady state control indices for feed composition 3, Petlyuk column (**SP**)	69
Table 4.3c:	Steady state control indices for feed composition 3, **SQF** scheme	70
Table 4.4c:	Steady state control indices for feed composition 3, **SQB** scheme	70
Table 4.5:	Steady state controllability indices for the optimized schemes	76
Table 4.6:	Open loop performance for feed rate disturbance	78
Table 4.7:	Open loop performance for feed composition disturbance	79
Table 4.8:	Closed-loop performance for feed rate disturbance	87
Table 4.9:	Closed-loop performance for feed composition disturbance	88
Table 5.1:	Emission factors of steam boiler per unit of heat delivered to the process	107
Table 5.2:	The flue gas emissions of Case 1	108
Table 5.3:	The flue gas emissions of Case 2	108
Table 5.4:	The flue gas emissions of Case 3	109
Table A1.1:	A_{ij} Coefficient matrix for NRTL	130
Table A1.2:	$(alpha)_{ij}$ Coefficient matrix for NRTL	130

Table A2.1:	A_{ij} Coefficient matrix for UNIQUAC	130
Table B.1:	Overall heat transfer coefficients	134
Table C.1:	Optimal scheme results of Case 1 based on U.S. utility prices	137
Table C.2:	Optimal scheme results of Case 1 based on European utility prices	138
Table C.3:	Optimal scheme results of Case 2 based on U.S. utility prices	139
Table C.4:	Optimal scheme results of Case 2 based on European utility prices	140
Table C.5:	Optimal scheme results of Case 3 based on European utility prices	141
Table C.6:	Optimal scheme results of equimolar feed, based on European utility prices and UNIQUAC property package	142
Table D.1:	Closed-loop performance for feed rate disturbance	143
Table D.2:	Closed-loop performance for feed composition disturbance	144

Chapter 1: Introduction

1.1. Motivation

During the last decades, in the chemical engineering milieu, there has been growing attempts to develop more energy efficient processes. The raising cost of energy and the concern for having a more environmentally sound industry impulse the study of technologies offering energy savings.

Although new separation methods are continuously being explored, distillation remains the most frequently used separation process. Distillation is both, energy intensive and inefficient. It accounts for around 3 % of the total world energy consumption and is one of the most energy consuming processes in chemical industry. Reduction of energy consumption in distillation has been actively studied in recent years. Process integration has been proven to be very successful in reducing the energy costs for conventional distillation arrangements. However, the scope for integration of conventional distillation columns into an overall process is limited due to practical constrains which often prevent integration of distillation columns with the rest of the process. Because of this, attention has been turned to the distillation operation it self. In this sense, conventional heat-integrated distillation columns and non-conventional distillation columns (complex columns arrangement) are to be considered. Conventional heat-integrated distillation columns have been given a special attention during the last decades due to their significant energy reduction. They consist of conventional distillation columns with energy exchange between some condensers and reboilers. On the other hand, a lot of research effort has been dedicated to non-conventional distillation arrangements.

Following the literature trend, for the case of ternary separation the conventional distillation arrangements are classified according to separation sequence as the direct sequence and the indirect sequence. Two different heat integrand schemes can be constructed out of each sequence depending on the direction of heat integration, namely forward heat integration and backward heat integration. Alternatively, non-conventional arrangements are basically schemes with a side section or a

prefractionator thermally coupled to a main column. Heat integration can be achieved also between the prefractionator and the main column for the sloppy separation sequence. These arrangements are also known as complex distillation arrangements and they became very attractive due to their ability of saving energy, but they still need more knowledge, understanding, and practical operation issues such as controllability to have strong implementation in the industry.

The main motivations of this thesis work are to extend the knowledge of energy-integrated distillation schemes that include the complex distillation arrangements also, and make them closer to implementation in industry. Some design, simulation, operation, and control aspects are analyzed, having the conventional distillation scheme as comparison basis.

1.2. The aims of this work

This work is based on studying and rigorous modeling (design, simulation, optimization, and control aspects) of various conventional and integrated distillation schemes for the separation of ternary mixture at different feed compositions. Economic evaluations of the distillation schemes are founded on rigorous simulation and optimization of each distillation scheme for minimum total annual cost (TAC). Thereafter, the controllability of the optimized schemes is studied, which includes the determination of steady state control indices, the open loop and closed-loop dynamic behavior. Overall evaluation of the best distillation schemes should be based on the combination of economic study, controllability study and environmental aspects. The main aims of this study is outlined below:

1. Design of various conventional and integrated distillation schemes, optimize the investigated alternatives rigorously by steady-state simulation, compare the energy-integrated schemes and the best conventional distillation scheme for better energy utilization of TAC savings.
2. Design and simulation of Petlyuk column for different feed compositions and evaluate its economic features for the given separation. A special emphasis laid on

the solution of the internal recycle streams, which represent important design problem by pinpointing the theoretical fractional recovery (β*).

3. Design and simulation of the complex distillation arrangements (sloppy heat-integrated schemes), applying the theoretical fractional recovery (β*) concept for designing these complex distillation schemes.
4. Compare the effect of applying different price structures (European and U.S. prices) on TAC savings and the ranking of the schemes.
5. Determine the steady-state control indices of economically optimum distillation schemes at the three different feed compositions and select the best control structure.
6. Study the open loop and closed-loop dynamic behavior of the optimum distillation schemes at equimolar feed composition. Investigate the closed-loop dynamic behavior for different control structures.
7. Estimate the flue gas emissions reductions due to energy-integration.

1.3. Approach

The Hyprotech's (HYSYS 1.1, 1996) professional simulation package is used for the modelling, steady-state and dynamic simulation of the distillation schemes. Steady-state control indices are determined by the use of MATLAB (Version 5.10.421, 1997).

The following methodological steps are implemented:

a) Shortcut design procedures are used to estimate:
   - the number of theoretical trays,
   - feed location and draw-off trays,
   - and the reflux ratio.

b) Steady-state rigorous simulation is carried out for the desired performance, the rigorous model of the package also used for sizing the different equipment items.

c) Steady-state control indices are determined for the economically optimum schemes at different control structures.

d) Dynamic simulation is carried out for the optimized schemes under feed rate and composition disturbances.

1.4. The scope and contribution

The scope of this thesis work is to separate a multi-component mixture into pure components by means of continuous distillation. Design, simulation, operation, and control aspects of different distillation arrangements for the separation of ternary mixture are studied. Economic evaluations of distillation schemes are made by rigorous optimization of each distillation scheme for minimum total annual cost (TAC) using steady state simulation. The controllability of the optimized schemes is studied, which include the determination of steady state control indices, the open loop and closed-loop dynamic behavior. Overall evaluation of the optimum distillation schemes are to be made based on the combination of economic study, controllability study and environmental considerations.

This study is devoted to non-ideal alcohol system of (ethanol, n-propanol, n-butanol) with high product purity of 99 % and three different feed compositions (0.45/0.1/0.45), (0.33/0.33/0.33), and (0.1/0.8/0.1). The economic features of different distillation schemes are investigated including (conventional distillation scheme, conventional heat-integrated scheme, Petlyuk column, and sloppy heat-integrated schemes) and compared to the best conventional distillation scheme.

The investigated schemes are:

i. Direct separation sequence without heat integration (**D**)
ii. Direct separation sequence with forward heat integration (**DQF**)
iii. Direct separation sequence with backward heat integration (**DQB**)
iv. Indirect separation sequence without heat integration (**I**)
v. Indirect separation sequence with forward heat integration (**IQF**)
vi. Indirect separation sequence with backward heat integration (**IQB**)

vii. Thermally coupled sloppy separation sequence (Petlyuk column) (**SP**)

viii. Sloppy separation sequence with forward heat integration (**SQF**)

ix. Sloppy separation sequence with backward heat integration (**SQB**)

The above mentioned schemes are designed, simulated rigorously, and then optimized for minimum total annual cost and compared with the best conventional distillation scheme for better energy utilization and saving in total annual cost (TAC). A particular emphasis is given to the question of fractional recovery of the middle component in the prefractionator and as a consequence to the internal recycles streams in the complex distillation arrangements (Petlyuk column and sloppy heat-integrated schemes). The effect of using higher and lower utility prices (European and U.S. prices) on the energy and total annul cost (TAC) saving are investigated for different types of energy-integrated schemes.

The controllability features of the distillation schemes that indicate better economic feature are investigated by determining their steady state control indices. According to the calculated steady-state control indices, open loop and closed-loop dynamic simulations have been carried out for the equimolar feed to investigate its dynamic behavior. The time constants, controller settings, overshoots, and the settling times are determined to characterize the controllability features of the schemes.

Finally, flue gas emissions of the optimum schemes are estimated for two different types of fuels (natural gas and petroleum oil).

This work is a contribution to the evaluation of the various distillation arrangements for the separation of multicomponenet mixtures considering their economic and controllability features. The work provides a better knowledge for the conventional and energy-integrated schemes. Energy requirements and controllability are the most emphasized design aspects. The complex distillation arrangements (Petlyuk column and sloppy heat-integrated schemes) are very attractive from energy point of view but their complexity makes them rare processes. The study of their properties has become principal parts of this work. This study can be considered as an extension to the

previous studies in the area of energy-integration and controllability of distillation columns.

1.5. Outline of the dissertation

To develop the objectives enunciated in the previous section, the thesis work has been distributed into seven chapters, covering the following aspects:

Chapter 1 is an introduction to the dissertation and its include, motivation, aims of the work, approach, the scope and contribution, and outlines of the dissertation.

Chapter 2 reviews the literature, it shows classifications of separation processes, then it covers the methods of energy savings in distillation systems with special emphasis on energy-integration methods such as heat-integrated columns for conventional and sloppy separation sequences, thermo-coupling method (e.g. Petlyuk column). This chapter covers also the controllability considerations and waste minimization.

Chapter 3 presents rigorous simulation and optimization procedures which is applied for conventional and energy-integrated distillation schemes in ternary mixture separations. The economic features of the distillation schemes are evaluated for different feed compositions and using different utility prices.

Chapter 4 covers the controllability of energy-integrated schemes. This study is performed in two steps, first steady-state control indices of the optimized schemes are determined, and then the best control structures are selected for further dynamic simulations. Open loop and closed-loop dynamic simulations are performed. The results of controllability study is presented, evaluated, and compared.

Chapter 5 shows that the energy-integrated schemes can provide not only energy savings and as a consequence cost saving, but further more cleaner environmental pollution by a considerable reduction of flue gas emissions. The share of conventional heat integrated scheme, Petlyuk column, and sloppy heat integrated schemes in reducing gas emissions is estimated.

Chapter 6 presents the conclusions of the different studies carried out in this work in addition to the major new results.

Chapter 2: Literature review

Chemical process industries covers large areas of our needs such as food supply systems, fuel availability, health care systems, clothing, housing, and transportation. Chemical engineers are encountered by a wide variety of problems in design, operation, control, troubleshooting, and even politics when dealing with environmental and economic aspects. The two main unit operations encountered in chemical process industry are the reactors and the separation units.

2.1. Separation processes

Separation processes includes:

- Removal of impurities from raw materials,
- Separation of products and by-products from raw materials (e.g. crude oil) and from reactor outputs,
- Removal of contaminants from liquid and gas effluent streams.

The most frequently used separation processes are: absorption, adsorption, ion exchange, chromatography, crystallization, distillation, drying, electrodialysis, evaporation, extraction, filtration, flotation, membranes, and stripping.

2.2. Classification of separation process

The separation is occurring by adding a separating agent, which takes the form of matter or energy. The degree of separation that may be obtained with any particular separation process is indicated by the *separating factor*, which is defined in the terms of product compositions (King, 1980):

$$\alpha_{ij}^{s} = \frac{x_{i1}/x_{j1}}{x_{i2}/x_{j2}} \qquad [2\text{-}1]$$

Separation processes can be classified according to the type of feed stream (heterogeneous or homogeneous) as shown in Figure 2.1. Homogeneous feed can be classified based on the type of controlling process either equilibrium process or rate

governed process, the equilibrium process can be classified depending on the type of separating agent (energy or mass).

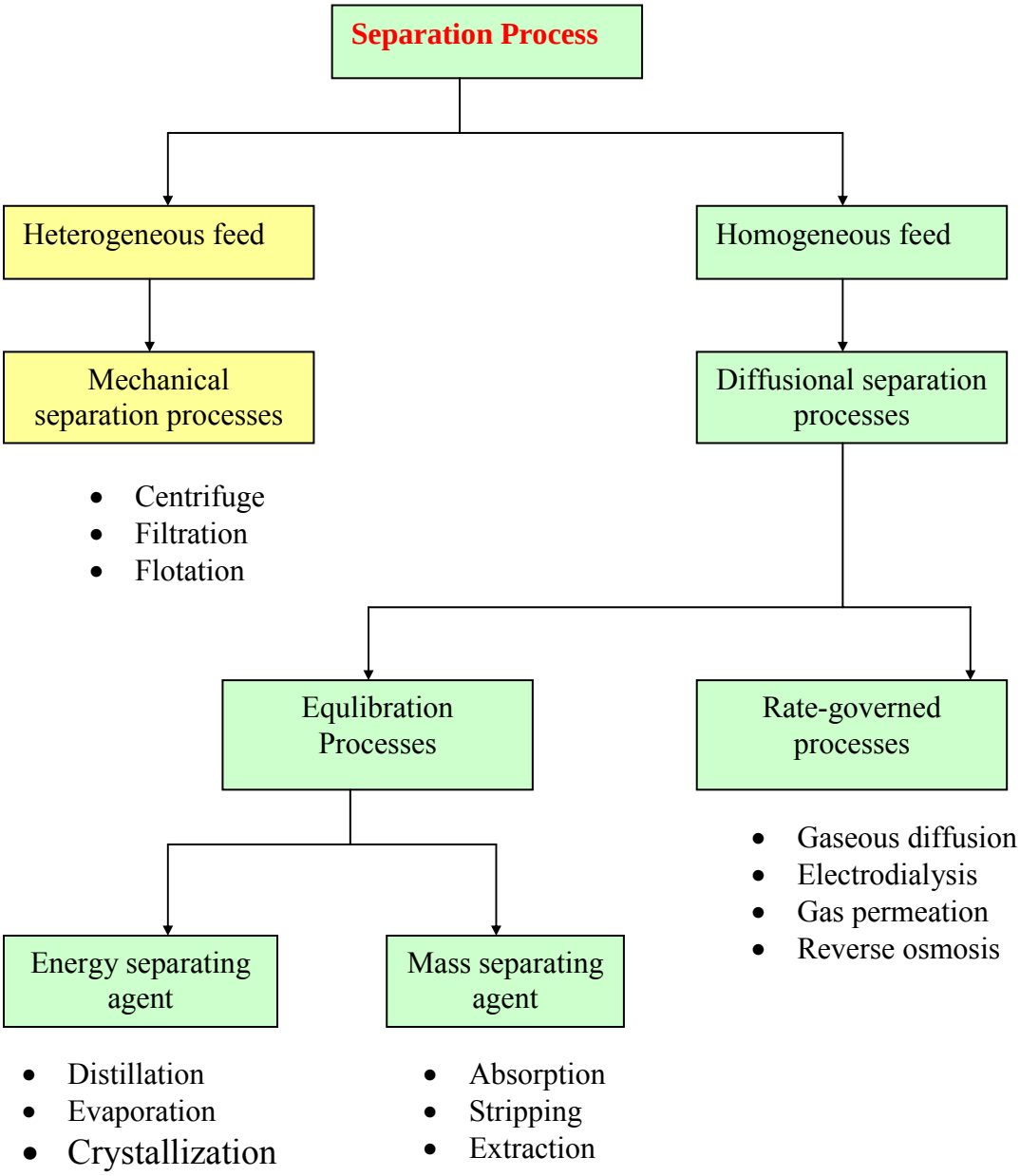

Figure 2.1: Classification of the main separation process

Benedict (1974) has classified multistage separation processes into three main categories according to the relative energy consumption for a certain separations at a given separation factor:

(i) *Potentially reversible processes*: In these processes, the work consumption can be reduced to its minimum based upon equilibration of immiscible phases,

which used only energy as separating agent (e.g. distillation, crystallization, and partial condensation).

(ii) *Partially reversible processes*: These processes include those equilibrium separation processes, which employ a stream of mass as a separating agent such as absorption, extractive distillation, and chromatography. Most of the steps are potentially reversible except for one or two, such as the addition of solvent, which inherently irreversible.

(iii) *Irreversible process*: In general these processes are rate-controlled separation process and all steps require irreversible energy input for separation. Membrane separation process and gaseous diffusion are typical examples.

2.3. Distillation unit

Distillation is the baseline of chemical industry. In the US for example about 40,000 columns are in operation, handling 90-95 % of all separations for product recovery and purification. Distillation has very wide applications in chemical process industry. These applications have a wide range from the separation of bulk petrochemicals such as propylene/propane and etheylbenzene/styrene to the cryogenic separation of air into nitrogen and oxygen. In petroleum industry distillation is used also to separate huge volumes of crude oil into gasoline and liquid fuels. The capital investments in distillation system in US alone amount to at least $ 8 billions (Humphrey, 1995).

Kunesh et al., (1995) has reasoned the popularity of distillation process to a number of bases:

- The capital investment for distillation scales as a function of capacity to about 0.6 power while other methods e.g., membranes tend to scale linearly with capacity. Thus distillation often has a distinct economic advantage at large throughputs.
- Unlike other separation methods, conventional distillation does not require a separating agent other than energy.
- A great deal of knowledge has been accumulated during the years about distillation such as, its operation, its limits, and reliable scaling-up of laboratory data. Confidence in distillation column design and its auxiliary equipment has

been developed. Similarly, direct experience with control systems and column transient response has been gained.

- Distillation is well supported with huge database of vapor/liquid equlibria (VLE).

Humphrey (1995) has mentioned the factors that favor distillation to be:

(i) Relative volatility is greater than 1.3,
(ii) Products are thermally stable,
(iii) Production rate is 5,000-10,000 lb./day or more, and
(iv) High corrosion rates and explosive reactions do not occur at distillation.

2.4. Distillation reversibility

Thermodynamically, the distillation process consists of the removal of entropy of mixing. The process requires exergy or work of separation. In a distillation process, exergy is provided by the input and the removal of heat at different temperature levels. Heat at high temperature is fed in the reboiler and heat at low temperature is removed in the condenser. Efficiency of distillation columns is very low because the actual exergy needed for a separation is much larger than the exergy for reversible separation. Reversible distillation is not practically attainable. Besides, only some product compositions can be obtained in a reversible multicomponent distillation (Agrawal et al., 1996). However, in any distillation process, the reversibility study is important for the improvement of the efficiency.

2.5. Energy requirement of distillation unit

Energy is the driving force for separation in distillation columns. There is a minimum energy requirement of separation, which represents the lower bound of energy consumed by the process. In actual industrial application, the energy consumption is much higher than the minimum requirement. This is due to irreversibility of the process, such as heat losses because of pressure drops, and temperature drops across reboliers and condensers (Fonyo, 1974).

The minimum reversible work requirements for the separation of homogenous mixture depend solely upon the composition, temperature and pressure of the mixture to be separated and upon the desired composition, temperature and pressure of the products. King (1980) has developed equation based on the analysis presented by Dodge (1944), Robinson and Gilliland (1950), and Hougen et al., (1950) for the minimum reversible mechanical work required in the ideal separation of a homogenous mixture into pure products at constant pressure and temperature:

$$W_{\min,T} = -RT\sum_{j} x_{jF} \ln\left(\gamma_{jF} x_{jF}\right), \qquad [2\text{-}2]$$

Where $W_{min,T}$ is the minimum work consumption per mole of feed, R is the gas constant and T is the absolute temperature. x_{jF} is the mole fraction and γ_{jF} is the activity coefficient of component j in the feed. If assuming ideal mixture, equation [2-2] yields:

$$W_{\min,T} = -RT\sum_{j} x_{jF} \ln x_{jF} \qquad [2\text{-}3]$$

When assuming ideal binary mixture with components A and B:

$$W_{\min,T} = -RT\left(x_A \ln x_A + x_B \ln x_B\right) \qquad [2\text{-}4]$$

Furthermore, W_{min} is also equal to the increase in Gibbs free energy, G:

$$W_{\min,T} = \Delta G_{sep} = \Delta H - T\Delta S\,, \qquad [2\text{-}5]$$

Where ΔH and ΔS is the change in enthalpy and entropy respectively.

The $W_{min,T}$ represents the lower bound of energy that must be consumed by the process. As mentioned earlier, for actual separation processes the energy requirement is much greater than the minimum work. Notwithstanding, $W_{min,T}$ represents a significant quantity which must be kept in mind during synthesis and comparison of different design alternatives (King, 1980).

In most separation processes energy is provided as heat rather than mechanical work. King (1980) defined the net consumption work of a process as the difference between the work that could have been obtained by a reversible heat engine from heat entering

the system and leaving the system. The ambient temperature, T_0, would be the other heat source or sink of the heat engine.

If heat, Q_H, is supplied to the system at high temperature, T_H, and heat, Q_L, leaves the system at low temperature T_L, the net work consumption, W_n, equals:

$$W_n = Q_H \frac{T_H - T_L}{T_H} - Q_L \frac{T_L - T_0}{T_L} \quad [2\text{-}6]$$

For a conventional distillation column the separation process is driven by heat input. If cooling water is used to remove heat in the condenser, equation [2-6] yields:

$$W_n = Q\left(1 - \frac{T_0}{T_R}\right), \quad [2\text{-}7]$$

Where $T_H = T_R$.

The thermodynamic efficiency, η, is defined as the ratio of the minimum reversible work consumption to the actual work consumption of the separation process

$$\eta = \frac{W_{\min}}{W_n} \quad [2\text{-}8]$$

2.6. Methods of energy conservation in distillation systems

Since energy prices are expected to increase in the future, energy conservation in the chemical industry is important. Also from an environmental point of view, savings in the use of energy is of upmost importance, because of reduced flue gas emissions of e.g. CO_2, NO_x, SO_x and particulates to the environment (Smith and Delaby, 1991). Due to the high-energy requirements of the distillation unit, one approach would be to totally replace distillation by other unit operations, such as absorption, desorption, adsorption, membrane processes, crystallization, recovery by chemical reactions, etc. (Huckins, 1978). However, by adopting these alternatives, higher capital costs relative to distillation are expected, especially at high capacity.

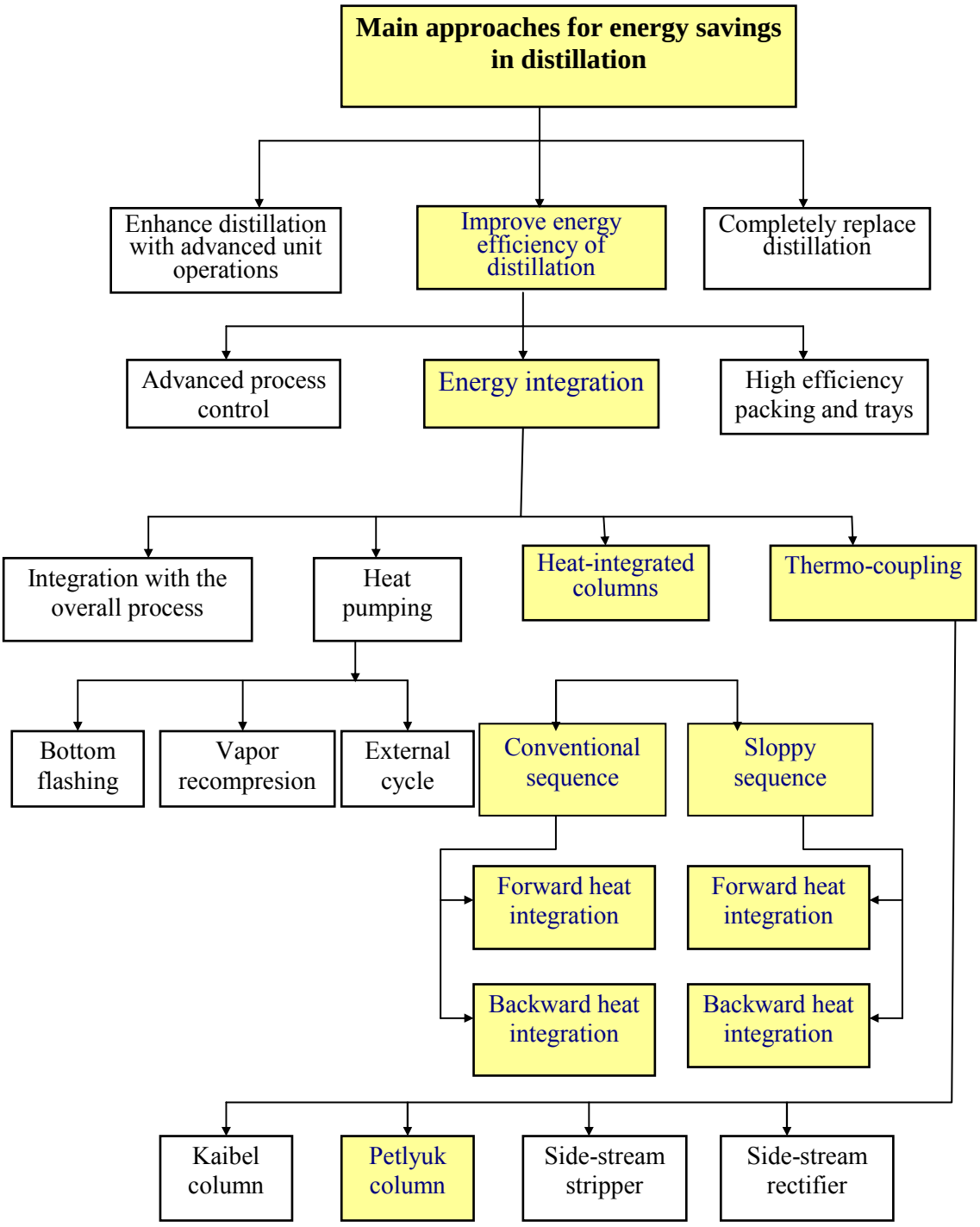

Figure 2.2: Main approaches for energy conservation in distillation systems

Enhancing distillation with other separation units to form a hybrid system can result in significant energy savings (Humphrey and Seibert, 1992). Another separation unit is grouped with the distillation unit, so that the second process refines the distillation product. This leads to a reduction in column reflux, and hence a reduction in energy use, and it also increases the column capacity. A systematic way of assessing energy

conservation of distillation systems is given by (Annakou, 1996) and it is modified according to this Ph.D. study as shown in Figure 2.2

Moreover, Mix et al. (1978) stressed the importance of improved instrumentation and process control. To obtain the desired purities in the product streams, operators operate the plants within a large margin of safety to ensure achievement of the specifications. This margin is vital for coping with fluctuations and upsets in the process. However, improved control will lead to reduce fluctuations, which allow for relaxation of the average product purity specifications, and thus a reduction in column reflux requirements. They discussed also the potential for energy requirement reduction by the means of tray and packing retrofit. They found that the characteristics that favor retrofit are few trays, high ratio of actual to minimum reflux, high pressure and large heats of vaporization. An increase in the number of equilibrium stages can usually be obtained by replacing distillation sieve trays with high efficient packing or trays. According to the Gilliland correlation, if the number of equilibrium stages is increased, reflux ratio and reboiler energy can be reduced.

Appropriate integration of distillation columns with the overall process can result in significant energy savings, e.g. (Smith and Linnhoff, 1988) or (Mizsey and Fonyó, 1990). Feed preheaters or precoolers and intermediate reboilers and condensers should be considered, if waste energy is accessible.

Heat pumping is an economical way to conserve energy in “stand alone” distillation columns when the temperature difference between the overhead and bottom of the column is small and the heat load is high (Mészáros and Fonyó, 1986) and (Fonyó and Benko, 1998). In a closed cycle heat pump an external fluid (refrigerant) is replacing the steam and cooling water. However, if the distillate is a good refrigerant vapor recompression can be applied. Bottom flashing should be considered if the bottom product is a good refrigerant. Because of less energy demand, the heat pump assisted distillation reduces the operating costs and occasionally can compensate the additional capital expenses of the compressor.

2.6.1. Conventional distillation schemes

These schemes consist of two simple distillation columns connected in such a way that one product of the first column is the feed of the second column. In literature, they are considered to be the conventional arrangements for ternary distillation. These arrangements have four column sections, two sections in each of the simple columns and each column with one feed and two product streams.

Two arrangements can be made from the conventional distillation schemes one is direct sequence (Figure 2.3 a) and the other is indirect sequence (Figure 2.3 b). In case of direct sequence, light component is drawn as an overhead product of column 1 and the binary bottom product (**BC**) are fed to column 2 where the intermediate component is drawn as overhead product and the heavy component as bottom product. On the other hand, in the case of indirect sequence, the heavy component is taken as bottom product of column 1 and the binary overhead product (**AB**) is fed to column 2 where light component is drawn as overhead product and intermediate component as bottom product.

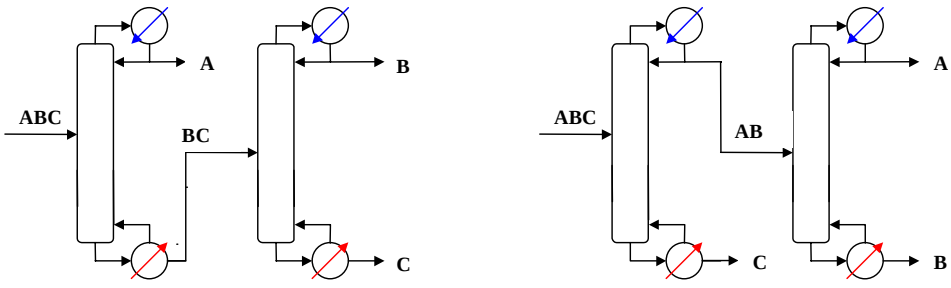

a) The direct sequence (**D**) b) The indirect sequence (**I**)

Figure 2.3: The conventional sequences for the separation of a ternary mixture

For an optimal direct sequence, the connecting stream is boiling liquid. In the same manner, for an optimal indirect sequence, the connecting stream is saturated vapor. The best conventional scheme from economic point of view is considered as the base case for comparison with non-conventional distillation arrangements.

2.6.2. Conventional heat-integrated schemes

Heat integrating between the two columns is one of the most efficient methods for reducing the amount of external heat. It is attempted by utilizing the overhead vapor from one of the columns to provide heat to the other so that reboiler of one column could be combined with condenser of the other in one heat exchanger. Usually the pressure of heat source column has to be increased to provide the temperature driving force needed in the heat exchanger.

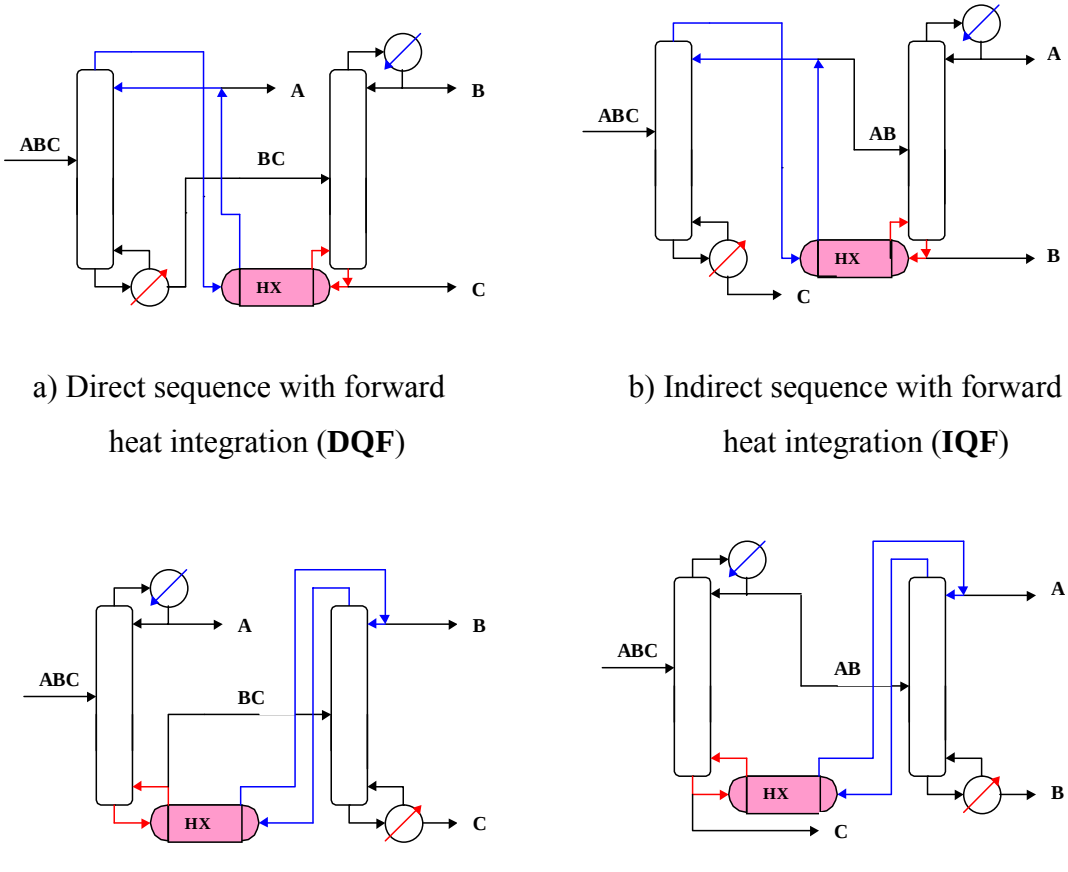

a) Direct sequence with forward heat integration (**DQF**)

b) Indirect sequence with forward heat integration (**IQF**)

c) Direct sequence with backward heat integration (**DQB**)

d) Indirect sequence with backward heat integration (**IQB**)

Figure 2.4**:** Heat-integrated sequences for separating a ternary mixture. The heat exchangers are noted by ”HX”

From the conventional sequences, four different heat integrated sequences can be constructed for the separation of a ternary mixture (Figure 2.4): the forward heat

integrated direct sequence (**DQF**); the backward heat integrated direct sequence (**DQB**); the forward heat integrated indirect sequence (**IQF**); the backward heat integrated indirect sequence (**IQB**).

In the forward heat integrated sequence, the first column boils up the second. Hence, the condenser of the first column and the reboiler of the second are replaced by a heat exchanger. The pressure of the first column is increased to meet the EMAT of the heat exchanger.

On the other hand, in the backward heat integrated sequence, the second column boils up the first. Therefore, the reboiler of the first column and the condenser of the second are replaced by a heat exchanger. Furthermore, the pressure of the second column is increased to meet the EMAT of the heat exchanger. When the choice of direct or indirect sequence is made, forward or backward heat integration must be considered. This consideration depends mostly on the heat duty of the condenser and reboiler of one column compared to the other, the temperature difference between the top of one column and that of the bottom of the other and on the magnitude of the increased pressure of the heat source column. When comparing the heat duties of the columns, it is usually found that they do not match. One solution is to install auxiliary equipment such as trim reboilers or condensers.

Mészáros and Fonyó (1988) presented several rules of thumb for selecting the best heat-integrated sequence:

1. Favor heat integration where additional heating is required
2. Avoid the use of a high temperature utility
3. Favor the heat integration which gives maximum heat exchange

Annakou (1996) suggested the following algorithm for selecting the best heat integrated sequence, based on the parameters shown in Table 2.1:

- Selected conventional scheme with new pressure *P'* that satisfy heat exchange requirement, then compare Q_{1C} to Q_{2R} and Q_{2C} to Q_{1R}.

- If $Q_{1C} < Q_{2R}$ and $\Delta T_{12} < \Delta T_{21}$ then choose forward heat integration. If $Q_{2C} < Q_{1R}$ and $\Delta T_{21} < \Delta T_{12}$ then choose reverse heat integration.
- If $Q_{1C} < Q_{2R}$ and $\Delta T_{21} < \Delta T_{12}$ or vice versa, then check both heat integrated sequences and choose the better one.
- Start rigorous modeling to satisfy the purity specifications as in the corresponding conventional sequences.

Table 2.1: Parameters for selecting the best heat-integrated sequence

P'_1	New pressure to satisfy the heat exchange requirement in column 1
P'_2	New pressure to satisfy the heat exchange requirement in column 2
Q_{1C}	Condenser heat duty for column 1
Q_{1R}	Reboiler heat duty for column 1
Q_{2C}	Condenser heat duty for column 2
Q_{2R}	Reboiler heat duty for column 2
ΔT_{12}	Temperature difference between top of column 1 and bottom of column 2
ΔT_{21}	Temperature difference between top of column 2 and bottom of column1

However, as with the rules of thumb, this algorithm may not give the optimal solution, because it does not take into account the possibility of changing the columns' design. For heat surplus in the case of forward heat integration, $Q_{1C} > Q_{2R}$, the reflux of the second column may be increased and the number of trays decreased, in order to balance the duties. Even though this requires a higher reboiler duty, there is no penalty in terms of energy consumption, because additional duty is obtained by heat integration. The option of decreasing Q_{1C} may not be possible due to the minimum reflux constraint (Bildea and Dimian, 1999).

Furthermore, if there is a heat deficiency, $Q_{1C} < Q_{2R}$, the reflux of the first column may be increased and the number of trays decreased. Still, the reboiler duty, Q_{1R}, must be increased. However, since the additional heat does not come from heat integration, there will be a penalty in terms of energy consumption. As for the previous case, decreasing Q_{2C} may not be possible due to the minimum reflux constraint. The same considerations apply for the reverse heat integration, though in this case Q_{2C} is higher compared to Q_{1R}

The impact on the optimal solution of increased capital costs for not balancing the duties because of the installation of an additional reboiler or condenser, only rigorous simulation and optimization can reveal. However, it is likely that high utility costs support the rules of thumb and the algorithm.

2.6.3. Thermo-coupling

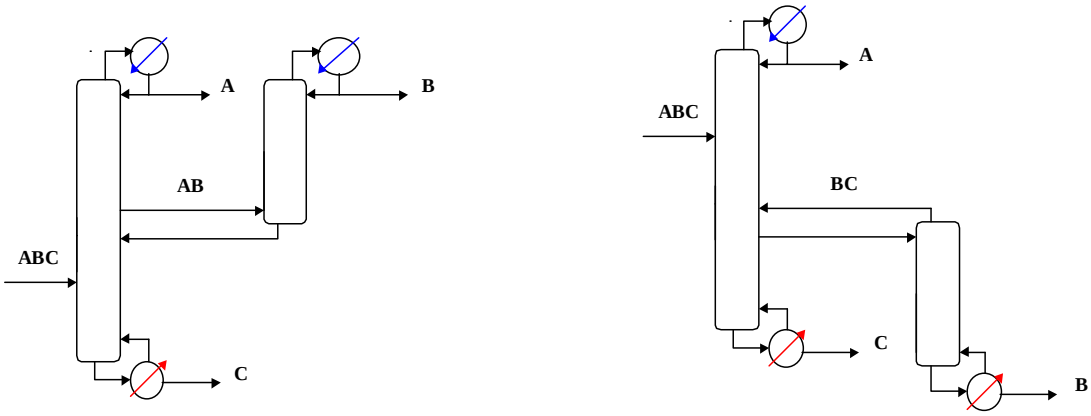

a) Column with side rectifier

b) Column with side stripper

c) The Petlyuk column

d) Dividing wall column (Kaibel column)

Figure 2.5: Thermally coupled systems

In the case of thermo-coupling, parts of the heat transfer necessary for the separation is provided through direct contact of the material flows. Also, a prerequisite for

thermo-coupling is that gas or liquid streams of the same composition should exist in different columns (Stichlmair and Stemmer, 1989). Four different thermo-coupled systems are shown in Figure 2.5.

2.6.4. Side rectifier column and side stripper column

These columns are partially thermally coupled and the thermal coupling is present at the connection between the two columns. They are columns with a side stream connected to a side section. This added section is a rectifier (column with side rectifier) or a stripper (column with side stripper). The number of sections of a column with side stripper or side rectifier is four.

The column with side rectifier consists of a column with sidestream connected to a side rectifier (Figure 3.a). In the sections adjusted to the feed, **A-BC** separation is performed to any desired extent. In the lower section of the first column, C is purified to any desired extent. The rectifier purifies product **B** to any desired extent. The column with side stripper consists of a column with sidestream connected to a side stripper (Figure 3.b). In the sections adjusted to the feed, **AB-C** separation is performed to any desired extent. In the upper section of the first column, **A** is purified to any desired extent. The stripper purifies **B** to any desired extent. Therefore, any specified recoveries or purities in the three products can be attained in both, a column with side rectifier and a column with side stripper.

2.6.5. The Petlyuk column and the divided wall column

The Petlyuk column (Petlyuk et al., 1965), also called the fully thermally coupled distillation column, consists of a prefractionator and a main column (Figure 2.5 c). In the prefractionator, the components **A** and **C** are first separated, which are the extremes in relative volatility, and therefore easily separated, while the **B** component is distributed both up and down. This is called a sloppy separation, in contrast to a sharp separation, where two components of adjacent relative volatility are separated. The components **A** and **B** are then separated in the upper (rectifying) part of the main column. Similarly, the components **B** and **C** are separated in the lower (stripping) part

of the main column. The main column has the three product streams and supplies the reflux and vapor streams required by the prefractionator. The Petlyuk column has six sections, two in the prefractionator and four in the main column. The reboiler and the condenser are in the main column.

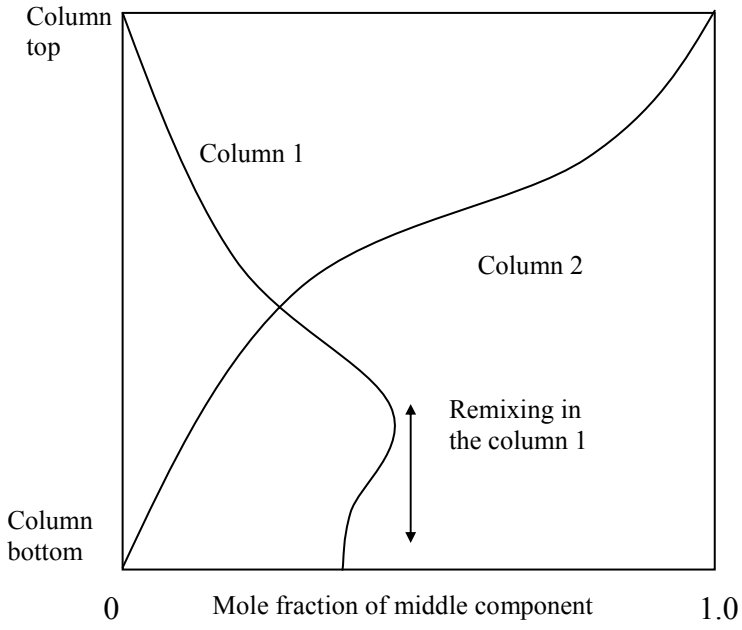

Figure 2.6: Composition profile of the middle component in direct sequence columns

The main advantage of the Petlyuk system is that there is no remixing of the middle component **B** in the prefractionator. Considering the first column of the direct sequence, the most volatile component, **A**, is separated from components **B** and **C**. The concentration of **B** raises to a maximum some way up the column. However, when it exits at the bottom, it has been diluted with a higher concentration of the least volatile component, **C**. This remixing means that energy has been wasted on separating **B** partway up the column, only to mix it again with **C**. Similarly, remixing also occur in the indirect sequence. Figure 2.6 shows the composition profiles of the direct sequence.

Trinatafyllou and Smith (1992) explained the remixing effect in a Petlyuk column and stated that the remixing effects can be avoided in Petlyuk column. From the composition profile of the middle component, **B**, in the Petlyuk system, shown in

Figure 2.7, it can be seen that no remixing occurs. It can also be noted that **B** is withdrawn as a product at the peak of the composition profile.

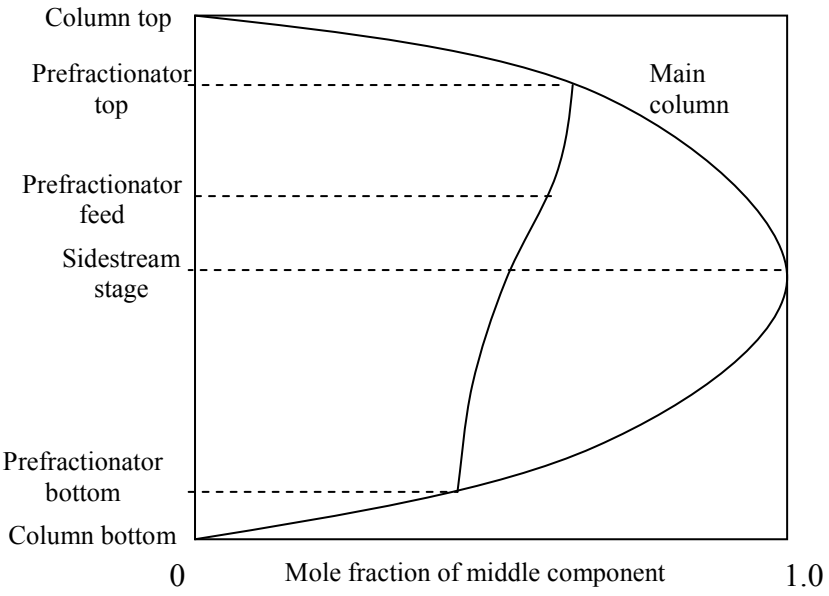

Figure 2.7: Composition profile of the middle component in the Petlyuk column

Another advantage of the Petlyuk column is that the composition of **B** in the feeds to the main column usually matches the composition of the feed trays (Figure2.7). While for sharp separations of more than two components, like in the conventional sequences, it is very difficult to find a tray with a composition close to that of the feed. The combination of no remixing of the middle component and reduced mixing at the feed tray adds up to between 20 and 30 per cent energy savings (Glinos and Malone, 1988).

Kaibel column (Figure 2.5 d) works the same way as the Petlyuk system, and if there is no heat transfer across the dividing wall, they are thermodynamically equivalent (Kaibel, 1987). Kaibel column is built in only one shell and a vertical wall divides its core in two parts that work as the prefractionator and the main column of the Petlyuk column, respectively. Combining the prefractionator and the main column into one column with a dividing wall, called the dividing wall column can make a reduction in capital costs.

In order to design the Petlyuk system, the flow rates of the internal recycle streams are of most importance. The fractional recovery of the middle component, β, in the top product is given by:

$$\beta = \frac{(D)(x_{D,B})}{(F)(x_{F,B})}, \qquad [2\text{-}9]$$

Where *D* and *F* are the respective flow rates of the overhead product and the feed, and x_D and x_F are the compositions in the overhead product and the feed, respectively, of the middle component, **B**.

Fidkowski and Krolikowski (1986) and also Rév (1990) have evaluated the theoretical fractional recovery, β^*, of the middle component in terms of relative volatilities. Then the energy consumption of the Petlyuk column is minimal. In the case of saturated liquid feed, yields:

$$\beta^* = \frac{\alpha_B - \alpha_C}{\alpha_A - \alpha_C}, \qquad [2\text{-}10]$$

Where α_i refers to the relative volatilities of the components **A**, **B**, and **C**. Hence, β^* can be used to estimate the internal recycle streams and the flow rates of the prefractionator. More theoretical reviews of the design model for the Petlyuk system can be found in e.g. Annakou (1996).

2.6.6. The sloppy separation systems

The sloppy systems can be resembled as a Petlyuk column, but without material flows from the main column to the prefractionator. However, like in the thermo-coupled systems, gas or liquid streams of the same composition exist in different columns (Figure 2.8).

The same sloppy separation takes place as in the prefractionator of the Petlyuk column. However, in contrast to the Petlyuk column, the heating and cooling requirement of the prefractionator is supplied through a reboiler and a condenser. In

the two main columns no remixing of the middle component occurs, just as in the main column of the Petlyuk column. The middle component is taken as a product in the bottom of the upper column and the top of the lower column. These two columns can easily be unified into one main column with a side stream.

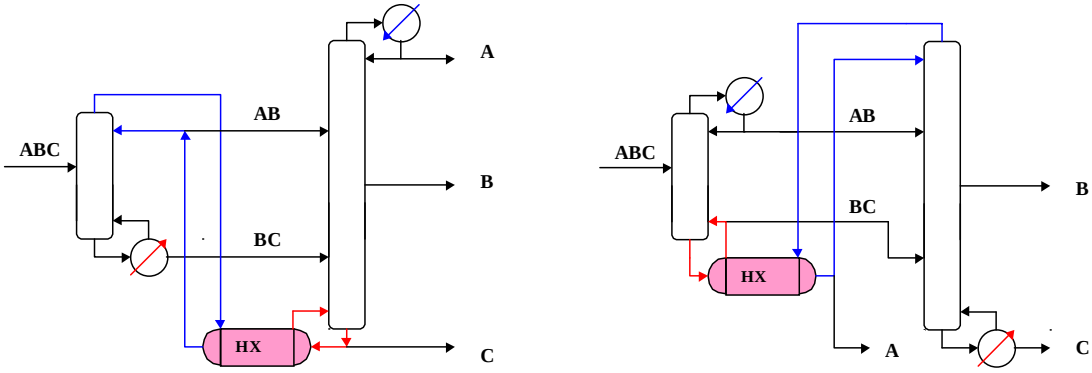

a) Sloppy sequence with forward heat integrated (**SQF**)

b) Sloppy sequence with backward heat integration (**SQB**)

Figure 2.8: The sloppy separtion systems. The heat exchanger is noted by ”HX”.

The heat integrated sloppy systems can be imagined as a heat integrated Petlyuk column, but with no material flow from the main column to the prefractionator. In the forward heat integrated sloppy system (Figure 2.8 a), the pressure of the prefractionator is increased to meet the temperature driving force necessary to boil up the main column. The opposite is the case in the backward heat integrated sloppy system (Figure 2.8 b).

To design the heat integrated sloppy systems, the same procedure as for the conventional heat integrated systems can be followed in combination with the design of the Petlyuk column. However, the use of the optimal fractional recovery, β^*, should be careful, since the pressures of the columns are usually different.

One of the early works in this area is the study of Tedder and Rudd (1978), who have analyzed the economic features of eight distillation schemes for the separation of ideal ternary mixtures. These distillation schemes include conventional direct and indirect

sequence, sidestrem strippers, sidestrem rectifiers, etc. However, Petlyuk column and Kaibel column have not been included. They have found that the regions of economic optimization for various designs depend on the ternary mixture separation system but also the changes in feed composition have characteristic effects on the total annual cost.

Fidkowski and Krolikowski (1986, 1987) have found an analytical solution of the Petlyuk column optimal operation, assuming ideal mixture, constant relative volatility, constant internal flow rates throughout the column and selected the fractional recovery of the middle component in the top product of the prefractionator as a decision variable. They have also compared the Petlyuk column to conventional sequence and other thermally coupled schemes shown in Figure 2.5. They have developed an optimization procedure for minimizing the vapor flow rate from the systems reboiler by using the Underwood method for calculating the minimum vapor flow rate. For the optimum fractional recovery of the middle component in the top product of the prefractionator they have used the formula based on the relative volatilites (Equation 2.10) introduced by Treybal (1968). They have found that the Petlyuk column is the least energy-consuming scheme. However, they have indicated that the rigorous methods must be used for design purposes.

Glinos and Malone (1988) have studied the sharp separation of ternary mixtures for several distillation alternatives including sidestream stripper, sidestream rectifiers, prefractionator, and Petlyuk column. In all cases they have focused on optimality regions in terms of the minimum total vapor rate generated by the reboilers. On the basis of this optimality measure they have developed approximate designs for the complex columns and compared them to the conventional direct and indirect schemes. For the Petlyuk column they have suggested that the multiple solutions can be easily bounded and the optimal solution is one that minimizes the total vapor flowrate in the whole system.

Carlberg and Westerberg (1989) have studied the thermally coupled columns using the vapor flowrates as bases. They have indicated that the recovery of the middle component in the prefractionator is not an independent variable because it depends on the recoveries of the light and heavy components.

Trinatafyllou and Smith (1992) have presented a shortcut design procedure for the design of the Petlyuk column. They have recognized that the flowrates in the main column are not independent of the vapor flow fed to the prefractionator and the specifications of the recoveries of the light and the heavy components in the prefractionator determine the vapor and liquid draw-off rates. They have compared the dividing wall column to the conventional schemes and found that about 30 % of the total cost can be saved. They have also emphasized the basic principle of Petlyuk et al., (1965) that in the case of Petlyuk column there is no remixing effect in the system, which would be a source of inefficiency in the separation, on the contrary, to simple distillation columns separating a ternary mixture.

Annakou and Mizsey (1996) have studied the design of Petlyuk column and investigated the role of β^* over the energy consumption and the total annual cost. They have found that their optimal β^* values are close to fractional recovery of the middle component β. They concluded that β is an important design parameter for the design of Petlyuk column.

Dunnebier and Pantelides (1998) has confirmed the conclusions of earlier work in this area that substantial benefits in both operating and capital costs may be achieved by the use of thermally coupled distillation column and possible saving up to 30 % are achieved comparing to conventional distillation columns.

In this work the design and optimization of Petlyuk column, sloppy schemes, conventional heat-integrated schemes, and the base case are addressed in chapter 3.

2.7. Controllability considerations

Traditionally plant design has been a mostly sequential discipline, where the control design is carried out after the plant has been designed. During plant design a number of basic plant performance requirements have to be ensured in order to obtain a design which provides acceptable operational performance.

Operability is the ability of the plant to provide acceptable static and dynamic operational performance. Operability includes flexibility, switchabilty, controllability and several other issues.

Grossmann and Morari (1984) have defined the operability as a general description for the ability of the plant to perform in a satisfactory way under conditions different from the nominal design conditions. They have outlined the major objectives of operability to be:

1. feasibility of steady-state operation for a range of different feed conditions and plant parameter variations,
2. smooth and fast change over and recovery from process disturbances,
3. reliable and safe operation despite equipment failures,
4. easy start up and shut down.

Rosenbrock (1970) defined controllability in more general terms: A system is called controllable if it is possible to achieve the specified aims of control, whatever these may be. By extension, the system is said to be more or less controllable according to the ease or difficulty of exerting control. Thus controllability may be viewed as a property of plant, which indicates how easy it is to control the plant to achieve the desired performance.

According to Nishida et al. (1981), the development of a control system requires:

- the specification of a set of control objectives,
- a set of controlled variables,
- a set of measured variables,
- a set of manipulated variables, and
- a structure interconnecting the measured and manipulated variables.

Morari (1983) has developed a useful measure to assess the inherent property of ease of controllability (resiliency). The Morari resiliency index (MRI) gives an indication of the controllability of a process. MRI depends on the controlled and manipulated

variables, but it does not depend on the pairing of these variables or on the tuning of controllers.

Yu and Luyben (1987) have followed almost the same procedure but indicate that the control system constitute of two main parts: the control structure, which is determined by the controlled and manipulated variables, and the controller structure, i.e., SISO controllers or one multivariable controller.

Mizsey (1991) has attributed the differences between the operability definitions to the fact that different methods work on different levels of process synthesis. Fisher et al. (1988) who work in the early stage of conceptual design express their goal in the operability analysis as to ensure the availability of adequate amount of equipment overdesign so that the process constrains can be satisfied in addition to minimizing the operating costs and overdesign costs over the entire range of predicted process disturbances. They have proposed an approach for control synthesis of a complete chemical process based on the hierarchical decomposition tool by Douglas (1985). They indicate for each hierarchical level the economically significant disturbances and the sets of the controlled and manipulated variables. For every level they check whether the number of manipulated variables is equal to the number of constrains plus operating variables (degree of freedom analysis) and based on that appropriate modifications should be decided.

2.7.1. Steady state control indices

Several tools are used for assessing the controllability and they are called steady-state control indices such as:

1) Relative Gain Array (RGA),
2) Condition Number (CN),
3) Morari Resiliency Index (MRI),
4) Niederlinski Index (NI).

Steady state gains are calculated for 3 × 3 multivariable systems. The following controllability indices are used (Luyben, 1990):

i) The Niederlinski index (NI), which is the determinant of the steady state gain matrix divided by the products of its diagonal elements.

$$NI = \frac{Det[k_p]}{\prod_{j=1}^{N} k_{pu}} \qquad [4\text{-}1]$$

where

k_p = matrix of steady state gains

k_{pu} = diagonal elements in steady state gain matrix

This method is a "necessary but not sufficient" condition for stability of a closed loop system with integral action. If the index is negative, the system will be unstable for any controller settings (i.e. integral instability). If the index is positive, the system may or may not stable. This index is useful for eliminating unworkable pairings at an early stage of design.

ii) The Morari resiliency index (MRI), which is the minimum singular value of the steady state gain matrix. The larger its value, the better is the control,

$$MRI = \underset{[G_{M(iw)}]}{\min} \sigma \qquad [4\text{-}2]$$

where $G_{M(iw)}$ is the open loop transfer function.

iii) The Relative gain array (RGA) is the Hadammard product of the steady state gain matrix and its inverse. Diagonal elements (λ_{ij}) close to unity indicate lower interactions. The RGA is a matrix of numbers. The ijth elements in the array is the ratio of the steady state gain between the ith controlled variable and the jth manipulated variable when all other manipulated variables are constant, divided by the steady state gain between the same two variables when all other controlled variables are constant.

iv) The condition number (CN), is the ratio of the maximum singular value of the steady state gain matrix to its minimum singular value.

$$CN = \frac{\sigma_{max}}{\sigma_{min}} \qquad [4\text{-}3]$$

The smaller CN, the better is the control (Papastathopoulou and Luyben, 1991).

2.7.2. Design of control structure

Chemical process are usually nonlinear and multivariable (MIMO) process and furthermore there exist some interactions between the variables in such a way that one variable may influence or be influenced by several other variables. These two facts make the choice of the control structure a difficult task. During final design, if we consider controllability, which works in the neighborhood of steady-state and the disturbances have low frequencies, linerizaed models and the tools of linear control theory can be used for the simulation and investigation of the process (Mizsey, 1991).

Wolff et al. (1995) considered the operation and control of the Petlyuk Column. Linear analysis tools and frequency-dependent plots are used to study the L-S-V control structure in decentralized feedback control strategy. This control structure consists in the control of **A** composition by L, the control of **B** composition by S and the control of **C** by V. From a linear point of view, they did not find major problems with the L-S-V control structure. However, they found serious problems related to the steady-state behavior if four compositions are specified and concluded that “holes” in the operation range would make it very difficult to control the four compositions.

Annakou et al. (1996) compared the controllability of the conventional heat-integrated column sequences and the Petlyuk Column for the separation of ternary mixtures. Through degrees of freedom analysis and steady-state multivariable control synthesis tools they have showed that both investigated schemes could be controlled by conventional decentralized control structures, although interactions among control loops is smaller for the conventional heat integrated systems.

Abdul et al. (1998) also studied the operation and control of Petlyuk Column. They suggested that both liquid and vapor splits are maintained constant at their nominal

values. Two control structures are considered in their work: L-S-V and D-S-V. The second one consists in the control of **A** purity by D, the control of **B** by S and the control of **C** by V. The steady-state Relative Disturbance Gain (RDG) of the two control structures are calculated to make an interaction analysis and simulations showed, according to The RDG results, that D-S-V control structure resulted in better control than L-S-V control structure.

Mizsey et al. (1998) have investigated the controllability of conventional-heat integrated schemes and the Petlyuk Column and found conventional heat-integrated schemes have less interactions comparing to Petlyuk column by measuring steady state control indices. The dynamic behaviour shows longer settling time and higher overshoots for the Petlyuk column comparing to conventional heat-integrated schemes, detunig is necessary due to strong interaction between its control loops.

Hernandez and Jimenez (1999) have carried out a comparison between energy requirement and controllability properties for three complex columns including the Petlyuk column. They have found that the schemes with side columns are economically competitive with Petlyuk column only for mixtures of low intermediate composition and when **B/C** split is harder than **A/B** separation. Schemes with side columns show better dynamic properties than Petlyuk column, and the amount of middle component has no effect on the control properties.

Bildea and Dimian (1999) have studied the relation between design and control of forward and backward heat integration of sloppy separation sequences and found the schemes are similar with respect to energy consumption, but very different with respect to dynamic behaviour. Forward heat integration is much easier to control, which can be due to the absence of a positive feedback of energy, which is usual in the backward heat integration.

Jimenez et al. (2001) have compared the controllability properties of thermally coupled distillation schemes with the conventional schemes and their results indicates that the energy-integrated schemes exhibit better control properties than the conventional schemes, and the Petlyuk column shows limited and unstable controllability results.

2.8. Environmental considerations

Energy economization plays very important role not only in the minimization of total cost in the chemical process industries but also in reducing or minimizing the flue gas emissions and the waste of the utilities of the chemical process industry (CPI). Waste in CPI can be classified into two main sources:

2.8.1. Process waste

The process waste is associated with three main sources:

(a) Waste is created in reactors through the formation of waste byproduct, also elsewhere in the plant (e.g. thermal decomposition),
(b) Waste is produced from separation and recycle systems through the inadequate recovery and recycling of valuable materials from waste streams,
(c) Waste produced from process operations such as start-up and shutdown of continuos processes, product changeover, equipment cleaning, etc.

2.8.2. Utility waste

Reducing energy requirement means a reduction in utility demand (i.e. less steam, cooling water, etc.). The basic sources of utility waste are result of the hot utilities and cold utilities. The basic units of utilities such as steam boilers, gas turbines, furnaces, and diesel engines produce gaseous waste associated with combustion process. The flue gas emissions, which are of concern to environmental protection are carbon dioxides, nitrogen oxides, and sulfur oxides (CO_2, NO_x, SO_x).

Smith and Delaby (1991) have divided the gaseous pollutants into three categories:

a) the long-lived species (CO_2, CH_4, N_2O, SO_2) responsible for global warming,
b) the soluble acidic oxides (NO_x, SO_x) responsible for acid deposition,
c) the other species which contribute to smog and health hazards (particulate such as metal oxides, hydrocarbons, carbon monoxide, etc.).

2.8.3. Waste treatment

The treatment of the waste after it has been created by the chemical processes or *end-of pipe treatment*. In this approach the waste is treated by some methods such as incineration, biological digestion, etc. The target of the *end-of-pipe treatment* is to destroy the waste but this cannot be achieved since it is already created. The waste can be concentrated or diluted, its physical or chemical form can be changed, but it cannot be destroyed (Smith, 1995). The real solution to this problem is not to create the waste from the start or in practical sense is to minimize the waste at the source that is *waste minimization* during the design stage.

Recently reducing or minimizing the waste at the source or in the design stage has been the focus of several papers. Douglas, who has presented a hierarchical approach for chemical process synthesis (Douglas, 1985, 1988), has modified his hierarchical procedure to include the waste reduction (1992). Berglund and Lawson (1991) have characterized waste as intrinsic and extrinsic wastes. Intrinsic wastes are inherent in the process configuration and extrinsic wastes are associated with the auxiliaries.

Mizsey (1994) has presented a systematic two level procedure for process waste elimination. He has suggested that the procedures of eliminating or minimizing the waste on the process or the plant level should be extended to a second level that is the factory level. This extension will enable the waste minimization methods to include not only one chemical process or plant but they can investigate more processes or plants trying to eliminate the global emission of the plants included in a chemical company.

In chapter 5 an estimation of the role of the energy-integrated schemes in reducing flue gas emissions is presented.

Chapter 3: Rigorous simulation and optimization

3.1. Introduction

Distillation is the most widely used separation technique in the petrochemical and chemical process industries for the separation of fluid mixtures despite its high-energy requirement. Significant energy savings can be reached by the use of complex distillation arrangements such as the side-stripper, the side-rectifier, the thermal (internal) *column coupling* (also known as Petlyuk column), the (external) *energy integration* (also known as energy integrated distillation system) and the heat pumping techniques.

Theoretical studies, e.g. Petlyuk et al. (1965), Stupin and Lockhart (1972), Fonyo et al. (1974), Stichlmair and Stemmer (1989), Annakkou and Mizsey (1996), and Emtir et al. (2001) have shown that the column coupling configurations are capable of achieving typically 30 % of energy savings compared to a conventional sequence. In addition, the coupling configuration can also be achieved with the so called dividing wall column, by placing a vertical wall in the middle of the column separating the feed from the side draw, e.g. Wright (1945), and Kaibel (1987). With this arrangement, reduction in capital cost can also be expected through the elimination of one of the column shells (but not the column internal). Despite the above advantages, industry has been reluctant to use the Petlyuk system and dividing wall columns and this is usually attributed to the lack of established design procedures and the fear of control problems.

This part of the dissertation compares the energy-integrated and thermally coupled configurations based on rigorous simulation and optimization for minimum total annual costs (TAC). The most common energy-integrated schemes are investigated not only theoretically studied but also used in industrial practice.

The following abbreviations are used for the studied distillation schemes and it is adopted from our previous study by Rev et al. (2001):

D: Direct separation sequence without heat integration (Fig. 2.3a)

DQF: Direct separation sequence with Forward heat integration (Fig. 2.4a)

DQB: Direct separation sequence with Backward heat integration (Fig. 2.4c)

I: Indirect separation sequence without heat integration (Fig. 2.3b)

IQF: Indirect separation sequence with Forward heat integration (Fig. 2.4b)

IQB: Indirect separation sequence with Backward heat integration (Fig. 2.4d)

SQF: Sloppy separation sequence with Forward heat integration (Fig. 2.8a)

SQB: Sloppy separation sequence with Backward heat integration (Fig. 2.8b)

SP: Thermally coupled sloppy separation sequence (Petlyuk column) (Fig. 2.5c)

3.2. Short-cut analysis

According to the previously performed short-cut analysis (Rév et al., 2001), in the case of sharp separation the sloppy separation path with forward, backward, or double heat integration (**SQF** and **SQB** schemes) is almost always capable of achieving as much energy savings as that of with the thermal coupling (Petlyuk column or dividing wall column, **SP**). Moreover, the conventional direct sequence and indirect sequence schemes with energy integration (**DQF**, **DQB**, **IQF** and **IQB** schemes) are, in some cases, also capable of achieving larger energy savings than that of the corresponding Petlyuk or dividing wall column configurations (**SP**).

The main corollaries of the short-cut analysis are the following:

- From energy point of view the energy-integrated and thermally coupled schemes are always better than the non-integrated ones.

- From energy point of view the energy-integrated schemes (**DQB**, **SQF**, and **SQB**) win in almost everywhere of the studied conditions. There is just a very small domain for **DQF** or **DQB** to win at very high ratio of **A** in the feed. All the integrated and coupled sloppy schemes are equivalent.

- Considering exergy loss, the integrated and thermally coupled schemes share the Gibbs composition triangle. There is a significant area where **SP** (Case 1) wins near the AC edge (Figure 3.1).

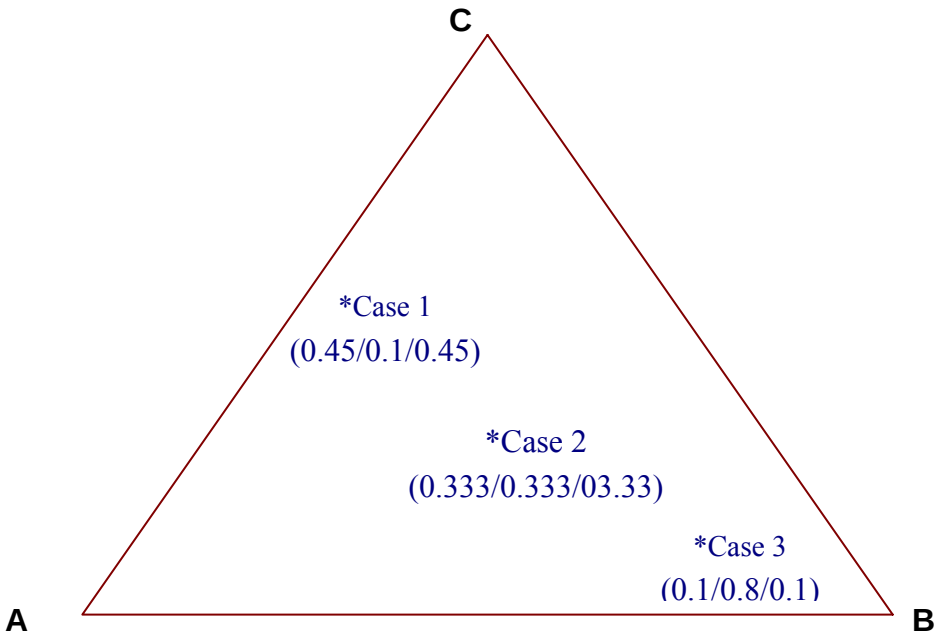

Figure 3.1: Composition triangle

According to the short-cut analysis, the forward or backward heat-integrated, as well as the double heat-integrated sloppy schemes (**SQF** and **SQB**) are equivalent, in energy term, to the thermally coupled sloppy schemes (**SP**, i.e. Petlyuk or dividing wall column configuration); and the heat-integrated schemes win, in exergy term,

almost everywhere of the studied conditions. These include a wide range of relative volatility ratios. The Petlyuk column has the greatest chance to win over the heat-integrated schemes at balanced relative volatility ratio. Even in that case, the heat-integrated schemes win over the Petlyuk column in the greatest part of the feed composition triangle; but the Petlyuk column yet proves to be the winner in a significant area of feed compositions especially al low concentration of middle component **B** (e.g. Case 1).

3.3. Rigorous case studies

The separation of (Ethanol – n-Propanol – n-Butanol) ternary mixture by several distillation schemes for 99 mole % product purity is studied at three different feed compositions (45/10/45), (333/333/333), and (10/80/10) in mole percent.

Table 3.1: Relative volatility and separation index for Rigorous Cases

	Case 1	Case 2	Case 3
α_{AB}	2.02	2.07	2.15
α_{AC}	4.67	4.72	4.79
α_{BC}	2.31	2.29	2.23
SI	0.87	0.90	0.96

The three different compositions are represented in composition triangle diagram (Figure 3.1) as Case 1, Case 2, and Case 3, their relative volatility and separation indices are shown in Table 3.1.

The feed and product specifications of the studied rigorous cases are given below:

Table 3.2: Feed and product specifications for Rigorous Case 1

Components	Feed stream		Product stream					
			Ethanol		n-Propanol		n-Butanol	
	kmol/h	Fraction	kmol/h	fraction	kmol/h	fraction	kmol/h	fraction
Ethanol (A)	135	0.45	134.87	0.99	0.14	0.005	0.00	0.00
n-propanol (B)	30	0.1	1.36	0.01	27.27	0.990	1.36	0.01
n-butanol (C)	135	0.45	0.00	0.00	0.14	0.005	134.87	0.99
Total	300	1.00	136.23	1.00	27.55	1.00	136.23	1.00

Table 3.3: Feed and product specifications for Rigorous Case 2

Components	Feed stream		Product stream					
			Ethanol		n-Propanol		n-Butanol	
	kmol/h	fraction	kmol/h	fraction	kmol/h	fraction	kmol/h	fraction
Ethanol (A)	100	0.333	99.50	0.99	0.49	0.005	0.00	0.00
n-propanol (B)	100	0.333	1.01	0.01	98.00	0.990	1.01	0.01
n-butanol (C)	100	0.333	0.00	0.00	0.49	0.005	99.50	0.99
Total	300	1.00	100.51	1.00	98.98	1.00	100.51	1.00

Table 3.4: Feed and product specifications for Rigorous Case 3

Components	Feed stream		Product stream					
			Ethanol		n-Propanol		n-Butanol	
	kmol/h	fraction	kmol/h	fraction	kmol/h	fraction	kmol/h	fraction
Ethanol (A)	30	0.10	28.79	0.99	1.21	0.005	0.00	0.00
n-propanol (B)	240	0.80	0.29	0.01	239.42	0.990	0.29	0.01
n-butanol (C)	30	0.10	0.00	0.00	1.21	0.005	28.79	0.99
Total	300	1.00	29.08	1.00	241.84	1.00	29.08	1.00

Hyprotech's HYSYS process simulator package is used for steady-state rigorous simulation in all studied cases. The objective function is total annual cost (TAC) minimization, which includes annual operating cost and annual capital cost. The utility prices for calculating the operating costs are given in Table 3.5.

Table 3.5: Utilities cost data

	High utility prices [(a)]		Low utility prices [(b)]	
Utility	Temperature (°C)	Price ($/ton)	Temperature (°C)	Price ($/ton)
LP-steam	160	17.7	160	6.62
MP-steam	184	21.8	184	7.31
Cooling water	30-45	0.0272	30-45	0.0067
Electricity	--------	0.1 $/kwh	---------	0.06 $/kwh
(a) Based on European prices (b) Based on U.S. prices				

3.4. Assumptions and techniques

The following simplified assumptions are made for the design, simulation, and optimization techniques of the distillation schemes:

a. NRTL thermodynamics property package and UNIQUAC are recommended by HYSYS user manual for predicting the properties of the non-ideal system like alcohol system, and the system parameters are given in Appendix A.

b. The feed to the first column in the sequence is saturated liquid at atmospheric pressure, the feed to the second column in the same sequence is saturated liquid at the pressure of the first column, and product streams are saturated liquid at the same column pressure.

c. The product rates are calculated by material balance, and the impurities of middle component product stream are symmetrically distributed.

d. The column diameters are selected so that the vapor velocity is between 65 and 70 % of the flooding velocity.

e. The effect of pressure drop across distillation columns and heat exchangers is considered to be negligible for such system.

f. Distillation column of plate type with valve tray column internals (Glitch type) and total condenser and reboiler are used.

g. The lower pressure column is kept at atmospheric pressure in order to use cooling water in the condenser.

h. Shell and tube heat exchangers are selected and the pressure of both columns is regulated to meet exchange minimum approach temperature (EMAT) = 8.5 ºC.

i. Cost of pipes, flash tanks, and pumping are ignored in this study. Moreover, variation for different schemes is small.

j. Plant lifetime is assumed, 10 years and operating hours are 8000 hr/year.

3.5. Optimization procedure

All studied schemes are simulated rigorously by HYSYS process simulator version 1.1 and the results of simulation are collected in HYSYS spreadsheet and then exported to Microsoft Excel where the final cost calculations for optimization is executed.

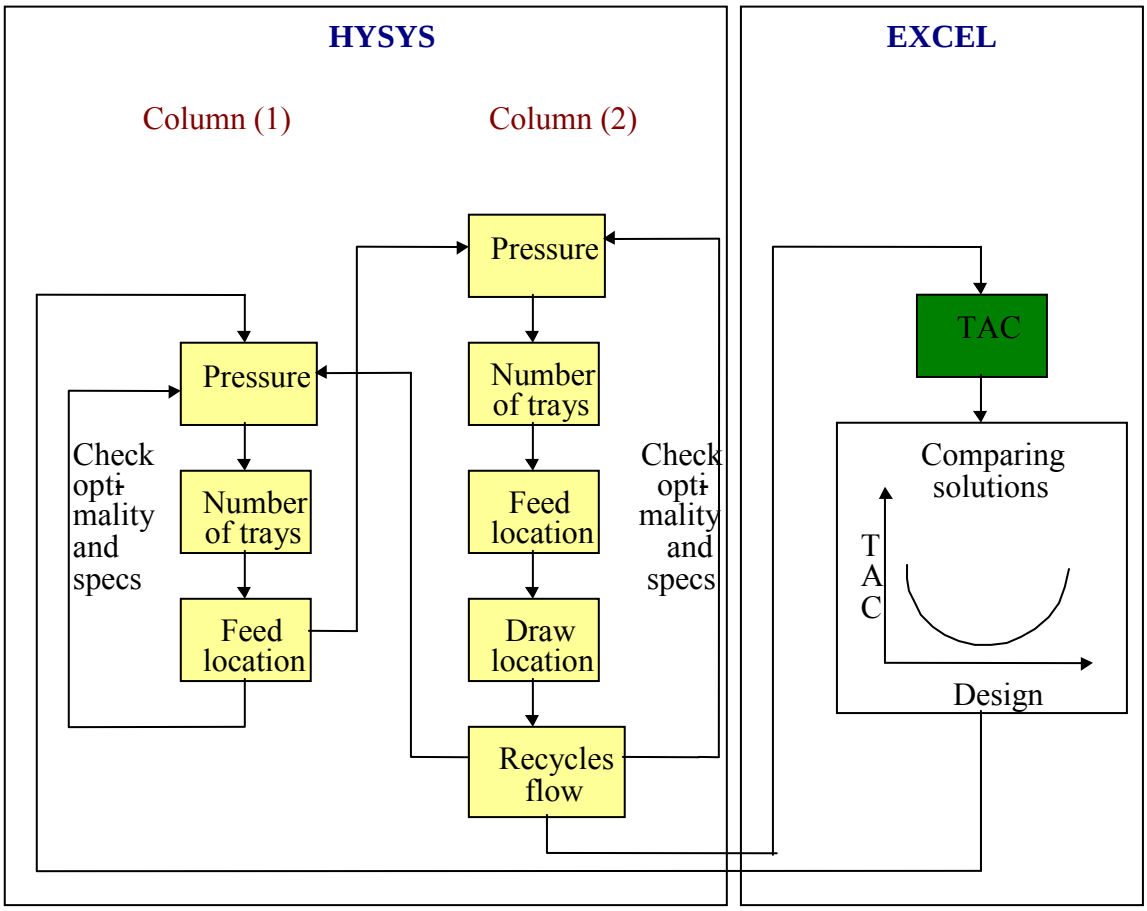

Figure 3.2: Simplified representation of the optimizing procedure

The optimization methodology applied in this study based on hand calculations by exploration of the objective function interactively over the domain in the following steps:

- Start from a visible solution,
- Change one of the manipulated variables and keep the others constant,

- Check the objective function and stop when it reaches the minimum,
- Keep the previous manipulated variable constant at the minimum objective function and tray another manipulated variable,
- Similarly until the objective function does not improve by changing any of the manipulated variables, at that point the optimization of the flowsheet reaches the global optimum.

Detailed column and heat exchanger costs are calculated using the default column and heat exchanger sizing of HYSYS simulator after each rigorous simulation run.

The capital costs executed in the Microsoft Excel spreadsheet based on the cost correlations of Douglas (1988), while Marshal and Swift indices have been used to update costs. The detailed descriptions of cost calculations are given in Appendix B. A simplified representation of the optimization procedure is shown in Figure 3.2. For each column system, the pressure, number of trays and feed location are considered as the optimization variables and they are manipulated until the optimal design is found. Optimization variables can be more in case of additional feeds, draws or recycle streams are present. In every simulation run design parameters (optimization variables) are changed, specifications and optimality are checked. The process simulations are stopped when the global optimal system design is achieved.

3.5.1. Optimization of conventional distillation schemes

The conventional distillation sequences (direct and indirect sequences) are optimized first, in order to provide a base case for the comparison of TAC savings for different energy-integrated schemes; the cheaper conventional scheme is selected as the base case. Also for comparison reasons, the feed entering the first column in the sequence is set to be saturated liquid at atmospheric pressure. The same also accounts for the final product streams. The feed to the second column is saturated liquid with a pressure equal to that of the first column.

For the direct sequence (D) and the indirect sequence (I), the following design parameters for each column are selected as optimization variables to obtain the specified purities:

i. Column pressure
ii. Feed location
iii. Number of stages

The feed properties such as composition, vapor fraction, pressure and flow rate have to be specified in HYSYS simulator environment, then the column pressure, the number of stages and feed location are specified as optimization variables. Two degrees of freedom are left for each column of the conventional sequences. These are used to maintain the convergence of the column by specifying the desired product purity and flow rate of one of the product streams.

According to Tedder and Rudd (1978), operating costs are high at low pressure, because refrigerants have to be used instead of cooling water. However, the total cost drops as the pressure increases, roughly up to the point where cooling water can be used. Furthermore, the total cost will rise again when the pressure is additionally increased, because the difference in relative volatilities between the components of the mixture decreases, making the separation more difficult. Therefore, the column pressures are set to meet heat exchange minimum approach (EMAT), equal to 8.5 °C, and for condensers operated with cooling water. The cooling water is assumed to enter at 30 °C and leave at 45 °C, which is the maximum allowed for cooling towers.

The initial starting point for all the optimization carried out when a feasible solution is found. For a certain number of trays the reflux ratio is evaluated by the HYSYS. The feed location to each column is adjusted by changing the location up and down until the lowest value of the reflux ratio is found needed to achieve the specified product purities. For each column sequence run the necessary data shown in Table 3.6 are exported to Excel and the final cost calculations are executed, giving the total annual costs.

Table 3.6: Data exported from HYSYS to Excel for each column

Description	Symbol	Unit
Theoretical numbers of trays	$N_{theoretical}$	
Column diameter	D	m
Heat duty, condenser	Q_{cond}	kJ/h
Heat duty, reboiler	Q_{reb}	kJ/h
Temperature of vapor to condenser	T_{cond}	°C
Temperature of reflux	T_{ref}	°C
Temperature of liquid to reboiler	T_{reb}	°C
Temperature of boil-up stream	T_{boil}	°C
Vapor flow rate to condenser	V_{cond}	kg mol/h
Reflux rate	L_{ref}	kg mol/h
Boil-up rate	V_{boil}	kg mol/h
Liquid flow rate to reboiler	L_{reb}	kg mol/h
Design pressure	P	kPa
Average viscosity of column liquid flow	μ	cP
Average relative volatility of key components	α	

The column diameter is calculated by HYSYS using the default settings of the tray sizing utility. Valve trays are chosen, the number of flow paths on each tray is set equal to one and maximum internal flows are at 65-70 % of the flooding.

The optimal column specifications are those that gave the minimum TAC. Since there is no recycled material or energy stream between the columns, the optimization is performed independently for each column. Hence, the optimal design is the combination of the two optimized column results and it will represent the global optimum.

3.5.2. Optimization of conventional heat-integrated schemes

The optimization procedure for heat-integrated schemes applied the same techniques and assumptions than those in conventional distillation schemes with the following modifications:

(a) Raise and adjust the operating pressure in the first or second column to keep EMAT at 8.5 °C.
(b) Keep the lower pressure column at atmospheric pressure.
(c) Due to energy recycling between columns the optimization variables (theoretical trays in columns 1 and 2) are interdependent.

To simulate and optimize the conventional heat-integrated schemes by HYSYS, a representative conventional scheme is first evaluated. This is done to get an initial estimate of the optimal heat integrated scheme. The following optimization variables are selected for the conventional heat-integrated schemes:

- Number of theoretical stages of column (1)
- Feed location of column (1)
- Number of theoretical stages of column (2)
- Feed location of column (2)

In case of forward heat integration, the temperature of the stream to the condenser of the first column is adjusted by increasing the column pressure, until it is 8.5 °C (EMAT) warmer than the steam to the reboiler of the second column.

Set the operating pressure for both columns and run it as conventional distillation with the desired purity in PFD_1 of HYSYS. Build another PFD_2 with the same configuration where heat integration is taking place by removal of reboiler and condenser and replaced by main heat exchanger. PFD_2 will converge by importing reflux stream and boil-up stream data from PFD_1. Manipulate the number of theoretical stages in column (1) and keep column (2) stages constant until minimum cost is achieved, then fix column (1) optimum stages and start to manipulate column

(2) stages till we get minimum total annual cost, which will represent the global optimum. Table 3.7 shows optimization results of direct sequence with backward heat integration (DQB) scheme for rigorous Case 2, which represent equimolar feed composition.

Table 3.7: Optimization results of **DQB** scheme for feed composition (0.333/0.333/0.333), using European utility prices (all costs in $/yr.)

Theoretical stages of column 1	Theoretical stages of column 2		
	30	31	32
45	1104694.0	1096472.5	1096320.9
46	1105509.4	1096247.5	1096447.6
47	1106324.7	**1096022.5**	1096574.3
48	1107140.0	1096143.8	1096649.8

3.5.3. Optimization of Petlyuk column

For the Petlyuk system, the prefractionator and the main column are not independent of each other since there are recycled streams between them. Therefore, the optimization is carried out dependently on both columns. The design parameters of the Petlyuk column are the followings:

i. The common pressure of the system
ii. Feed location of the prefractionator
iii. Number of trays in the prefractionator
iv. Feed locations of the main column
v. Draw location of the middle component (sidestream location)
vi. The amount of liquid from the main column to the prefractionator
vii. The amount of vapor from the main column to the prefractionator

Unlike the conventional and heat integrated sequences, which are built in the PFD in HYSYS, the Petlyuk column is built in the column environment subflowsheet. This is done for the reason of faster convergence. A column section without reboiler or

condenser as a prefractionator is added to the main column and connected through recycle streams.

The internal recycle streams (feed locations) L_{12} and V_{21} are located on the same tray. The same accounts for L_{21} and V_{12}. (Figure 4.2) This is obvious since the feed streams from the prefractionator are located at the trays in the main column with the closest corresponding composition.

After specifying the feed to the prefractionator, the common pressure, feed locations, and number of trays of the columns, five degrees of freedom are left. These are used to control two product stream rates, two purity specifications and one internal recycle stream. The optimization variables are:

- Prefractionator theoretical trays
- Main column theoretical trays
- Prefractionator reflux rate or boil up rate

Feed locations and main column draw rate location are adjusted to achieve minimum reflux ratio in the main column. Usually Petlyuk column is optimized by estimating the theoretical stages of the prefractionator and main column, evaluating the internal streams rates by using theoretical fractional recovery of the middle component β^* in terms of relative volatility as initial estimate. Run the system to get the desired purity and products rates in a feasible solution. The optimization variables (prefractionator stages, main column stages, and internal streams) are changed one by one and interchangeable until global optimum solution is achieved.

3.5.4. Optimization of sloppy heat-integrated schemes

These schemes are the combination of the Petlyuk column and conventional heat-integrated schemes where the heat is recycled and integrated between the two

columns (prefractionator and main column) by changing the pressure so both columns are interdependent during optimization. The optimization variables are:

- Prefractionator theoretical trays
- Main column theoretical trays
- Distillate or bottom product rate of the prefractionator

Two PFD has to be build in HYSYS, one for the scheme with out heat integration and the other for the heat integrated scheme and the initial values for reflux and boil up stream are imported from the scheme without heat integration to be able to converge the integrated scheme. As initial estimate, the distillate or product rate of the prefractionator is calculated from the theoretical fractional recovery of the middle component β^* in terms of relative volatility.

3.6. Optimal fractional recovery of the middle component

This parameter is taking into account in some schemes (Petlyuk column **SP**, **SQF**, and **SQB**) schemes as a design parameter and it is represented by β and its equal to the amount of middle component in the overhead of the prefractionator over the amount of middle component in the feed. The optimal value of the fractional recovery of the middle component (β_o) is calculated for the investigated optimal schemes and it is compared to the theoretical fractional recovery of the middle component (β^*) which is based on the relative volatility as follows for saturated liquid feed:

$$\beta^* = \frac{\alpha_B - \alpha_C}{\alpha_A - \alpha_C}, \qquad [3\text{-}1]$$

As sown in Table 3.8, it is found that the results of β^* and β_o is almost identical in case of Petlyuk column and **SQB** scheme where the prefractionator is at atmospheric pressure.

Table 3.8: Comparison of theoretical and optimal fractional recovery of the middle component

Schemes	Case 1, (0.45/0.10/0.45)		Case 2, (0.333/0.333/0.333)		Case 3, (0.10/0.80/0.10)	
	β^*	β_o	β^*	β_o	β^*	β_o
Petlyuk column (**SP**)	0.36	0.35	0.35	0.37	0.33	0.33
TAC ($/yr)	1.03E+06	1.03E+06	1.28E+06	1.28E+06	1.61E+06	1.61E+06
SQF scheme	0.39	0.32	0.37	0.33	0.35	0.35
TAC ($/yr)	1.27E+06	1.24E+06	1.24E+06	1.18E+06	1.14E+06	1.14E+06
SQB scheme	0.36	0.35	0.35	0.35	0.33	0.33
TAC ($/yr)	1.28E+06	1.28E+06	1.19E+06	1.19E+06	1.09E+06	1.09E+06

Consequently theoretical fractional recovery β^* can be used as initial design parameter for Petlyuk column (**SP**) to determine the optimum solution of the recycle streams and theses results are in agreement with the previous study of Annakou and Mizsey (1996). This design parameter is found to be valid for sloppy separation sequences (**SQF** and **SQB** schemes). In case of **SQF** scheme, due to the high pressure of the prefractionator a slight deviation is found in the optimal fractional recovery β_o from the theoretical values β^* especially in Case 1 and Case 2. In general TAC is not affected and the overall ranking of the schemes still the same. These results indicate that using of β^* as initial estimate is recommended in order to save effort and time on calculations.

3.7. Results of conventional distillation schemes

These schemes are the conventional non-integrated schemes and considered as the base case for the energy-integrated schemes. From the optimization result (Tables 3.9, 3.10, and 3.11), its clear that the TAC of the schemes increases as the concentration of the middle component increases. In case of indirect sequence a significant saving in energy costs can be obtained by using partial condenser in upstream columns for indirect sequences.

Table 3.9: Optimization results of direct scheme

	Direct scheme (**D**)		
	Case (1)	Case (2)	Case (3)
Heat load (J/hr)	19.75E+09	24.05E+09	30.04E+09
Capital cost ($/yr.)	1.22E+05	1.42E+05	1.65E+05
Operating cost ($/yr.)	1.41E+06	1.72E+06	2.15E+06
TAC ($/yr.)	1.53E+06	1.86E+06	2.31E+06

Table 3.10: Optimization results of indirect scheme, **BC** in liquid phase

	Indirect scheme (**I**)		
	Case (1)	Case (2)	Case (3)
Heat load (J/hr)	23.22E+09	27.01E+09	30.90E+09
Capital cost ($/yr.)	1.37E+05	1.53E+05	1.68E+05
Operating cost ($/yr.)	1.66E+06	1.93E+06	2.21E+06
TAC ($/yr.)	1.79E+06	2.08E+06	2.38E+06

Table 3.11: Optimization results of indirect scheme, **BC** in vapor phase

	Indirect scheme (**I**)		
	Case (1)	Case (2)	Case (3)
Heat load (J/hr)	18.10E+09	22.91E+09	29.24E+09
Capital cost ($/yr.)	1.33E+05	1.54E+05	1.82E+05
Operating cost ($/yr.)	1.29E+06	1.64E+06	2.09E+06
TAC ($/yr.)	1.42E+06	1.79E+06	2.27E+06

The use of a partial condensed not only avoids using a utility, but also reduces the condenser duty of the upstream column and the reboiler duty of the second column. Reduction in TAC can be achieved if the **BC** stream is fed to the second column as vapor phase, this result is due to the reduction in both condensing duty of the first column and the reboiler duty of the second column.

3.8. Results of the energy-integrated schemes

Two radically different cost structures are taken into account in the conventional and energy-integrated schemes. One of them is a high utility price structure corresponding to prices in Europe; the other one is a low utility price structure that corresponds to prices in the U.S. The effect of the high and low utility costs is demonstrated in Case 1 and Case 2; therefore, Case 3 is studied with the European cost structure only. Valve trays (of Glitsch type) are considered as column internal.

3.8.1. Results of Case 1 are collected in Table C.1 and Table C.2 (Appendix C). Here the feed is situated near the **AC** edge. The presence of component **B** in the feed is just 10 %; the presence of components **A** and **C** are equimolar to each other. The two tables correspond to the two subcases of U.S. and European utility prices.

The winners and their rate of winning are collected in Table 3.12. **SP** wins, in total annual cost savings compared to the base case **D**, with 4 % and 3 % above **DQB**, and with 7 % and 6 % above **IQF**. The Petlyuk column is better than the others in both of its lower operating and capital costs.

Table 3.12: Winning schemes in Case 1 (10 % middle component)

No.	U.S. prices		European prices	
	scheme	TAC savings %	scheme	TAC savings %
1	**SP**	28	**SP**	33
2	**DQB**	24	**DQB**	30
3	**IQF**	21	**IQF**	27
4	**SQF**	21	**IQB**	27

According to the short-cut analysis, at this feed composition the Petlyuk column (**SP**) ought to win over one of the integrated schemes with approximately 40 %. According to Tables C.1 and C.2, however, in case of the lower utility costs (U.S. price structure) the handicap of **DQB** behind **SP** is just 5.7 % in TAC, 8 % in capital costs, and 4.8 % in operating costs. In case of the higher utility costs (European price structure), the handicap of **DQB** behind **SP** is again no more than 4.9 % in TAC, 7.8 % in capital costs, and 4.8 % in operating costs.

3.8.2. Results of Case 2 are collected in Table C.3 and Table C.4 (Appendix C). Here the feed is equimolar in the components. The winners and their rate of winning are collected in Table 3.13. According to the short-cut analysis, at this feed composition the Petlyuk scheme (**SP**) ought to win over one of the integrated schemes with approximately 20 %. On the contrary, **SP** does not win in any of the two rigorous subcases. These cases are investigated also with sieve trays, and got the same qualitative results (not listed here).

Table 3.13: Winning schemes in Case 2 (equimolar feed)

No.	U.S. prices		European prices	
	scheme	TAC savings %	scheme	TAC savings %
1	**SQF**	36	**DQB**	41
2	**SQB**	36	**SQF**	36
3	**DQB**	35	**SQB**	36
4	**SP**	28	**SP**	31

Instead of **SP**, the integrated sloppy schemes **SQF** and **SQB** win in the case of U.S. utility prices. However, they are just 1 % better above **DQB**, in TAC savings compared to the base case **D**. According to Tables C.3-C.4, in case of the lower utility costs (U.S. price structure) the handicap of **DQB** behind **SQF** and **SQB** is just 1.8 % and 0.8 % in TAC, 4.2% and 3.5 % in capital costs, and 0.9 % and -0.6% in operating costs. (In the latest figure, **DQB** is better in operating costs over **SQB**).

In case of the higher utility costs (European price structure) the schemes change place. Here **DQB** wins over the sloppy schemes. The handicap of **SQF** and **SQB** behind **DQB** is 7.3 % and 8.2 % in TAC, and 9.3 % and 11.5 % in operating costs, while they have better capital cost figures with 3.4 % and 4.8 %. The Petlyuk system (**SP**) is not in the first three places in this feed composition (Case 2); and it is just at the 4th place, with great handicap, in both of utility price structures.

3.8.3. Results of Case 3 are collected in Table C.5 (Appendix C). Here the feed is situated near the **B** node. The presence of component **B** in the feed is 80 %; the presence of components **A** and **C** are equimolar to each other. Just the subcase of the European utility prices is shown. As the ratio of component **B** increases in the feed, the energy demand of the separation increases, and the energy costs become dominating.

Table 3.14: Winning schemes in Case 3 (80 % middle component)

No.	European prices	
	scheme	TAC savings %
1	**SQB**	53
2	**SQF**	51
3	**DQB**	32
4	**SP**	30

The schemes **DQF**, **IQF**, and **IQB** are proved inferior to the others, as the energy costs are dominant; therefore, they are omitted. The conventional indirect scheme (**I)** is however included for comparison. The winners and their rate of winning are collected in Table 3.14.

In accordance with the results of the short-cut analysis, this is the place where the integrated sloppy schemes (**SQB** and **SQF**) win. The Petlyuk column (**SP**) is again at the 4th place behind the 3rd rank **DQB**. The handicap of the **DQB** scheme behind **SQB** and **SQF** is 44 % and 38 % in TAC, 4.1 % and 11.4 % in capital costs, and 52 % and 43 % in operating costs.

3.9. Sensitivity of the TAC savings

In this economic study the schemes are classified according to the ranking in TAC savings. The effect of different cost parameters on the TAC savings are investigated:

(a) **Utility prices**: The results of using different utility prices are presented in Table 3.12-3.13 and it shows that TAC savings is affected by using low and high utility prices and the ranking of the winning schemes are changing (e.g. Case 2) and these results prove that the TAC savings is sensitive to the utility prices.

(b) **Project life**: The change in the project life does not influence the TAC savings and the ranking of the schemes are the same (Tables 3.15-3.17).

(c) **Marshal and swift index**: The effect of changing M&S index is negligible in all the cases (Tables 3.15-3.16).

Table 3.15: TAC savings (%) for 10 years project life, Europe utility prices and (M & S index = 1056.8)

	D	**DQF**	**IQF**	**DQB**	**IQB**	**SP**	**SQF**	**SQB**
Case 1	0	1	27	30	27	33	19	17
Case 2	0	19	26	41	23	31	36	36

Table 3.16: TAC savings (%) for 10 years project life, Europe utility prices and (M & S index = 1093.9)

	D	**DQF**	**IQF**	**DQB**	**IQB**	**SP**	**SQF**	**SQB**
Case 1	0	1	27	29	26	33	19	16
Case 2	0	19	27	41	23	32	37	36

Table 3.17: TAC savings (%) for 5 years project life, Europe utility prices and (M & S index = 1056.8)

	D	**DQF**	**IQF**	**DQB**	**IQB**	**SP**	**SQF**	**SQB**
Case 1	0	1	23	26	23	30	17	14
Case 2	0	17	23	37	19	29	33	33

3.10. Conclusions of the economic study

A general rule governing the ranks of the studied schemes according to total annual costs (TAC) is the increasing heat duty requirement with increasing concentration of component B in the feed. The schemes with energy integration are sensitive for the heat duty while the Petlyuk column without energy integration (but thermal coupling) is not. The savings in TAC of Petlyuk columns are uniformly about 30 % to 33 % in all the three cases. A comparison between the optimized schemes is shown in Figure 3.3 for the European utility prices.

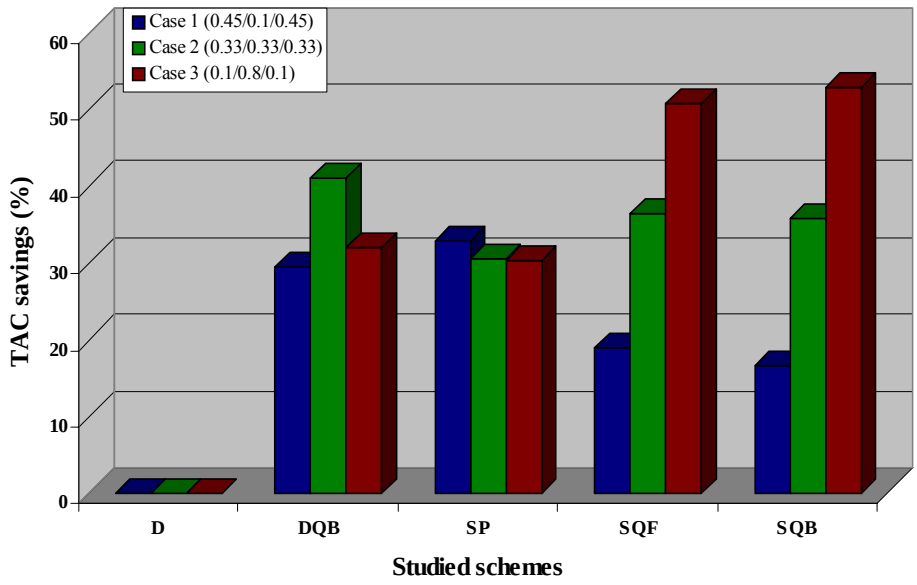

Figure 3.3: Comparison of TAC savings in optimized schemes for European utility prices

CASE 1: Here the Petlyuk column (**SP**) is the winner with 28 and 33 % savings in U.S. utility price and European utility price respectively. There is no qualitative ranking difference considering the two price structures. The second ranked direct sequence with backward heat integration (**DQB**) with 24 and 30 % savings that cannot be more because of low heat duty. It is back just with 3%. The forward heat integrated sloppy scheme (**SQF**, 21 % savings) is just the 4th ranked in case of U.S. utility prices, probably because there is an **AB→C** energy integration that involves a pressure shift and use of high pressure steam.

CASE 2, U.S. utility prices: Here the Petlyuk column is not amongst the best schemes. Direct sequence with backward heat integration (**DQB**) with 35% savings is at the 3rd place backed just with 1 % by both forward heat integrated sloppy scheme (**SQF**) and backward heat integrated sloppy scheme (**SQB**) by their 36% savings.

CASE 2, European utility prices: Here the direct sequence with backward integration (**DQB**) is the winner with 41% savings. Both the 2nd ranked forward integrated sloppy schemes (**SQF**, 36% savings) and the 3rd ranked backward integrated sloppy scheme (**SQB**, 30% savings) involve unpreferable integration **AB→C** or the even wider boiling point gap **A→C** comparing to the **B→BC** integration in the winner scheme.

CASE 3: This is the case where the heat integrated sloppy schemes, namely the 1st ranked backward heat integrated sloppy scheme (**SQB**, 53 % savings) and the 2nd ranked forward integrated sloppy scheme (**SQF**, 51 % savings) come to play since the heat duty is really high. The Petlyuk column (**SP**) with its 30 % savings is just 4th behind the 3rd ranked direct sequence with backward integration (**DQB**, 32 % savings).

Comparing the optimization results of rigorous simulations to the corollaries of the short-cut analysis, the domain where the thermally coupled system wins is even much lower, and is constrained to a small area near the **AC** edge of the composition triangle

at balanced relative volatility ratio. At balanced relative volatility ratio and equimolar feed composition, as well as near the node of pure **B**, the Petlyuk column takes only the fourth place behind the heat-integrated schemes at European and U.S. price structures (Case 2 and Case 3). Yet, the Petlyuk column wins over the heat-integrated schemes at 10 % middle component in the feed. Its advantage, in total annual costs, over the second best (heat-integrated) scheme is no more than 5-6 %.

Considering all the energy, cost, operability and flexibility viewpoints, the advantageous application of the thermally coupled systems, if it exists indeed, is constrained to a very small range of relative volatility ratio, feed composition, and price structure. This small range is situated somewhere around balanced relative volatility ratio **A/B** to **B/C**, small amount of the middle component **B** (e.g. Case 1), balanced presence of the two swing components **A** and **C** in the feed or a little bit shifted to the direction of **C**.

On the other hand, the integrated sloppy schemes win, in a great TAC percent, at high **B** ratio in the feed, while the conventional heat integrated schemes, **DQB** in our particular case, is the best choice at equimolar feed.

In this economic study the optimized schemes are classified according to the ranking in TAC savings. Since the difference in TAC savings between the optimized schemes is a few percentages, a further aspect will be taken into consideration. Controllability features become critical in these cases and Chapter 4 will focus on the controllability aspects.

Chapter 4: Controllability study of energy-integrated schemes

The rigorous economic study is supported in this work by controllability studies in order to combine economic and controllability evaluations so that the final selection will be based on both studies. According to the economic results, the best conventional heat integrated scheme, Petlyuk column, and sloppy separation sequence with forward and backward heat integration have to be investigated for further controllability study.

4.1. Steady-state control indices

Degrees of freedom analysis and steady-state multivariable control structure synthesis tools show that all the schemes can be controlled by conventional decentralized control structures. However, in the case of conventional heat integrated scheme heuristics and also the steady state control indices show that the interaction among the control loops is less than in the case of Petlyuk column and sloppy separation with forward and backward heat integration.

This part of the work deals with the evaluation of optimum schemes based on the combination of the economic and controllability results of the investigated schemes for the separation of ternary mixture.

4.1.1. Studied schemes

Four energy-integrated schemes are investigated for steady state control indices and these schemes are selected based on the results of economic study as follows: direct sequence with backward heat integration (**DQB**), Petlyuk column (**SP**), sloppy separation sequence with forward and backward heat integration (**SQF**) and (**SQB**).

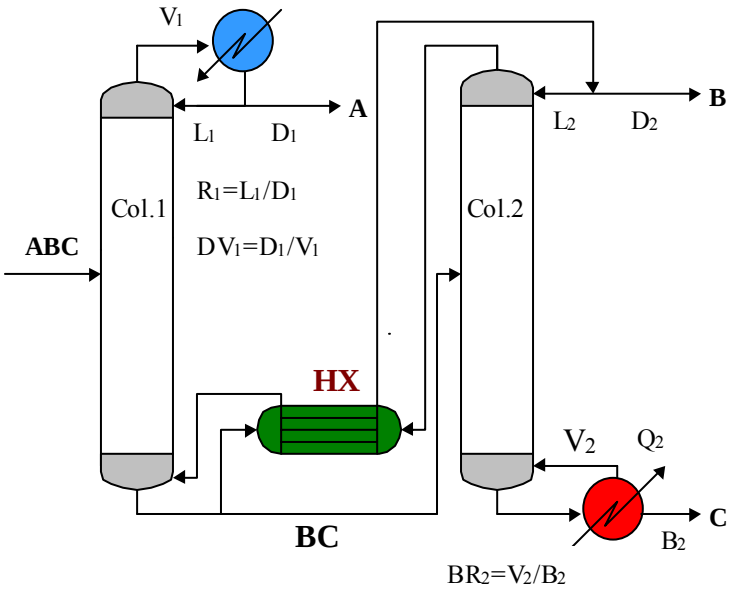

Figure 4.1: Direct sequence with backward heat integration (**DQB**) indicating its manipulated variables

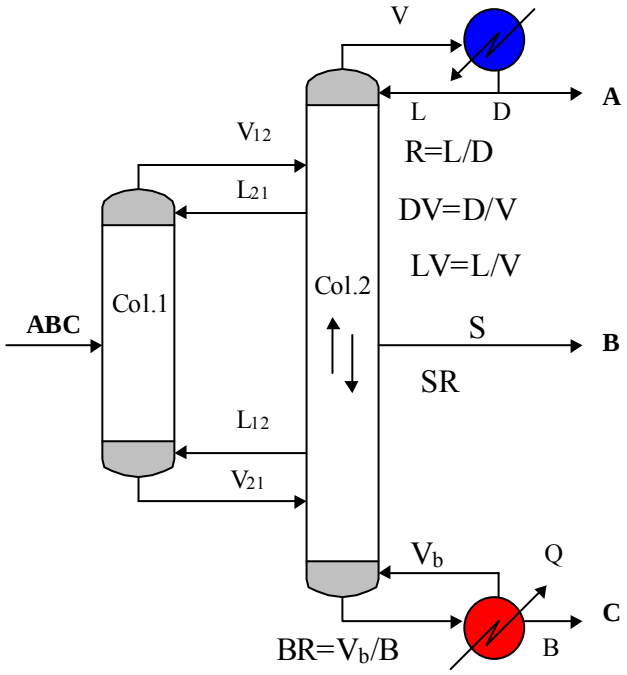

Figure 4.2: Petlyuk column (**SP**) indicating its manipulated variables

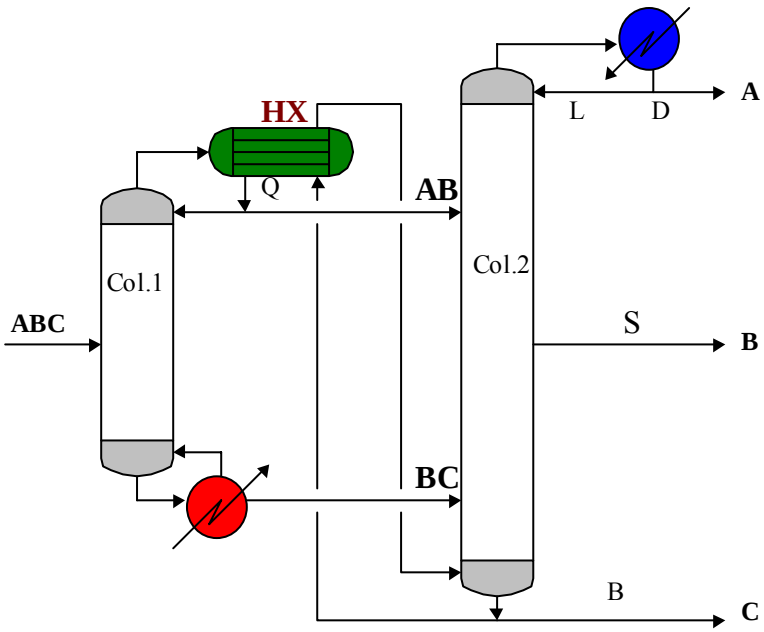

Figure 4.3: Sloppy sequence with forward heat integration (**SQF**) indicating its manipulated variables

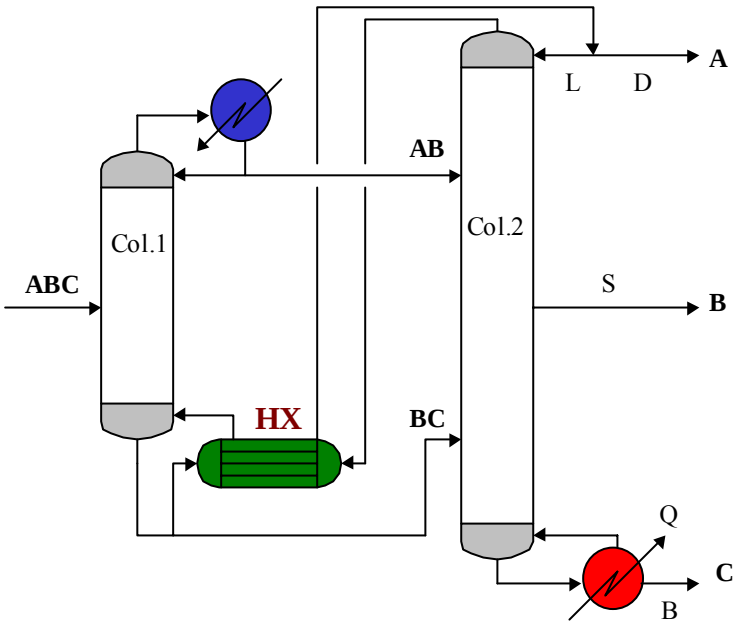

Figure 4.4: Sloppy sequence with backward heat integration (**SQB**) indicating its manipulated variable

The controllability study is based on the degree of freedom analysis tools for both energy-integrated schemes. First, the controlled and manipulated variables are selected on the basis of engineering judgment and secondly, the possible pairing of these controlled and manipulated variables for composition control loops are analyzed. Three feed compositions are selected for the steady state control indices analysis of (ethanol/n-propanol/n-butanol) ternary mixture as follows:

a) Feed composition 1: (0.45/0.1/0.45) feed composition and 99 % product purity, which is the only point where Petlyuk column is competitive with the other energy integrated schemes from the economic point of view.

b) Feed composition 2: (0.333/0.333/0.333) feed composition and 99 % product purity, where the conventional heat integrated scheme is the best in TAC saving.

c) Feed composition 3: (0.1/0.8/0.1) feed composition and 99 % product purity, where the sloppy separations with forward and backward heat integration are the winners in TAC savings.

The controlled variables of all the studied schemes are the composition of the product streams, which is denoted as $\mathbf{X_A}$, $\mathbf{X_B}$, and $\mathbf{X_C}$. The possible manipulated variables for the conventional heat integrated schemes are: L_1, D_1, R_1, DV_1, LV_1, D_2, L_2, R_2, B_2, Q_2, BR_2 (Figure 4.1), and for Petlyuk column and sloppy separation sequence with forward and backward heat integration are: L, D, R, S, B, Q, DV, LV, BR (Figures 4.2, 4.3, and 4.4).

Three of the manipulated variables are selected as control structure of the investigated scheme based on the degree of freedom analysis. The steady state control indices are calculated by increasing one of the manipulated variables (m1-m2-m3) by 1 % and keeping the other two constants.

4.1.2. Results of steady-state control indices for feed composition 1

The analysis of the investigated possible control structures of direct sequence with backward heat integration (**DQB)** scheme shows that structures like (D_1-L_2-Q_2), (D_1-R_2-Q_2), (D_1-L_2-BR_2), (L_1-L_2-Q_2), (L_1-R_2-Q_2), (R_1-L_2-Q_2), (R_1-R_2-Q_2), and (R_1-R_2-B_2) are showing negative RGA, and higher values of RGA which indicates strong interactions between control loop so that they are excluded from further dynamic investigations.

The remaining control structures with relativity high MRI, low CN, and λ_{ij} values close to unity are considered as promising candidates for further dynamic investigations (Table 4.1a). (D_1-L_2-B_2), (D_1-R_2-B_2), (DV_1-D_2-B_2), and (L_1-D_2-Q_2) are recommended for further dynamic simulations due to their control indices values which is showing higher MRI index, Lower CN, and the most diagonal elements (λ_{ij}) are close to unity.

Table 4.1a: Steady state control indices for **DQB** scheme, feed composition 1

m1-m2-m3	NI	MRI	CN	λ_{11}	λ_{22}	λ_{33}
D_1-L_2-B_2	1.089	0.123	9.312	1.000	0.919	0.919
D_1-D_2-Q_2	1.672	0.058	55.907	1.000	0.598	0.598
D_1-R_2-B_2	1.063	0.114	10.332	1.000	0.941	0.941
DV_1-L_2-B_2	1.090	0.033	31.601	1.000	0.917	0.917
DV_1-D_2-B_2	1.212	0.117	40.982	0.816	0.825	1.009
L_1-D_2-Q_2	1.656	0.040	16.585	1.000	0.604	0.604
L_1-D_2-B_2	1.340	0.058	68.953	0.738	0.739	1.002
L_1-L_2-B_2	1.088	0.027	36.506	1.000	0.919	0.919
L_1-R_2-B_2	1.063	0.027	36.275	1.000	0.940	0.940
L_1-D_2-BR_2	1.456	0.041	17.871	1.000	0.687	0.687
LV_1-D_2-B_2	1.155	0.080	55.241	0.812	0.863	1.049
R_1-L_2-B_2	1.092	0.027	37.190	1.000	0.916	0.916
R_1-D_2-Q_2	1.702	0.039	16.105	1.000	0.587	0.587
R_1-D_2-B_2	1.245	0.053	83.954	0.813	0.797	0.972
R_1-D_2-BR_2	1.474	0.040	18.030	1.000	0.678	0.678

The analysis of the alternative composition control structures investigated with the corresponding steady state control indices for Petlyuk column (**SP)**, sloppy heat-integrated schemes **SQF**, and **SQB** (Tables 4.2a, 4.3a, and 4.4a) show that, the control structures (DV-S-Q), (L-S-Q), (LV-S-Q), (L-S-BR), (L-SR-Q), (R-S-Q), and (R-S-BR) are excluded from further dynamic investigations due to their negative RGA values, which indicate serious interactions between control loops.

Table 4.2a: Steady state control indices for Petlyuk column (**SP**), feed composition 1

m1-m2-m3	NI	MRI	CN	λ_{11}	λ_{22}	λ_{33}
D-S-Q	2.244	0.064	60.428	1.158	0.519	0.453
D-S-BR	1.411	0.046	100.862	1.255	0.733	0.657
DV-S-B	1.422	0.097	44.058	0.644	0.863	1.185
L-S-B	1.885	0.033	127.130	0.506	0.648	1.273
R-S-B	1.509	0.027	163.117	0.601	0.752	1.346
S-L-B	1.349	0.033	127.308	0.387	0.730	1.273

(S-L-B) is excluded also due to heuristic dynamic consideration (Papastathopoulou and Luyben, 1991). (D-S-Q), (DV-S-B) and (L-S-B) are good candidates for further dynamic simulation investigations although their control indices are poor comparing to **DQB** scheme.

Table 4.3a: Steady state control indices for **SQF** scheme, feed composition 1

m1-m2-m3	NI	MRI	CN	λ_{11}	λ_{22}	λ_{33}
D-S-Q	15.324	0.003	1334.400	1.663	0.082	0.063
D-S-BR	24.189	0.003	1368.600	1.500	0.054	0.038
DV-S-B	8.376	0.005	829.509	0.119	1.248	1.368
L-S-B	3.274	0.001	5370.000	0.294	0.450	3.804
R-S-B	6.129	0.002	2114.000	0.156	0.187	1.480
S-L-B	0.284	0.001	5404.700	0.561	3.510	3.825

Table 4.4a: Steady state control indices for **SQB** scheme, feed composition 1

m1-m2-m3	NI	MRI	CN	λ_{11}	λ_{22}	λ_{33}
D-S-Q	474.657	0.049	32.610	1.210	0.012	0.002
D-S-BR	98.351	0.052	30.821	1.213	0.045	0.008
DV-S-B	1.183	0.032	151.997	0.856	0.844	0.985
L-S-B	1.224	0.009	518.692	0.813	0.820	1.011
R-S-B	1.167	0.010	495.208	0.850	0.859	1.012
S-L-B	4.893	0.009	537.742	0.180	0.204	1.022

4.1.3. Conclusion of feed composition 1

Steady state control indices of **DQB** scheme are much better than **SP**, **SQF**, and **SQB** schemes, this is due to structure of these schemes where all the controlled products are drawing from the same column and the flow rates of the top and bottom products are high comparing to the side product, consequently the interactions between control loops are expected to be higher in the case of sloppy separation schemes comparing to **DQB** scheme. The control structures candidates for **DQB** scheme is more than that of **SP**, **SQF**, and **SQB** and theses results shows that **DQB** scheme is more flexible and had less control loops interactions. According to the steady state control analysis tools, avoid the use of reboiler duty as manipulated variable in all the cases except when it is combined with distillate rate as control variable for the top product stream. The best candidates for **DQB** scheme is the control structure that contains D_1 and B_2 as manipulated variables and these streams posses the highest streams rates in the set.

4.1.4. Results of steady-state control indices for feed composition 2

This is known as feed composition 2 where the feed composition is equimolar. The same strategy of feed composition 1, which means all control structures with negative NI or Negative RGA's are excluded, control structures with low RGA's indicates strong interactions between control loops are also eliminated.

The result of steady state control indices for **DQB** scheme is shown in Table 4.1b. The same control structures, which is excluded in feed composition 1 is also in feed composition 2 except (R_1-R_2-B_2) control structure that is showing positive result.

The (D_1-L_2-B_2), (D_1-R_2-B_2), (L_1-D_2-Q_2), (DV_1-D_2-B_2), and (L_1-D_2-B_2) control structures are recommended for further dynamic investigations due to their control indices values which is showing higher MRI index, Lower CN, and the most diagonal elements (λ_{ij}) are close to unity. (DV_1-D_2-B_2) and (L_1-D_2-B_2) are showing the best control indices values, but it has no industrial applications due to difficult in controlling two products compositions by the same flow rate stream in the same column and violations in material balance will take place. This will be investigated by dynamic simulation later.

Table 4.1b: Steady state control indices for **DQB** scheme, feed composition 2

m1-m2-m3	NI	MRI	CN	λ_{11}	λ_{22}	λ_{33}
D_1-L_2-B_2	1.167	0.047	18.220	1.030	0.857	0.829
D_1-D_2-Q_2	1.805	0.097	10.450	1.030	0.514	0.550
D_1-R_2-B_2	1.114	0.054	16.528	1.000	0.897	0.897
DV_1-L_2-B_2	1.170	0.042	20.251	1.000	0.855	0.855
DV_1-D_2-B_2	1.058	0.384	3.691	0.946	0.945	0.999
L_1-D_2-Q_2	1.707	0.081	8.802	1.047	0.589	0.586
L_1-D_2-B_2	1.435	0.292	4.020	0.689	0.686	1.015
L_1-L_2-B_2	1.169	0.043	20.028	1.000	0.855	0.855
L_1-R_2-B_2	1.033	0.035	25.554	1.085	0.968	0.883
L_1-D_2-BR_2	1.559	0.095	7.704	1.000	0.641	0.641
LV_1-D_2-B_2	1.071	0.398	3.554	0.937	0.932	0.997
R_1-L_2-B_2	1.176	0.043	19.723	1.000	0.850	0.850
R_1-D_2-Q_2	1.812	0.085	8.557	1.010	0.553	0.553
R_1-D_2-B_2	1.062	0.231	5.937	0.947	0.941	0.995
R_1-R_2-B_2	1.082	0.033	26.884	1.038	0.924	0.889
R_1-D_2-BR_2	1.529	0.090	8.302	1.002	0.654	0.655

The results of Petlyuk column (**SP**), sloppy heat-integrated schemes **SQF**, and **SQB** are shown in the Tables (4.2b, 4.3b, and 4.4b).

Table 4.2b: Steady state control indices for Petlyuk column (**SP**), feed composition 2

m1-m2-m3	NI	MRI	CN	λ_{11}	λ_{22}	λ_{33}
D-S-Q	2.356	0.242	4.942	1.002	0.455	0.425
D-S-BR	1.179	0.186	7.703	1.039	0.857	0.824
DV-S-Q	0.809	0.249	6.027	0.980	0.454	1.243
DV-S-B	5.674	0.164	10.552	0.134	1.015	1.145
L-S-B	5.716	0.090	14.974	0.161	0.728	1.007
R-S-B	3.291	0.074	22.601	0.231	1.019	1.174
S-L-B	1.201	0.090	14.979	0.367	0.751	1.008

In all these three schemes the excluded control structures due to negative or poor control indices are the same and similar to feed composition 1, except (DV-S-Q) control structure which is showing positive result is in feed composition 2. The (D-S-BR) control structure shows the best RGA diagonal elements which indicates minimum interactions between control loops. The ratio control seems to be better for minimizing the interactions between control loops (Annakou et al., 1996 and Mizsey et al., 1996).

Table 4.3b: Steady state control indices for **SQF** scheme, feed composition 2

m1-m2-m3	NI	MRI	CN	λ_{11}	λ_{22}	λ_{33}
D-S-Q	1.637	0.130	9.515	0.999	0.642	0.610
D-S-BR	1.063	0.097	15.133	1.014	0.949	0.927
DV-S-Q	0.831	0.281	4.720	1.079	0.644	1.200
DV-S-B	11.348	0.215	7.453	0.068	0.995	0.994
L-S-B	7.020	0.072	17.699	0.128	0.693	0.969
R-S-B	4.837	0.060	25.430	0.159	0.981	1.061
S-L-B	1.196	0.072	17.871	0.466	0.708	0.974

The control structures of (D-S-Q), (DV-S-B), (D-S-BR) and (L-S-B) are recommended for further dynamic simulation investigations.

The overall result of feed composition 2 shows improvement in the steady state control indices comparing to feed composition 1, especially in **SP**, **SQF**, and **SQB** schemes. **DQB** scheme still has the advantages of better steady state control indices with respect to other investigated schemes.

Table 4.4b: Steady state control indices for **SQB** scheme, feed composition 2

m1-m2-m3	NI	MRI	CN	λ_{11}	λ_{22}	λ_{33}
D-S-Q	9.164	0.102	11.483	0.916	0.452	0.109
D-S-BR	5.763	0.093	13.502	0.961	0.659	0.155
DV-S-B	1.046	0.111	13.856	0.938	0.964	1.018
L-S-B	1.165	0.058	25.014	0.852	0.880	1.007
R-S-B	1.048	0.053	29.077	0.937	0.965	1.018
S-L-B	6.727	0.058	25.026	0.127	0.148	1.007

4.1.5. Conclusion of feed composition 2

For equimolar feed composition, the steady state control indices have been improved especially for sloppy separation schemes. This can be explained due to the previous fact that all the controlled products are drawing from the same column with similar flow rates ranges; the interactions between control loops are becoming less comparing to feed composition 1.

4.1.6. Results of steady-state control indices for feed composition 3

The possible control structure candidates are shown in Table 4.1c for **DQB** scheme. The excluded control structures are selected based on the similar assumption used for feed composition 1 and feed composition 2.

The streams that contain D_2 as manipulated variable for controlling $\mathbf{X_B}$ proved to be the best in CN and MRI values. The (D_1-L_2-B_2), (D_1-R_2-B_2), (L_1-D_2-Q_2), (D_1-D_2-Q_2), and (L_1-D_2-BR_2) control structures are recommended for further dynamic investigations due to their control indices values which is showing higher MRI index, Lower CN, and the most diagonal elements (λ_{ij}) are close to unity.

Table 4.1c: Steady state control indices for **DQB** scheme, feed composition 3

m1-m2-m3	NI	MRI	CN	λ_{11}	λ_{22}	λ_{33}
D_1-L_2-B_2	1.107	0.035	26.746	1.000	0.903	0.903
D_1-D_2-Q_2	1.117	0.376	4.240	1.000	0.896	0.896
D_1-R_2-B_2	1.058	0.034	28.597	1.000	0.945	0.945
D_1-L_2-BR_2	0.894	0.036	19.706	1.000	1.119	1.119
DV_1-L_2-B_2	1.103	0.034	27.143	1.000	0.907	0.907
DV_1-D_2-B_2	1.073	0.155	8.039	0.927	0.925	1.012
L_1-D_2-Q_2	1.106	0.144	9.655	1.000	0.905	0.905
L_1-D_2-B_2	1.102	0.110	12.252	0.904	0.898	1.015
L_1-L_2-B_2	1.103	0.034	27.239	1.000	0.907	0.907
L_1-R_2-B_2	1.056	0.033	29.354	1.000	0.947	0.947
L_1-D_2-BR_2	1.046	0.144	7.113	1.000	0.956	0.956
LV_1-D_2-B_2	1.085	0.611	2.203	0.918	0.919	1.009
R_1-L_2-B_2	1.103	0.034	27.152	1.000	0.907	0.907
R_1-D_2-Q_2	0.737	0.147	9.687	1.000	1.357	1.357
R_1-R_2-B_2	1.065	0.033	29.472	1.000	0.939	0.939
R_1-D_2-BR_2	1.046	0.146	7.019	1.000	0.956	0.956

Table 4.2c: Steady state control indices for Petlyuk column (**SP**), feed composition 3

m1-m2-m3	NI	MRI	CN	λ_{11}	λ_{22}	λ_{33}
D-S-Q	1.216	0.318	4.649	0.841	0.876	0.822
D-S-BR	1.012	0.496	2.291	1.026	1.003	0.959
DV-S-Q	0.352	0.105	15.631	2.981	0.878	2.840
DV-S-B	3.146	0.123	59.061	0.197	1.758	0.665
L-S-B	7.702	0.166	8.849	0.126	0.958	0.352
L-S-BR	0.527	0.101	12.332	1.902	0.902	1.961
R-S-B	2.579	0.099	73.180	0.240	1.759	0.722
R-S-BR	0.894	0.124	9.174	1.152	0.879	1.164
S-L-B	4.506	0.167	8.835	0.090	0.178	0.353

For sloppy separation schemes the results of steady state control indices are showing in Tables (4.2c, 4.3c, and 4.4c). After excluding the negative and poor control indices, these results proved to be the best in steady state control indices comparing to feed composition 1 and feed composition 2 and structures like (D-S-Q), (D-S-BR), (DV-S-Q), and (L-S-B) are good candidates for further dynamic investigations.

Table 4.3c: Steady state control indices for **SQF** scheme, feed composition 3

m1-m2-m3	NI	MRI	CN	λ_{11}	λ_{22}	λ_{33}
D-S-Q	1.174	0.141	10.362	0.971	0.885	0.852
D-S-BR	1.043	0.390	3.141	1.018	0.972	0.937
DV-S-Q	0.611	0.148	10.008	1.710	0.888	1.636
DV-S-B	5.264	0.108	71.230	0.129	1.798	0.432
L-S-B	9.641	0.241	6.464	0.109	0.883	0.103
L-S-BR	0.380	0.088	15.781	2.615	0.887	2.764
R-S-Q	0.186	0.036	41.698	5.589	0.924	5.371
R-S-B	3.204	0.081	94.962	0.214	1.803	0.550
R-S-BR	0.922	0.156	7.974	1.107	0.848	1.167
S-L-B	6.376	0.231	6.907	0.107	0.107	0.293

Table 4.4c: Steady state control indices for **SQB** scheme, feed composition 3

m1-m2-m3	NI	MRI	CN	λ_{11}	λ_{22}	λ_{33}
D-S-Q	1.172	0.357	4.440	0.976	0.881	0.852
D-S-BR	1.026	0.483	2.625	1.027	0.986	0.946
DV-S-Q	0.201	0.068	27.358	4.930	0.865	4.962
DV-S-B	9.854	0.113	54.802	0.078	1.617	0.312
L-S-B	42.571	0.240	6.940	0.023	0.951	0.168
L-S-BR	0.709	0.188	7.731	1.406	0.880	1.522
R-S-B	11.510	0.087	70.437	0.067	1.624	0.302
R-S-BR	0.939	0.183	6.916	1.082	0.854	1.154
S-L-B	6.874	0.239	6.982	0.108	0.087	0.159

4.1.7. Conclusion of feed composition 3

In this case where the composition of the middle component is the highest, sloppy heat-integrated schemes **SQF** and **SQB** proved to be the best in economic features. The steady state control indices are showing the best indices comparing to the previous cases, which means the middle component concentration plays important role in the interactions inside the column and as this concentration increases less interactions are expected.

4.1.8. Conclusions of the steady state control indices study

Steady-state control analysis is carried out for the optimum schemes by investigating their control indices (Niederlniski index (NI), Morari resiliency (MRI), and RGA). The results show the following:

1. The schemes are controllable with decentralized controller structures.
2. Petlyuk column and sloppy heat integrated schemes shows poor indices and strong interactions in composition 1.
3. Feed compositions 2 and 3 show better controllability indices than the same schemes of feed composition 1.
4. Direct sequence with backward heat integration (**DQB**) is always the best from steady-state control analysis point of view.

These results have to be verified by dynamic simulations in the next section.

4.2. Dynamic simulations

This part of the study deals with the analysis of the dynamic behavior of conventional and energy-integrated schemes by addressing the stabilization and the composition control of the schemes through decentralized feedback control. In order to find out which are the best control structures, different control structures are systematically analyzed and compared under performance of open loop and closed-loop dynamic simulation.

The general control objectives considered in this work are stabilization, to maintain composition of the products at set points, and to maintain the operation close to minimum energy consumption. Composition control objective consists of the control of the three-product purity.

4.2.1. Level control

In distillation columns, the reboiler and reflux drum are large enough to absorb fluctuations. Because of that, in this work, proportional controllers have been implemented in both level control loops.

According to Luyben (1990), in real plants, most liquid levels represent material inventory used as surge capacity. In these cases, it is unimportant where the level is, as long as it is between some maximum and minimum values. Because of that, proportional controllers are often used to control liquid levels, in order to give smooth changes and filter out fluctuations in flowrates affecting downstream units.

The tuning of the proportional controllers has been done in such a way that the control valve is wide open when the tank is 80 % full, and the control valve is closed when the tank is 20 % full. According to this, the tuning of the level controllers are determined first and the controllers parameters are calculated based on Tyreus-Luyben cycling method.

4.2.2. Composition control

Generally, direct composition measurements will lead to better composition control than temperature measurements. Besides, temperature can be a very poor indicator of composition for multicomponent mixtures. In this work, composition measurements are considered, and sample points are located at the product streams.

PI controllers are the controllers implemented in the composition control loops. The integral mode of a feedback controller is required to avoid steady state offset resulting from disturbances. It is usually combined with the proportional mode in a proportional integral (PI) controller.

4.2.3. Controllers Tuning

PI-controllers are used for composition control system (CC-S) and P-controllers for level control system (LC-S). Tuning of the schemes controller loops by using Tyreus-Luyben cycling method can be summarized below:

(a) Install the control loops for the scheme, which include LC-S and CC-S.

(b) P-controller is set for LC-S with constant controller gain value equal to ($K_C = 4$) in all schemes.

(c) PI-controller is recommended for the three CC-S. They are tuned individually by estimating P-controller only and increasing the controller gain (K_C) until the loop reach a stability limit.

(d) The ultimate gain (K_U) and the ultimate frequency (P_U) can be found at the stability limit, then from these constants, tuning values for PI-controller (K_C and τ_C) can be determined by using Tyreus-Luyben settings parameters, using these parameters the CC-S are expect to be stable after three oscillations.

Tyreus-Luyben controller setting parameters:

$$K_C = \frac{K_U}{3.2} \quad [4\text{-}4]$$

and

$$\tau_C = 2.2 * P_U \quad [4\text{-}5]$$

where:

K_C = Controller gain

τ_C = Controller reset time

K_U = Ultimate gain

P_U = Ultimate frequency

Switching all the three CC-S loops on, strong interactions take place and detunning factors are necessary.

4.2.4. The Biggest Log-modulus Tuning (BLT)

The Tyreus-Luyben settings are often not adequate for multivariable system. For multivariable systems, it is needed a procedure that simultaneously tunes all controllers, taking into account the interaction that exist among the loops. The Biggest Log-modulus Tuning (BLT) is a way to accomplish the job. It provides settings that work reasonably well in many processes. These settings may not be optimum, because they tend to be conservative. However, they guarantee stability and yield tunings that give a reasonable compromise between stability and performance in multivariable systems (Luyben, 1992).

The BLT method is based on the Tyreus-Luyben equations. The ultimate gain and ultimate frequency of each loop are calculated in the classical Single Input Single Output (SISO) way. A detuning factor F_{BLT} is assumed, which should be greater than 1. The larger the F_{BLT} value, the more stable the system will be, but more sluggish will be the system response. The gains of all feedback controllers (K_C) are calculated by dividing the Tyreus-Luyben gains by F_{BLT}. The feedback controllers integral time (τ_C) are calculated by multiplying the Tyreus-Luyben integral time by F_{BLT}.

4.2.5. A case study

The controllability study of equimolar feed composition of (ethanol – n-propanol – n-butanol) is carried out based on the preliminary operability study of that feed composition investigated in the previous section. This study is based on the economic features of the studied schemes, steady state control indices of the schemes, and the analysis of dynamic features of these schemes. HYSYS flowsheet simulator is used for steady-state and dynamic simulation for this study using feed capacity of 100 kmol/h, 99 mole % product purity, and UNIQUAC thermodynamic property package, and the same optimization procedure of the previous economic study are followed. Optimization results are shown in (Table C.6) and it can be summarized with respect to TAC savings as follows:

- The energy-integrated schemes are always more economical than the conventional distillation schemes.

- **DQB** scheme shows the maximum savings comparing to the other schemes with 37 %. DQF shows the lowest value with 16 %,

- the sloppy schemes show similar savings: 34 % for **SQF** and 33 % for **SQB**,

- Petlyuk column (**SP**) shows the highest utility demand comparing to other energy integrated structures and it has only 29 % saving,

- **SQF** and **SQB** schemes have the lowest values of utility demand but because of using middle pressure steam the utility cost will be higher and they become the second ones according to **TAC** saving classification.

4.2.6. Steady state control indices of the case study

In these investigated schemes the product compositions ($\mathbf{X_A}$, $\mathbf{X_B}$, $\mathbf{X_C}$) are controlled and the proper set of manipulated variables is determined. The manipulated variables for the direct sequence (**D**), direct sequence with forward heat integration (**DQF**), and

direct sequence with backward heat integration (**DQB**) scheme are the following: distillate of column 1 (D_1), reflux flow of column 1 (L_1), distillate of column 2 (D_2), reflux flow of column 2 (L_2), bottom rate of column 2 (B_2).

Table 4.5: Steady state controllability indices for the optimized schemes

Studied Schemes	NI	MRI	CN	λ11	λ22	λ33
D, (D_1-L_2-B_2)	1.137	0.099	8.890	1.000	0.880	0.880
D, (L_1-D_2-Q_2)	1.995	0.065	32.113	1.000	0.500	0.500
D, (L_1-D_2-B_2)	1.865	0.234	4.934	0.580	0.540	0.920
DQF, (D_1-L_2-B_2)	1.136	0.024	36.320	1.000	0.880	0.880
DQF, (L_1-D_2-Q_2)	1.890	0.033	21.290	1.000	0.530	0.530
DQF, (L_1-D_2-B_2)	1.678	0.226	5.240	0.586	0.595	1.020
DQB, (D_1-L_2-B_2)	1.093	0.023	39.660	1.000	0.910	0.910
DQB, (L_1-D_2-Q_2)	2.283	0.040	18.110	1.000	0.440	0.440
DQB, (L_1-D_2-B_2)	1.540	0.246	5.040	0.647	0.645	1.000
SP, (D-S-Q)	3.515	0.182	6.890	1.000	0.320	0.280
SP, (L-S-B)	7.438	0.089	14.380	0.130	0.570	0.990
SQF, (D-S-Q)	6.470	0.010	137.400	1.000	0.250	0.150
SQF, (L-S-B)	4.030	0.008	158.100	0.250	0.250	0.998
SQB, (D-S-Q)	5.080	0.038	33.310	0.997	0.470	0.196
SQB, (L-S-B)	1.287	0.022	64.388	0.770	0.827	1.000

The manipulated variables for Petlyuk column (**SP**), sloppy sequence with forward heat integration (**SQF**), sloppy sequence with backward heat integration (**SQB**) are heat duty of main column (Q), side product flow (S), and distillate rate of main column (D), and reflux rate of main column (L). Ratio control structures are not considered.

According to the previous results of steady-state control analysis, the best control structures are evaluated for this case study by determining its control indices; Niederlinski index (NI), the Morari resiliency index (MRI), the relative gain array (RGA), and the condition number (CN).

The results of steady-state control indices are shown in Table 4.5 indicating the following:

(i). base case (**D**) and conventional heat-integrated schemes (**DQF** and **DQB**) show less interactions,

(ii). the steady state control indices of (D_1-L_2-B_2) manipulated variables selection for **D**, **DQF**, and **DQB** schemes prove to be better than those of (L_1-D_2-Q_2) and (L_1-D_2-B_2),

(iii). serious interactions can be expected for the sloppy schemes (**SQF** and **SQB**) and for the Petlyuk column (**SP**) due to poor RGA values and also for other indices,

(iv). in case of **SP**, **SQF**, and **SQB** schemes the selection of (L-S-B) set of manipulated variables is better than (D-S-Q) set according to RGA values.

(v). RGA proved to be more representative for this system and the set of control structures (manipulated variables) which have values of λ_{ij} close to unity are expected to show less interaction.

The results of steady-state control indices are verified by further dynamic simulation, which includes the study of open loop and closed-loop dynamic behavior of the schemes under feed rate and feed composition disturbance.

4.2.7. Open loop dynamic simulation

In distillation, the main time constants are given by the composition dynamics. High purity columns have very large open-loop time constants. However, the use of feedback changes the dynamics and the closed-loop time constants may become much shorter.

During the dynamic simulations equimolar feed composition ($\mathbf{X_A}$= 0.333, $\mathbf{X_B}$ =0.333, $\mathbf{X_C}$ =0.333) and feed rate of 100 kmol/h are selected as base case. The disturbances are always the same and at the same time for all schemes, with 100 to 100.5 kmol/h

for feed rate disturbance, and (0.333/0.333/0.333) to (0.33/0.34/0.33) for feed composition disturbance.

In open loop dynamic simulation, the schemes are studied without installation of any composition or level controller and the time constants of the different transient behaviors are measured.

4.2.8. Results of open loop dynamic simulation

The time constant of each product composition (ethanol, n-propanol, and n-butanol) are measured as shown in Tables 4.6-4.7 for feed rate and feed composition disturbances.

Table 4.6: Open loop performance for feed rate disturbance

Studied schemes	Ethanol ($\mathbf{X_A}$) Time constant (time unit)	n-Propanol ($\mathbf{X_B}$) Time constant (time unit)	n-Butanol ($\mathbf{X_C}$) Time constant (time unit)	Average time constant (time unit)
D	16	8	3	9
DQF	20	11	2	11
DQB	14	9	6	10
SP	16	5	6	9
SQF	16	3	5	8
SQB	23	13	11	16

The arithmetic average time constant are calculated for the various studied distillation schemes in order to classify the schemes for lower and higher time constant in case of open loop dynamic behavior. Figures 4.5-4.16 show the plots of feed rate and feed composition disturbances for the open loop dynamic simulations

Table 4.7: Open loop performance for feed composition disturbance

Studied schemes	Ethanol ($\mathbf{X_A}$) Time constant (time unit)	n-Propanol ($\mathbf{X_B}$) Time constant (time unit)	n-Butanol ($\mathbf{X_C}$) Time constant (time unit)	Average time constant (time unit)
D	12	10	6	9
DQF	15	5	19	13
DQB	11	13	6	10
SP	14	7	4	8
SQF	14	2	6	7
SQB	36	9	9	18

The results of open loop dynamic simulation show that **SQB** is a significantly slower scheme compared to the other investigated schemes and it has the highest time constant. The reason can be the opposite direction of material and energy flows. The rest of the studied schemes show similar order of magnitude for the average time constants.

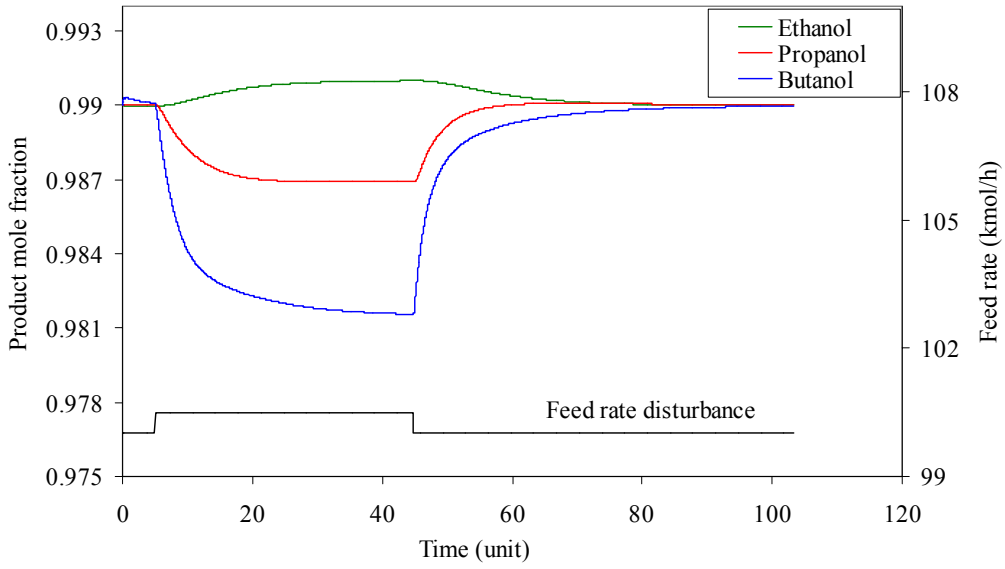

Figure 4.5: Open loop transient behavior of direct sequence (**D**) for feed rate disturbance

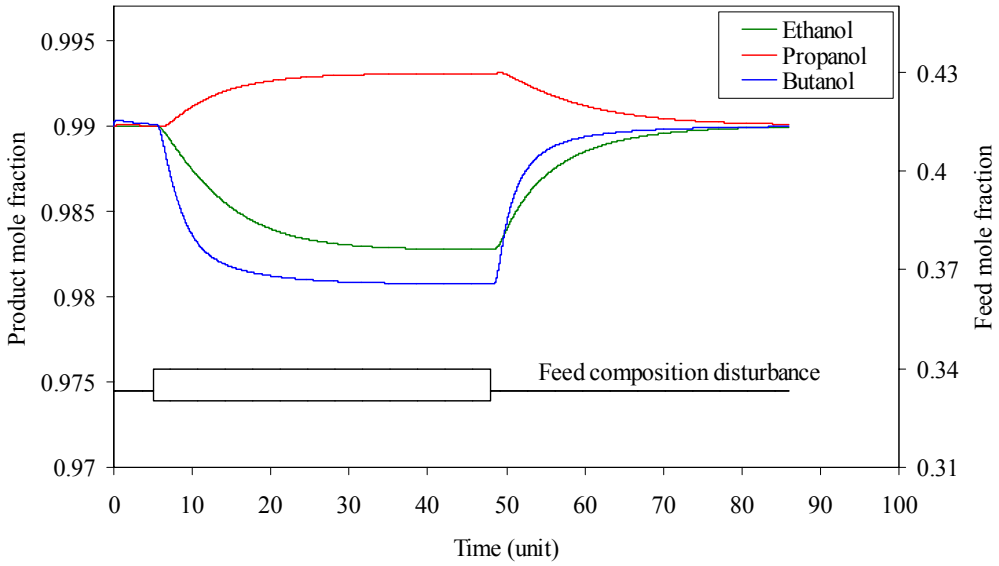

Figure 4.6: Open loop transient behavior of direct sequence (**D**) for feed composition disturbance

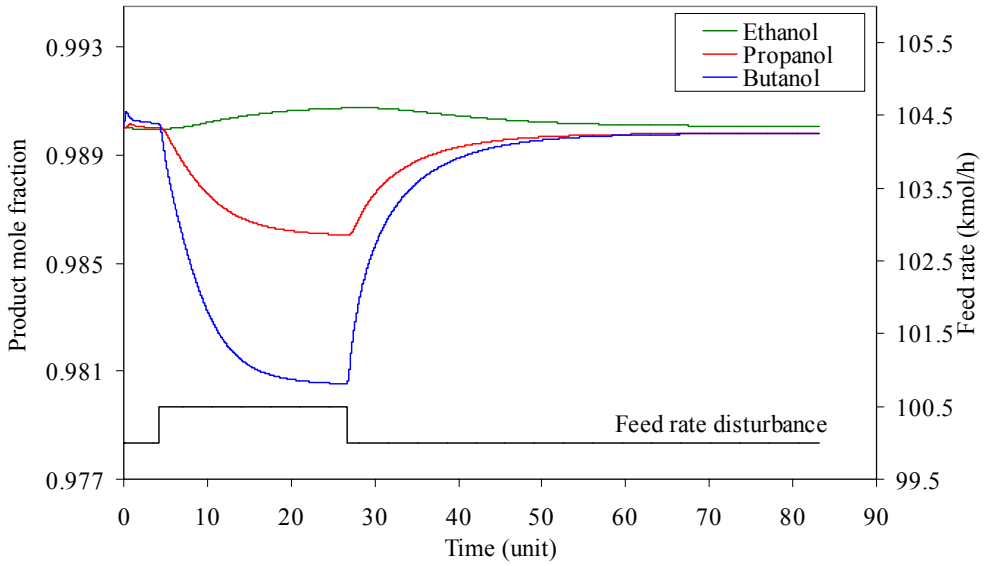

Figure 4.7: Open loop transient behavior of **DQB** scheme for feed rate disturbance

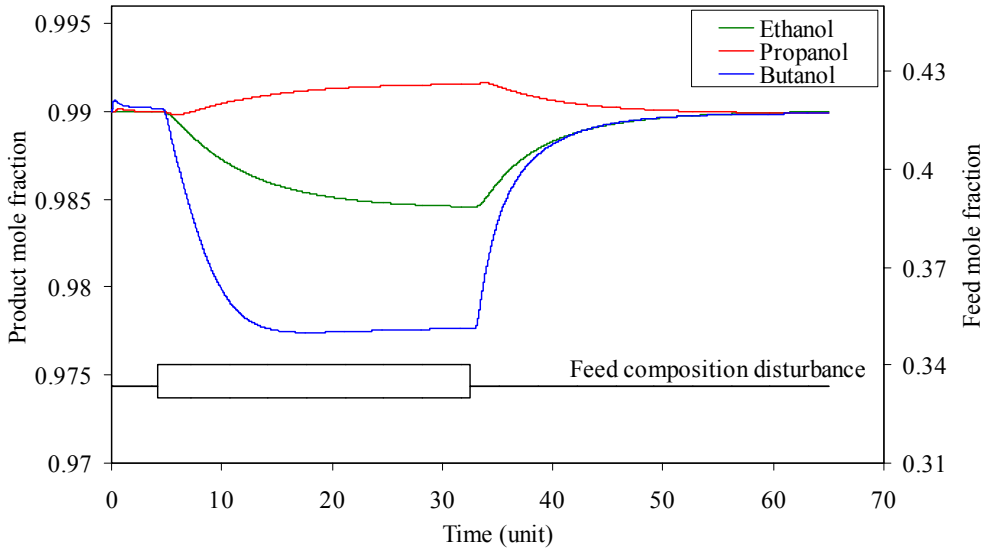

Figure 4.8: Open loop transient behavior of **DQB** scheme for feed composition disturbance

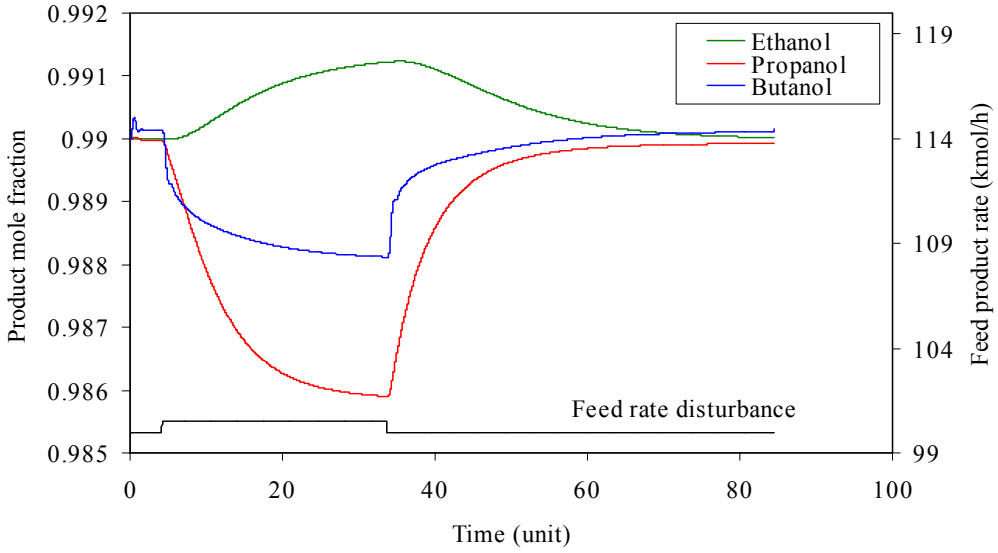

Figure 4.9: Open loop transient behavior of **DQF** scheme for feed rate disturbance

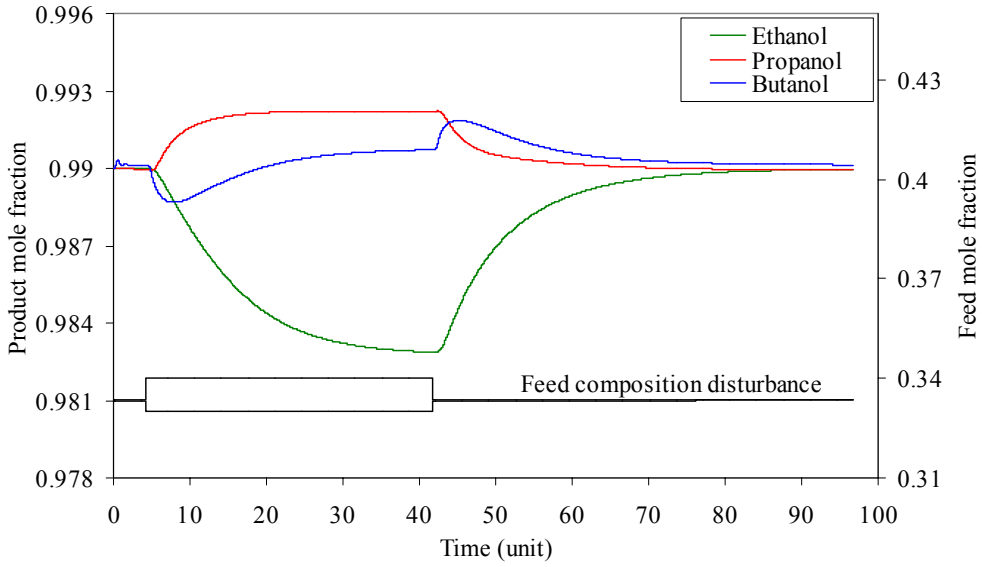

Figure 4.10: Open loop transient behavior of **DQF** scheme for feed composition disturbance

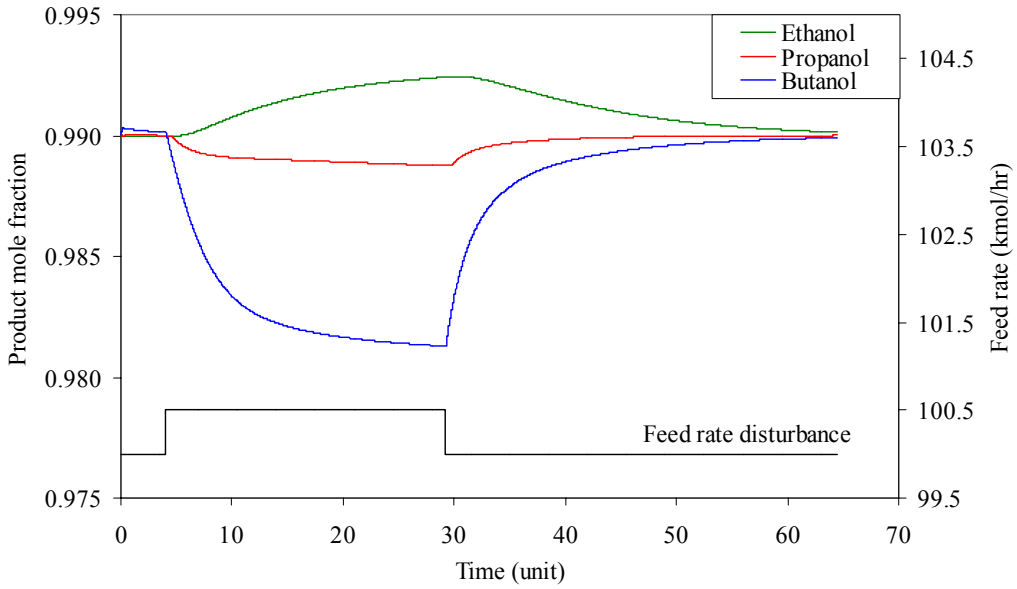

Figure 4.11: Open loop transient behavior of Petlyuk column (**SP**) for feed rate disturbance

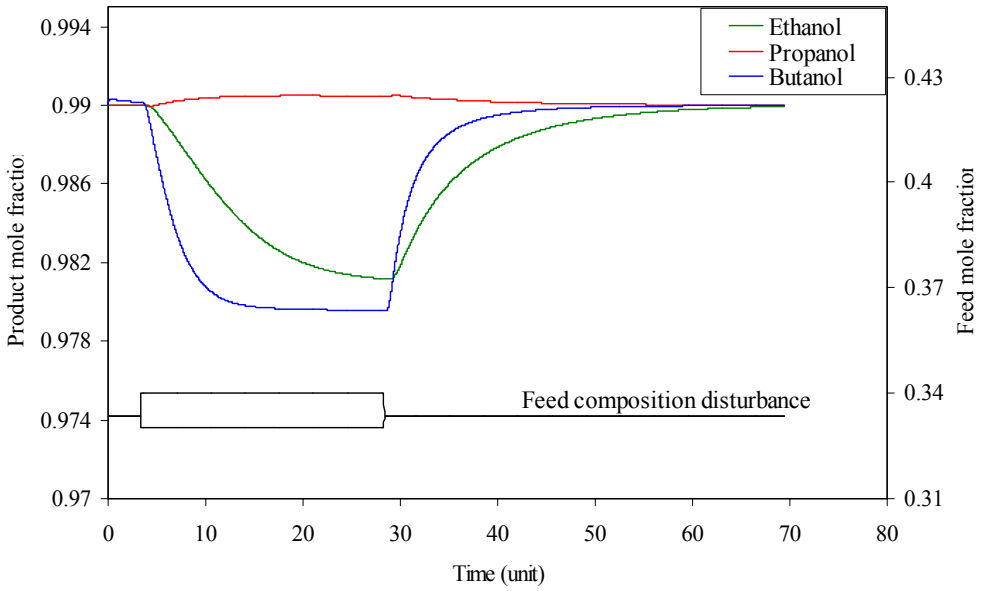

Figure 4.12: Open loop transient behavior of Petlyuk column (**SP**) for feed composition disturbance

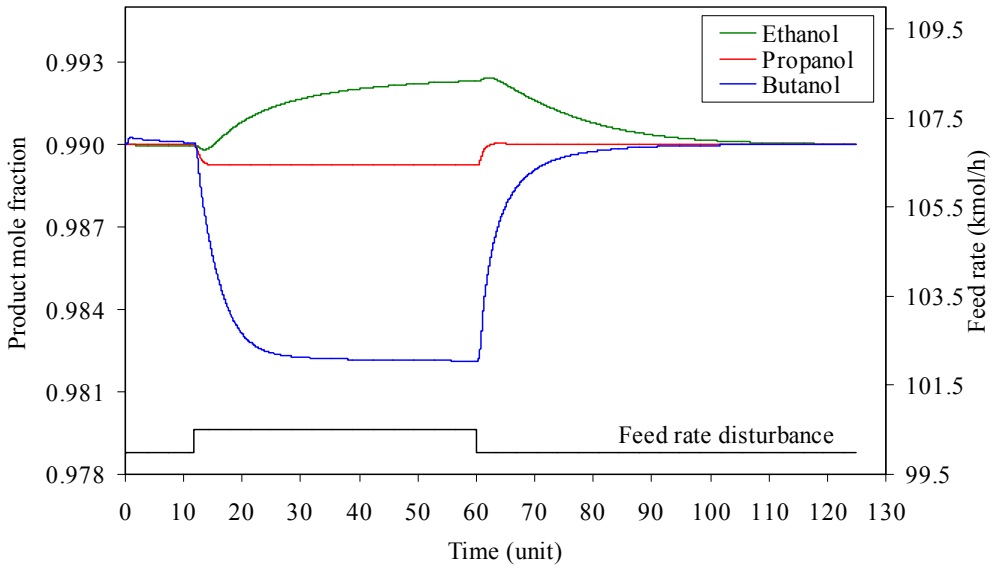

Figure 4.13: Open loop transient behavior of **SQF** scheme for feed rate disturbance

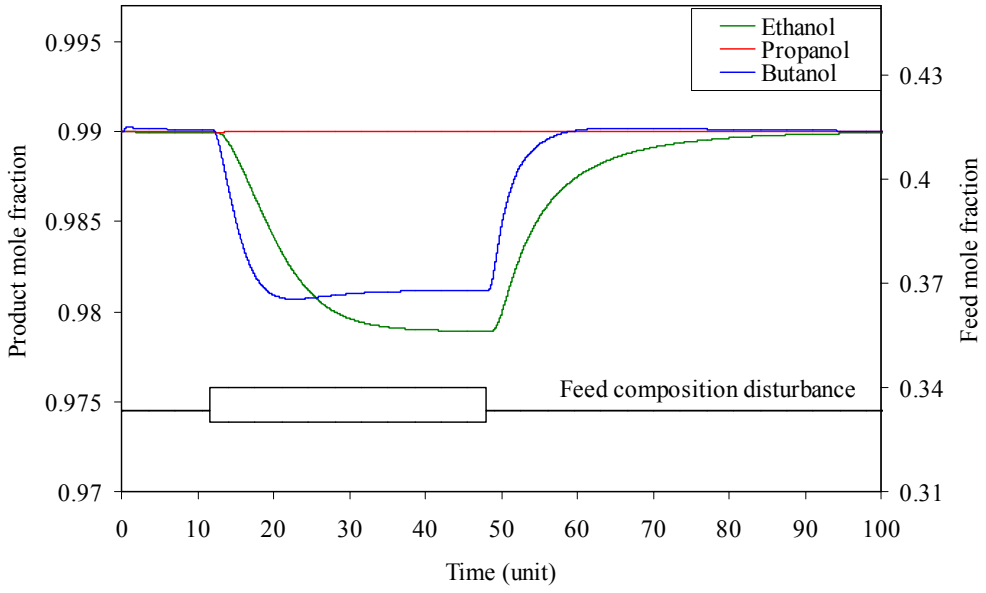

Figure 4.14: Open loop transient behavior of **SQF** scheme for feed composition disturbance

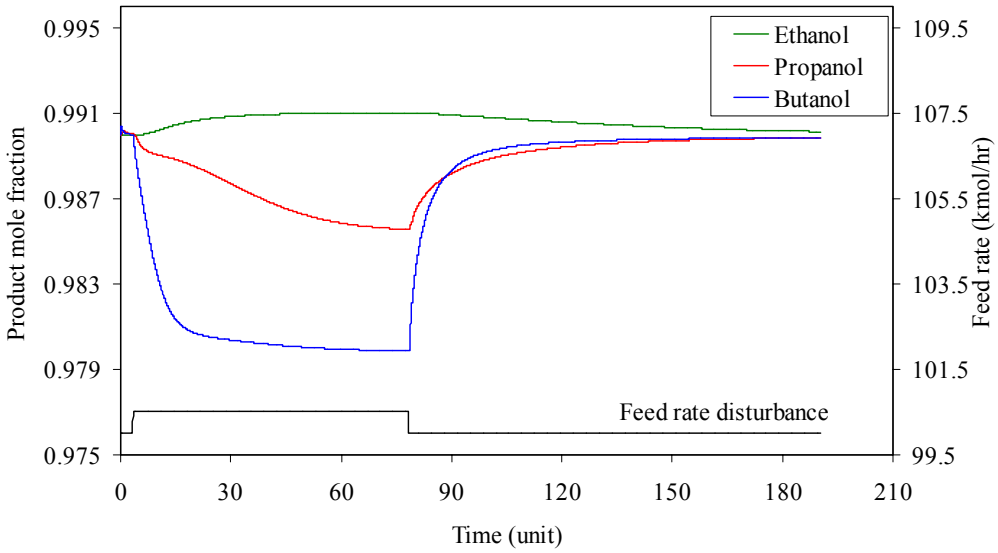

Figure 4.15: Open loop transient behavior of **SQB** scheme for feed rate disturbance

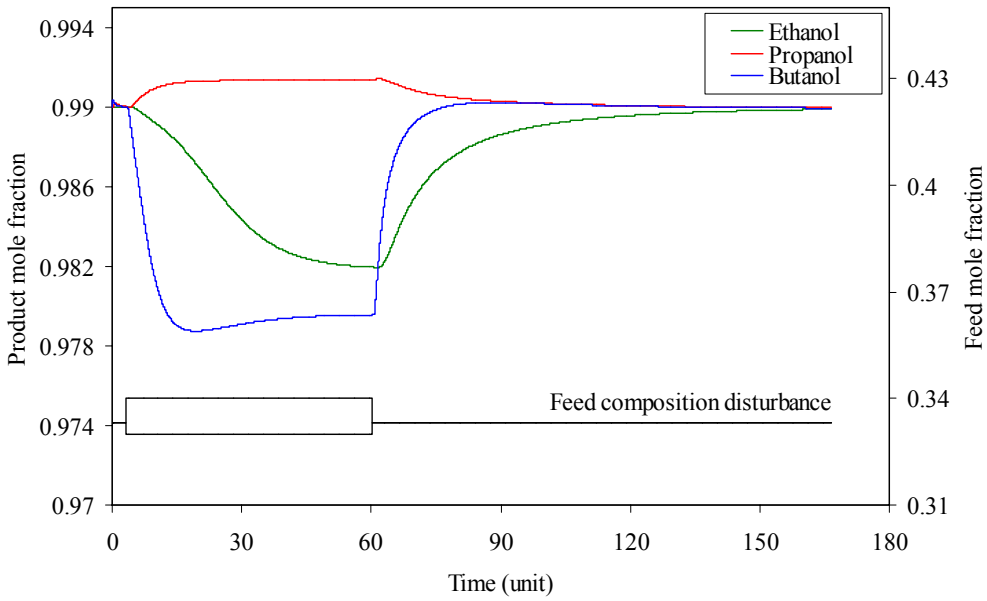

Figure 4.16: Open loop transient behavior of **SQB** scheme for feed composition disturbance

4.2.9. Closed-loop dynamic simulation

In closed-loop dynamic simulation a composition controller and level controller have to be installed. The best control structures are selected according to the results of their steady state control indices. PI-controllers are selected for simulations with closed composition control loops (closed-loop dynamic simulation) and P-controllers for the material balance control loops (level control) are used. The controller tunings are determined by the Tyreus-Luyben cycling method.

Closed-loop simulations are carried out for feed rate and composition disturbance. The settling time, overshoots, and product of settling time and overshoots (PSO) are determined and compared to characterize the dynamic behavior of the schemes. PSO values are expected to be proportional to integral square error (ISE) of the control loop. To eliminate interactions between control loops and achieve a stable operation, detuning factors are used.

4.2.10. Results of closed-loop dynamic simulation

Closed loop dynamic behavior of conventional and energy-integrated schemes for different sets of manipulated variables are shown in Figures 4.17-4.28. The investigated schemes are evaluated by taking the summation of settling time, overshoots, and PSO for each product composition.

The results of the studied schemes are summarized in Tables 4.8 and 4.9 and show that the base case (**D**) and the conventional heat-integrated schemes (**DQF** and **DQB**) are the fastest in closed-loop dynamic behavior by showing lower settling time, overshoots, and PSO values comparing to the other investigated schemes (**SP**, **SQF**, and **SQB**). Comparing the control structures used, (D_1-L_2-B_2) set of the manipulated variables proves to be faster than the (L_1-D_2-Q_2) and (L_1-D_2-B_2). The D-B structures originally believed to be unworkable but investigated and recommended by Skogestad (1997) show less favorable performance.

Table 4.8: Closed-loop performance for feed rate disturbance

Studied schemes	Σ ST	Σ OS	Σ PSO	F_{BLT}
D (D_1-L_2-B_2)	10.580	0.010	0.075	1.3
D (L_1-D_2-B_2)	32.740	0.011	0.227	1.0
DQF (D_1-L_2-B_2)	11.620	0.006	0.051	1.3
DQF (L_1-D_2-Q_2)	20.100	0.012	0.178	1.0
DQF (L_1-D_2-B_2)	36.550	0.012	0.346	1.0
DQB (D_1-L_2-B_2)	23.330	0.024	0.310	3.0
DQB (L_1-D_2-Q_2)	26.750	0.033	0.751	1.0
DQB (L_1-D_2-B_2)	34.250	0.034	0.677	1.0
SP (L-S-B)	30.610	0.023	0.238	2.0
SP (D-S-Q)	39.440	0.020	0.262	5.0
SQF (L-S-B)	40.500	0.057	0.813	2.0
SQF (D-S-Q)	59.960	0.042	0.903	3.0
SQB (L-S-B)	70.150	0.030	0.799	6.0
SQB (D-S-Q)	150.000	0.031	1.564	20

The Petlyuk column shows good dynamic behavior in closed-loop disturbance compared to sloppy heat-integrated schemes (**SQF** and **SQB**) although the economic features of sloppy schemes are better than the Petlyuk column. (L-S-B) control structure proves to be faster in closed-loop dynamic simulation than (D-S-Q) set in case of Petlyuk column and sloppy schemes.

Table 4.9: Closed-loop performance for feed composition disturbance

Studied schemes	Σ ST	Σ OS	Σ PSO	F_{BLT}
D (D_1-L_2-B_2)	14.200	0.006	0.044	1.3
D (L_1-D_2-B_2)	21.200	0.021	0.264	1.0
DQF (D_1-L_2-B_2)	13.160	0.003	0.025	1.3
DQF (L_1-D_2-Q_2)	23.340	0.041	0.631	1.0
DQF (L_1-D_2-B_2)	31.950	0.081	1.951	1.0
DQB (D_1-L_2-B_2)	16.530	0.019	0.133	3.0
DQB (L_1-D_2-Q_2)	37.850	0.130	3.790	1.0
DQB (L_1-D_2-B_2)	44.840	0.130	3.512	1.0
SP (L-S-B)	28.390	0.043	0.441	2.0
SP (D-S-Q)	42.680	0.064	0.907	5.0
SQF (L-S-B)	41.600	0.017	0.261	2.0
SQF (D-S-Q)	68.290	0.030	0.789	3.0
SQB (L-S-B)	104.850	0.076	3.398	6.0
SQB (D-S-Q)	107.310	0.083	4.654	20

Forward energy-integrated schemes (e.g. **DQF** and **SQF**) prove to be better than backward energy-integrated schemes (**DQB** and **SQB**), and this can be due to stronger interactions that can take place because of the opposite directions of energy and materials flows.

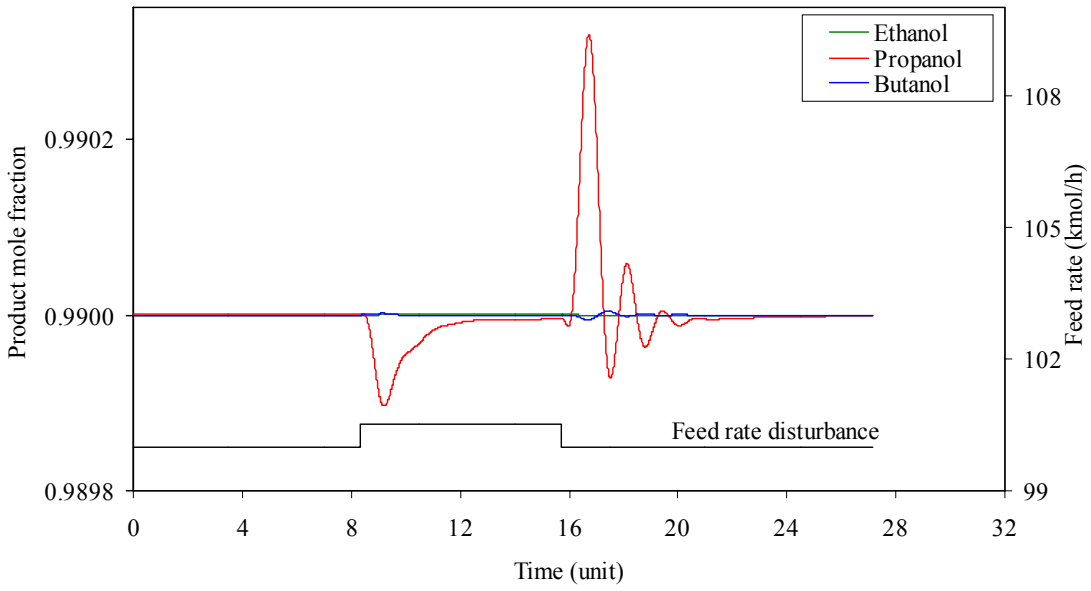

Figure 4.17: Closed-loop transient behavior of direct sequence (**D**) for feed rate disturbance using (D_1-L_2-B_2) manipulated variables

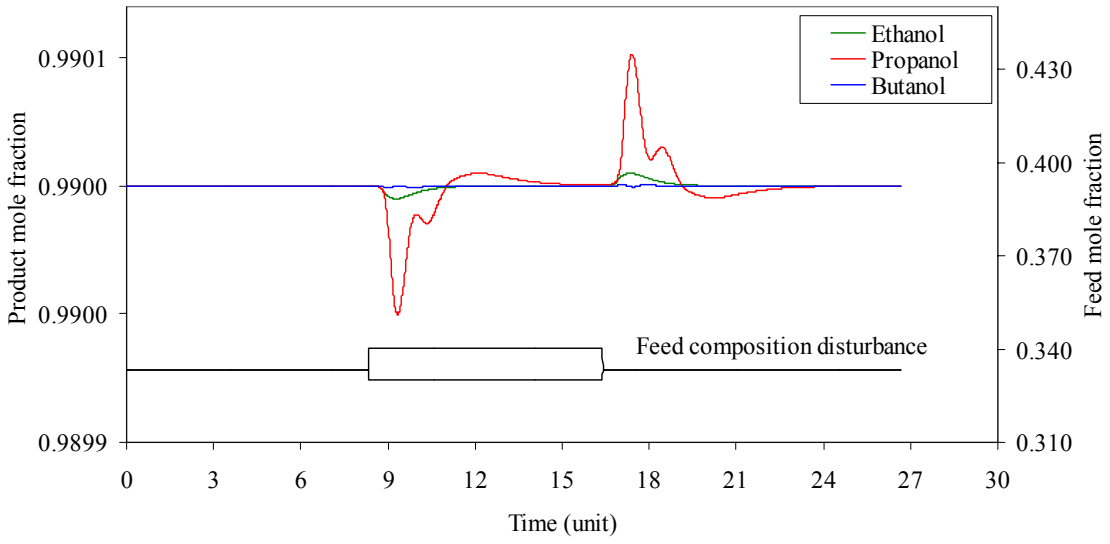

Figure 4.18: Closed-loop transient behavior of direct sequence (**D**) for feed composition disturbance using (D_1-L_2-B_2) manipulated variables

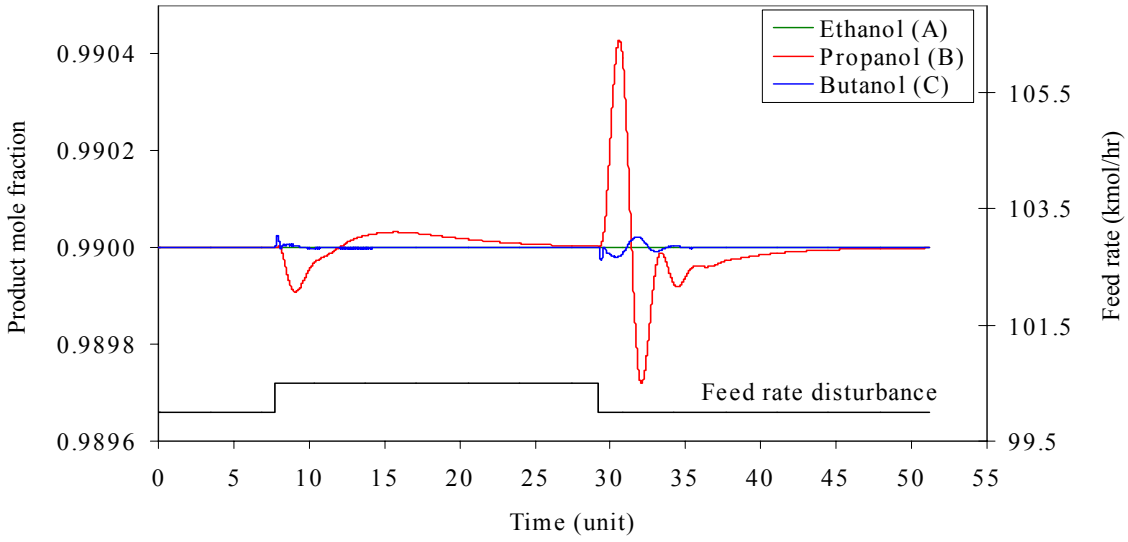

Figure 4.19: Closed loop transient behavior of direct sequence (**D**) for feed rate disturbance using (L_1-D_2-B_2) manipulated variables

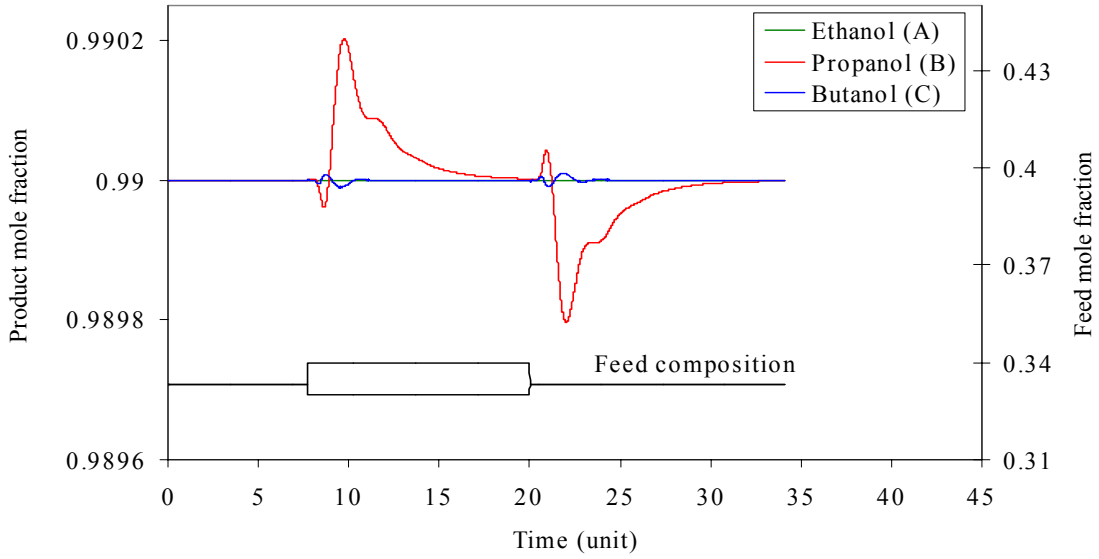

Figure 4.20: Closed-loop transient behavior of direct sequence (**D**) for feed composition disturbance using (L_1-D_2-B_2) manipulated variables

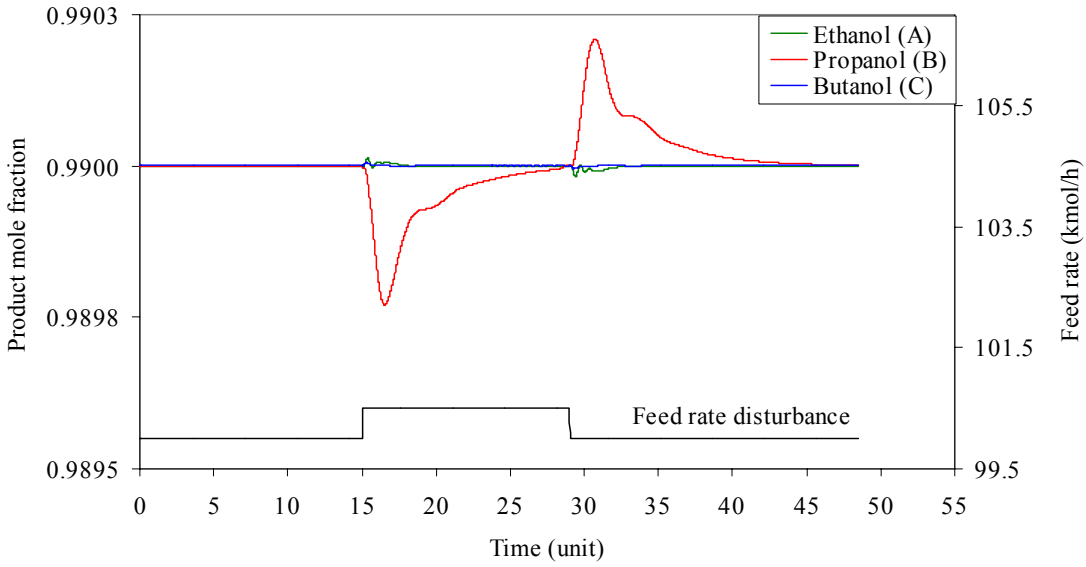

Figure 4.21: Closed-loop transient behavior of **DQB** scheme for feed rate disturbance using (D_1-L_2-B_2) manipulated variables

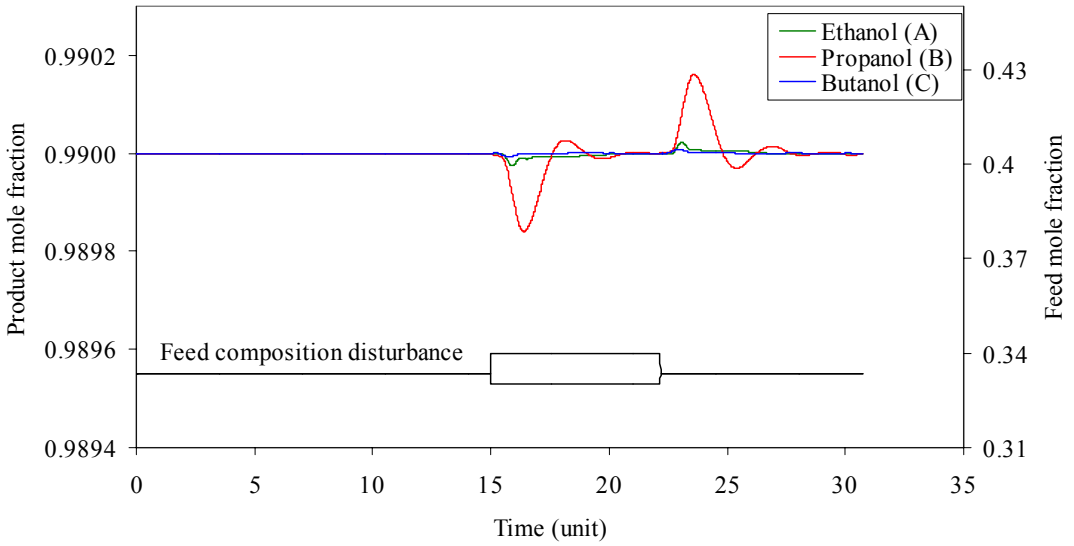

Figure 4.22: Closed-loop transient behavior of **DQB** scheme for feed composition disturbance using (D_1-L_2-B_2) manipulated variables

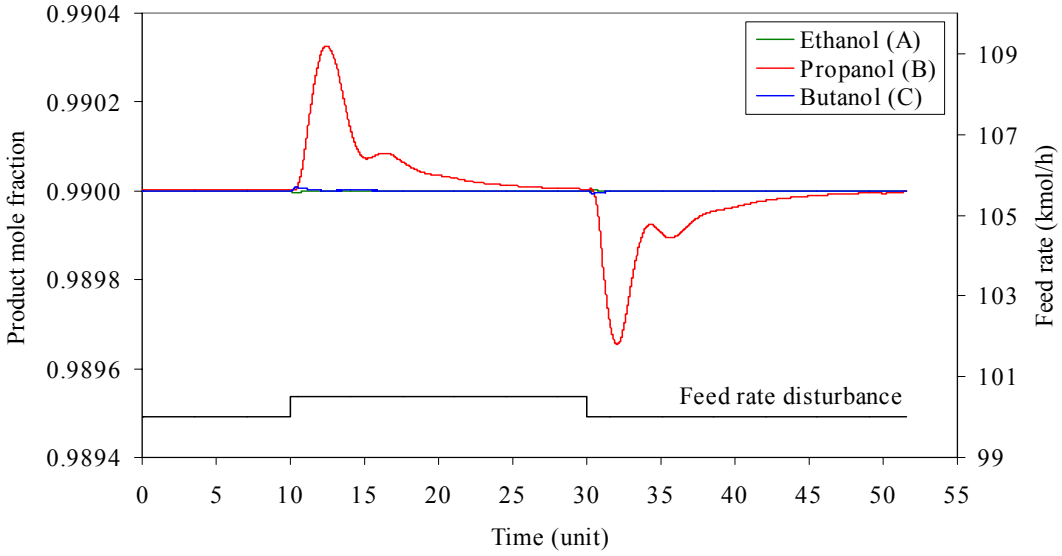

Figure 4.23: Closed-loop transient behavior of **DQB** scheme for feed rate disturbance using (L_1-D_2-B_2) manipulated variables

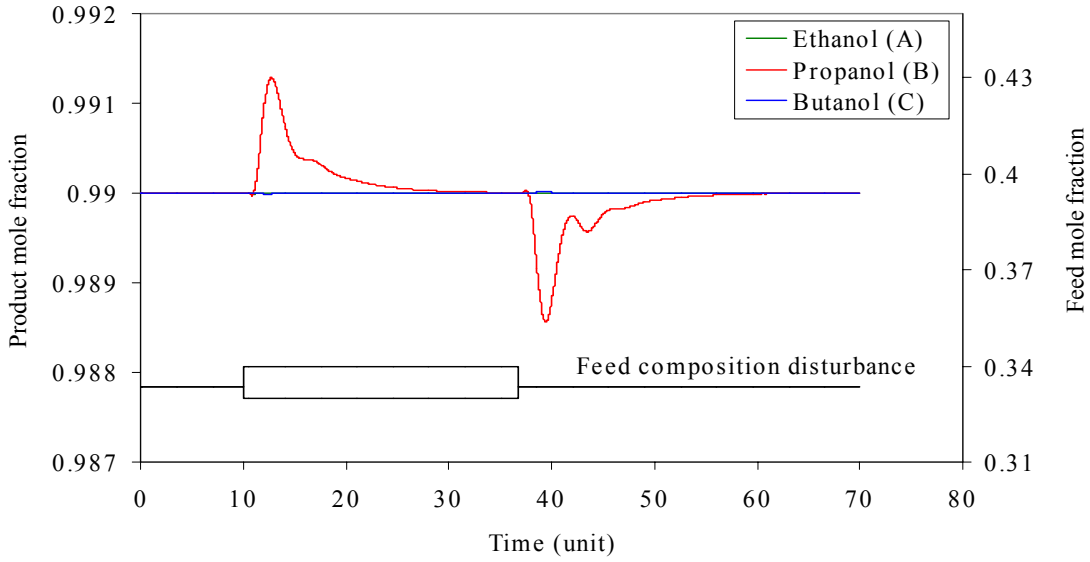

Figure 4.24: Closed-loop transient behavior of **DQB** scheme for feed composition disturbance using (L_1-D_2-B_2) manipulated variables

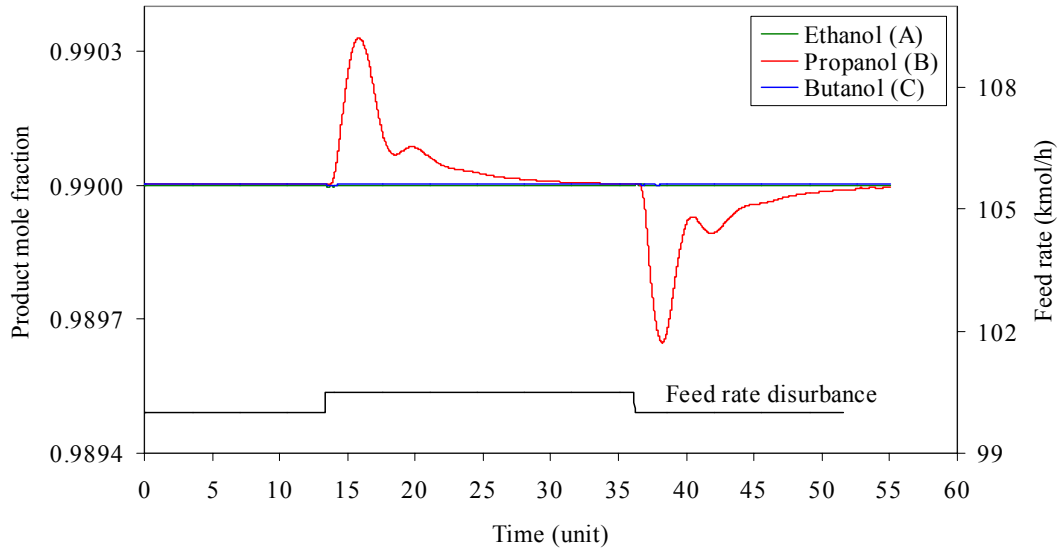

Figure 4.25: Closed-loop transient behavior of **DQB** scheme for feed rate disturbance using (L_1-D_2-Q_2) manipulated variables

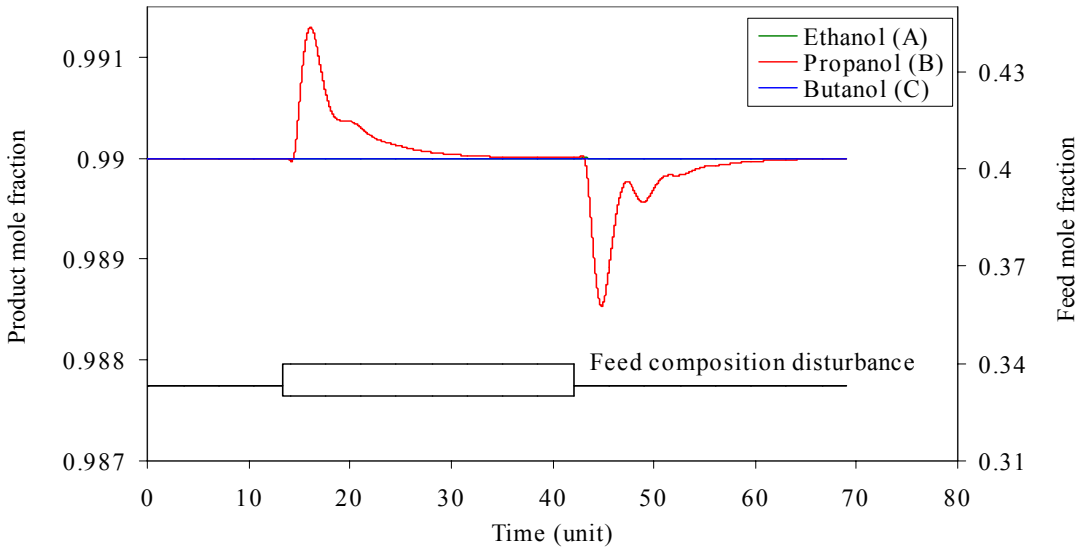

Figure 4.26: Closed-loop transient behavior of **DQB** scheme for feed composition disturbance using (L_1-D_2-Q_2) manipulated variables

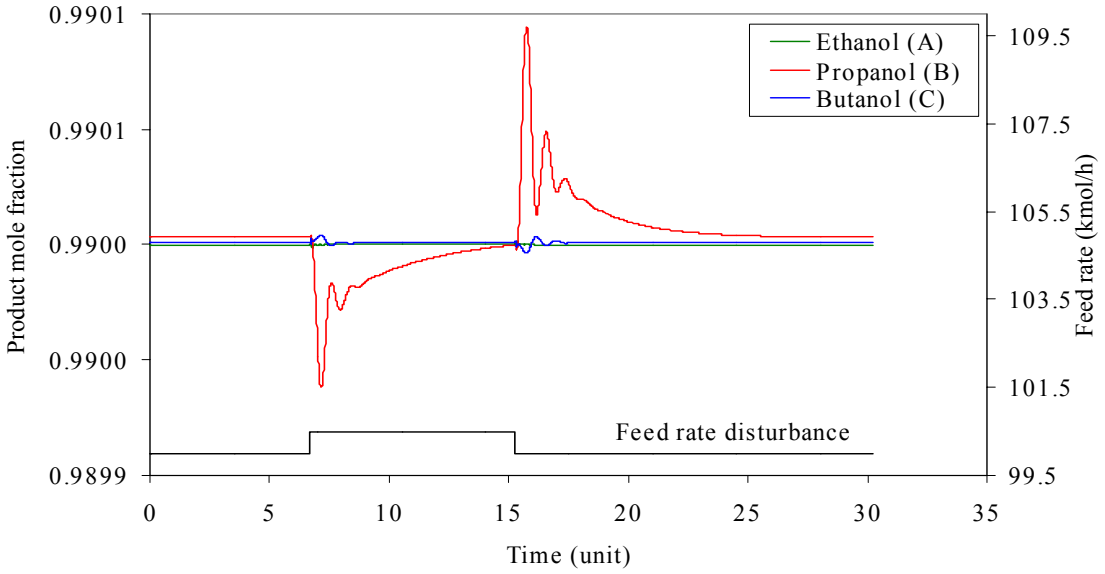

Figure 4.27: Closed-loop transient behavior of **DQF** scheme for feed rate disturbance using (D_1-L_2-B_2) manipulated variables

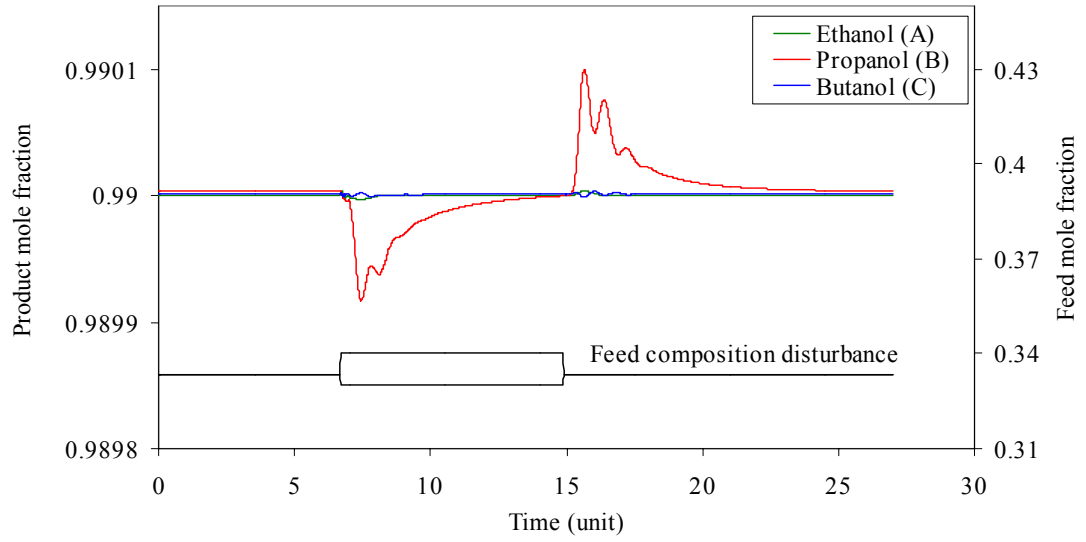

Figure 4.28: Closed-loop transient behavior of **DQF** scheme for feed composition disturbance using (D_1-L_2-B_2) manipulated variables

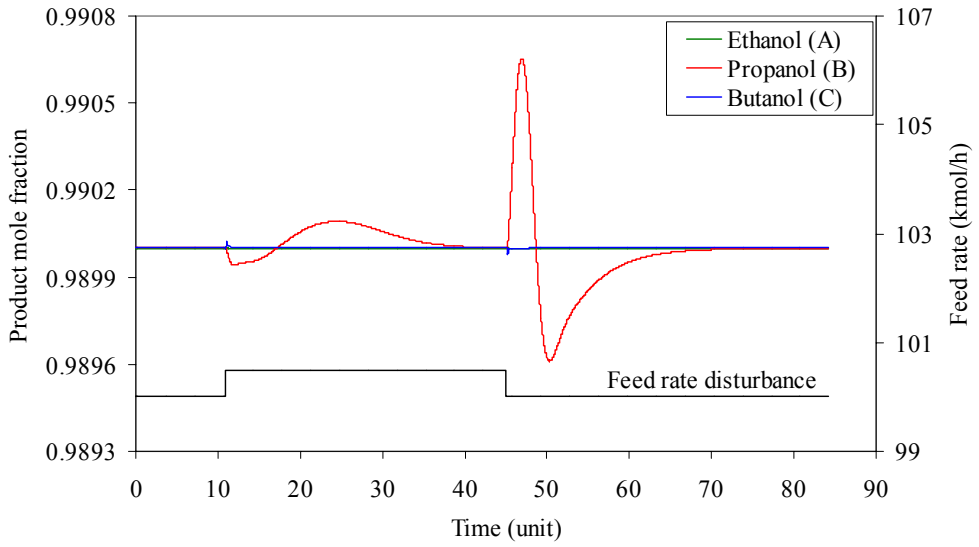

Figure 4.29: Closed-loop transient behavior of **DQF** scheme for feed rate disturbance using (L_1-D_2-B_2) manipulated variables

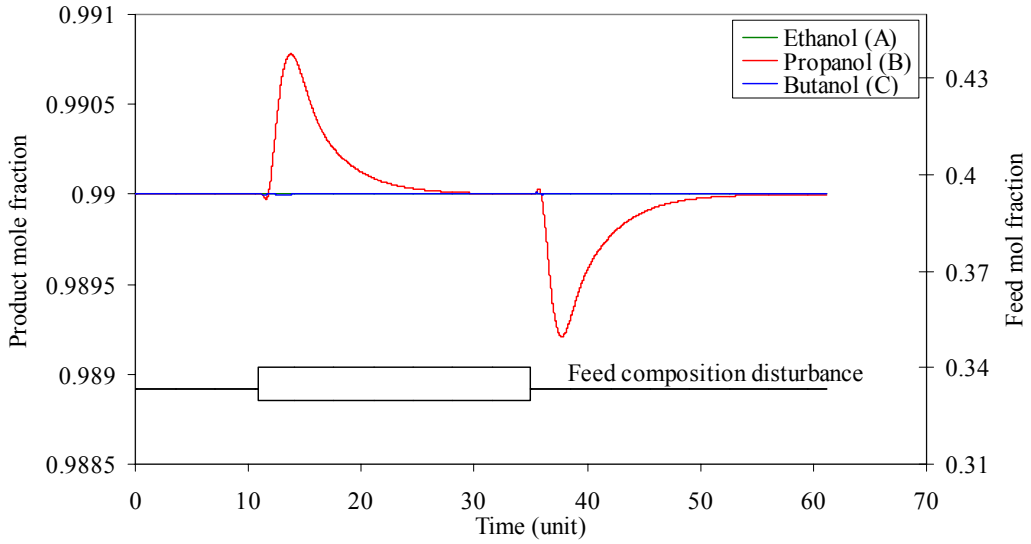

Figure 4.30: Closed-loop transient behavior of **DQF** scheme for feed composition disturbance using (L_1-D_2-B_2) manipulated variables

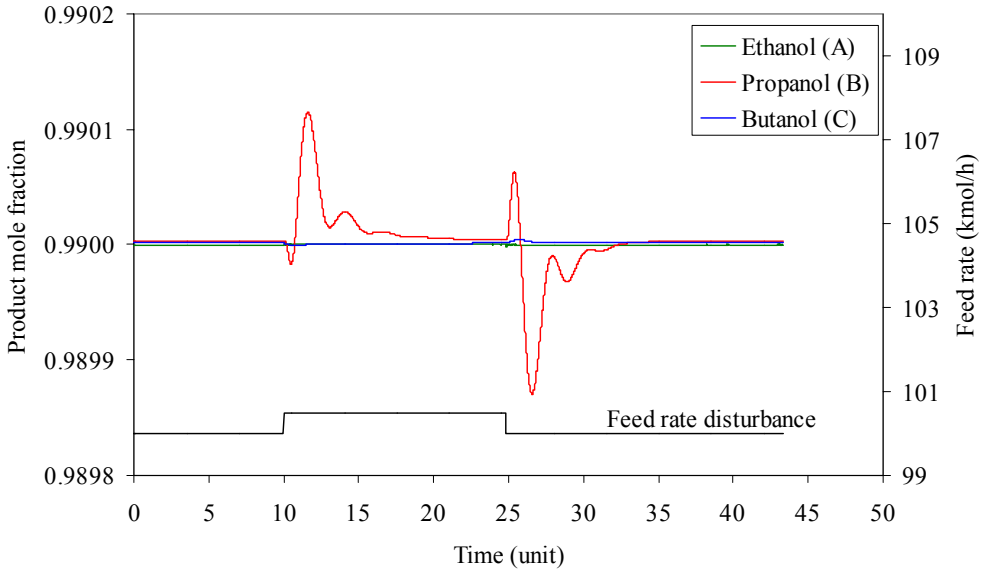

Figure 4.31: Closed-loop transient behavior of **DQF** scheme for feed rate disturbance using (L_1-D_2-Q_2) manipulated variables

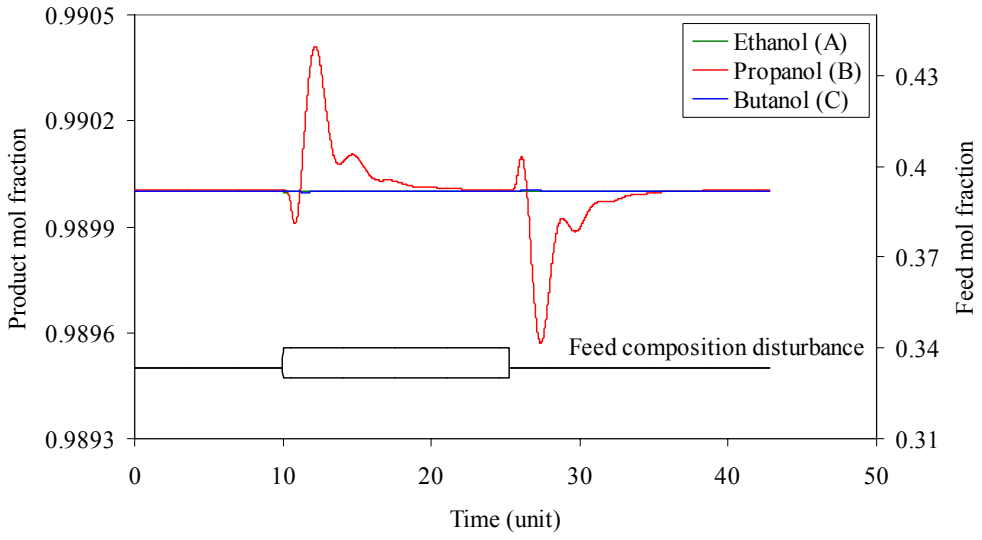

Figure 4.32: Closed-loop transient behavior of **DQF** scheme for feed composition disturbance using (L_1-D_2-Q_2) manipulated variables

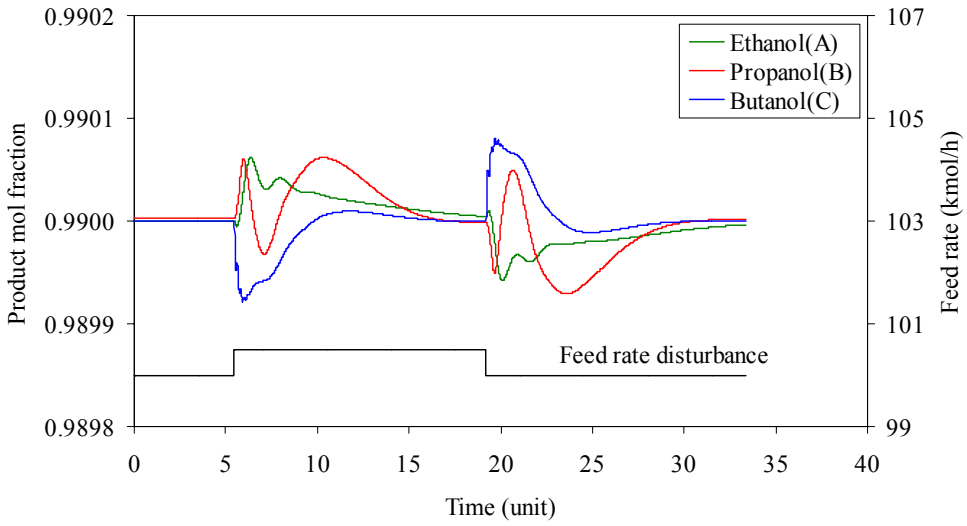

Figure 4.33: Closed-loop transient behavior of Petlyuk column (**SP**) for feed rate disturbance using (D-S-Q) manipulated variables

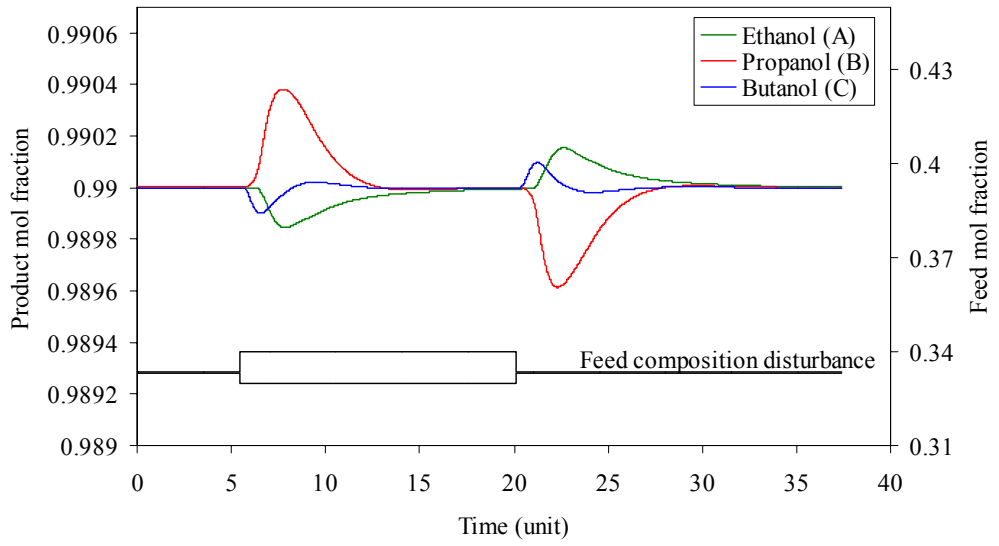

Figure 4.34: Closed-loop transient behavior of Petlyuk column (**SP**) for feed composition disturbance using (D-S-Q) manipulated variables

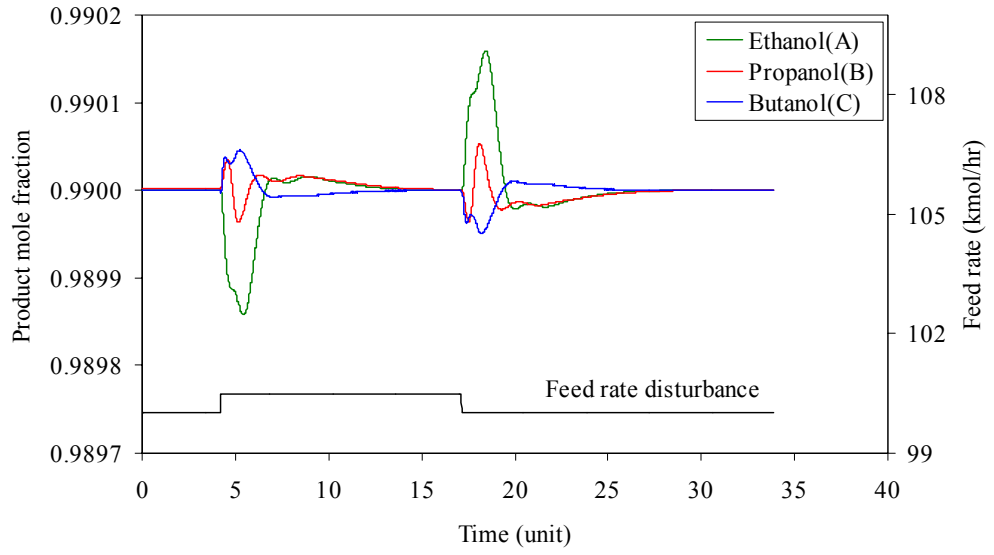

Figure 4.35: Closed-loop transient behavior of Petlyuk column (**SP**) for feed rate disturbance using (L-S-B) manipulated variables

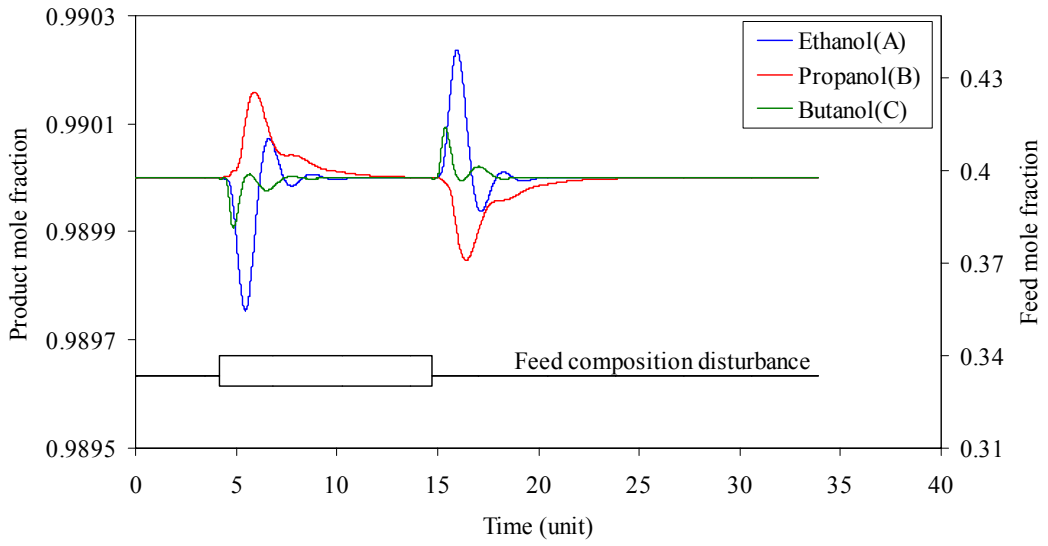

Figure 4.36: Closed-loop transient behavior of Petlyuk column (**SP**) for feed composition disturbance using (L-S-B) manipulated variables

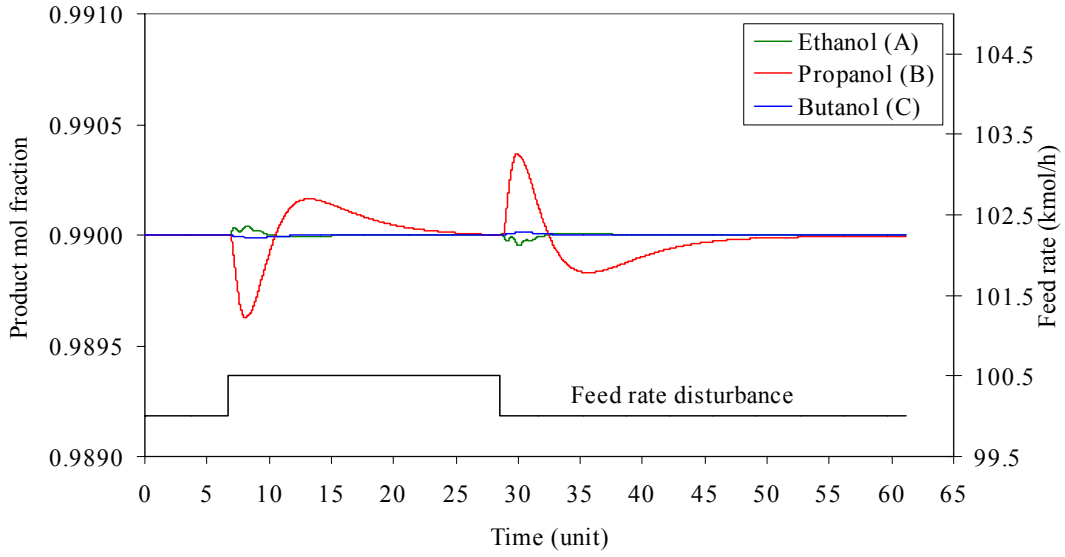

Figure 4.37: Closed-loop transient behavior of **SQF** scheme for feed rate disturbance using (D-S-Q) manipulated variables

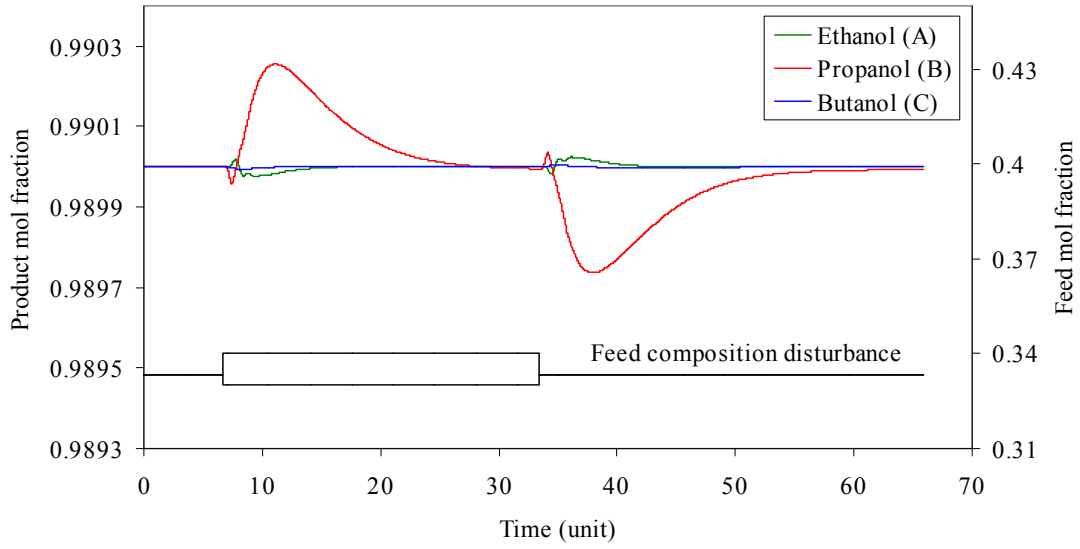

Figure 4.38: Closed-loop transient behavior of **SQF** scheme for feed composition disturbance using (D-S-Q) manipulated variables

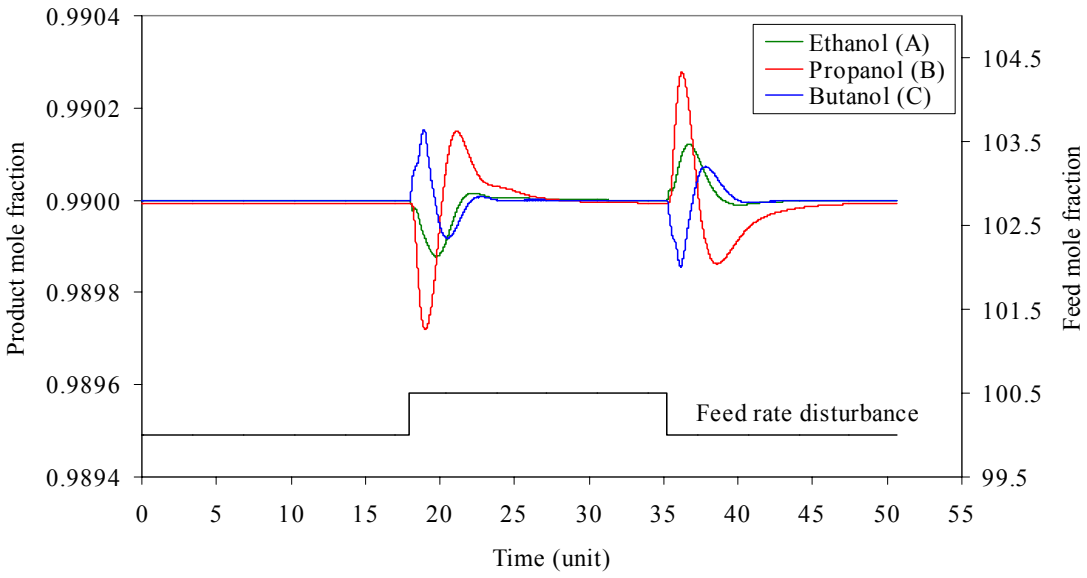

Figure 4.39: Closed-loop transient behavior of **SQF** scheme for feed rate disturbance using (L-S-B) manipulated variables

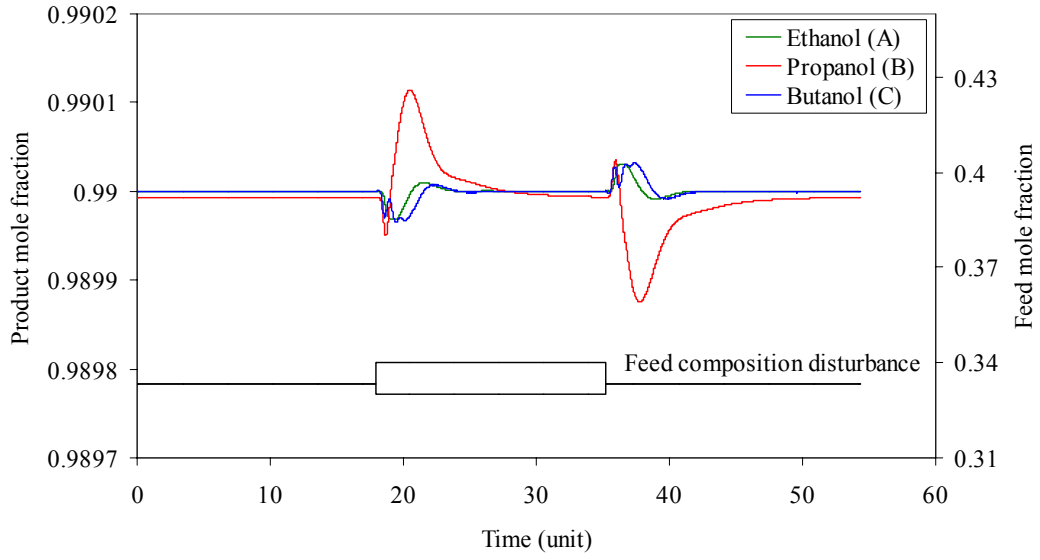

Figure 4.40: Closed-loop transient behavior of **SQF** scheme for feed composition disturbance using (L-S-B) manipulated variables

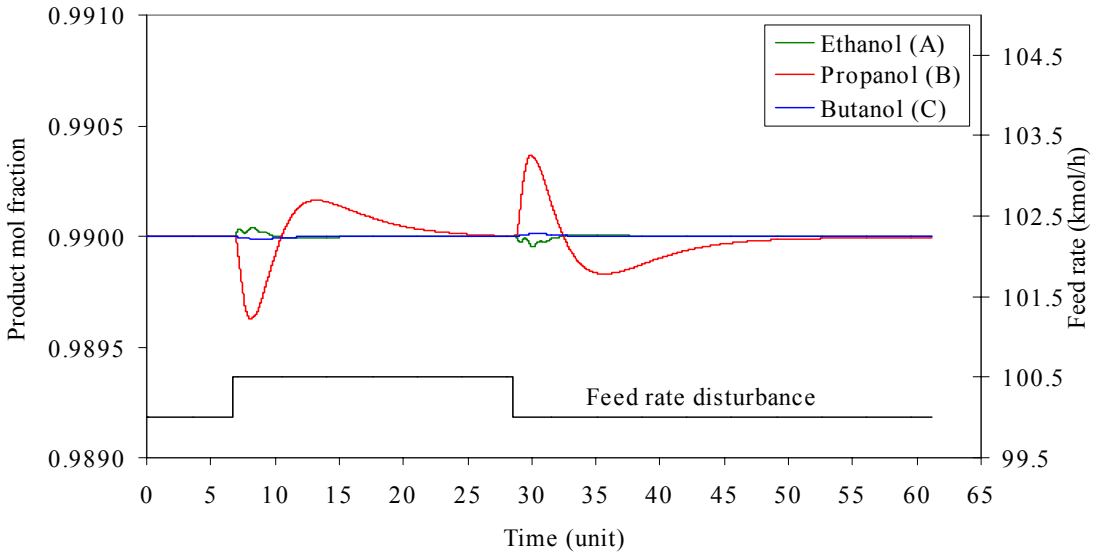

Figure 4.41: Closed-loop transient behavior of **SQF** scheme for feed rate disturbance using (D-S-Q) manipulated variables

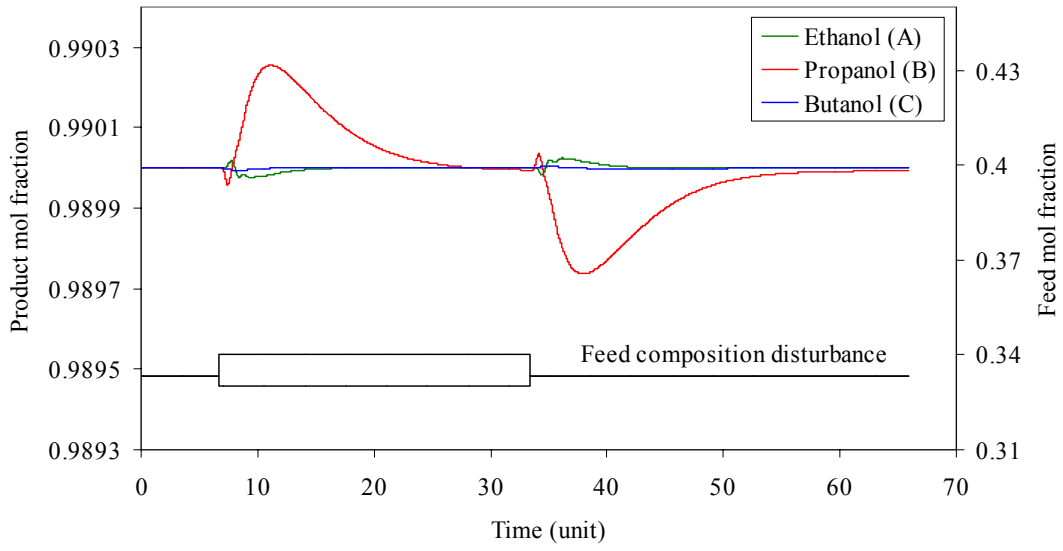

Figure 4.42: Closed-loop transient behavior of **SQF** scheme for feed composition disturbance using (D-S-Q) manipulated variables

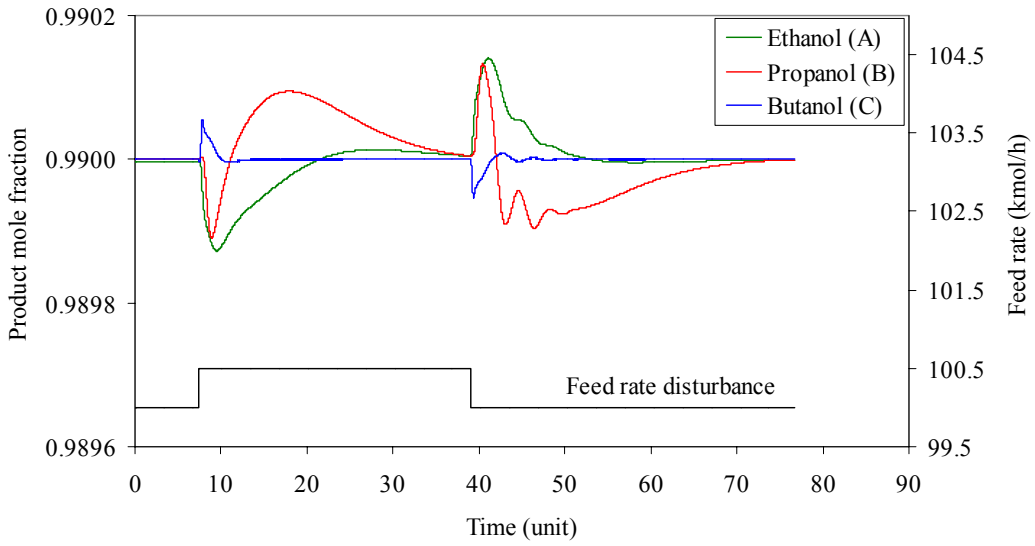

Figure 4.43: Closed-loop transient behavior of **SQB** scheme for feed rate disturbance using (L-S-B) manipulated variables

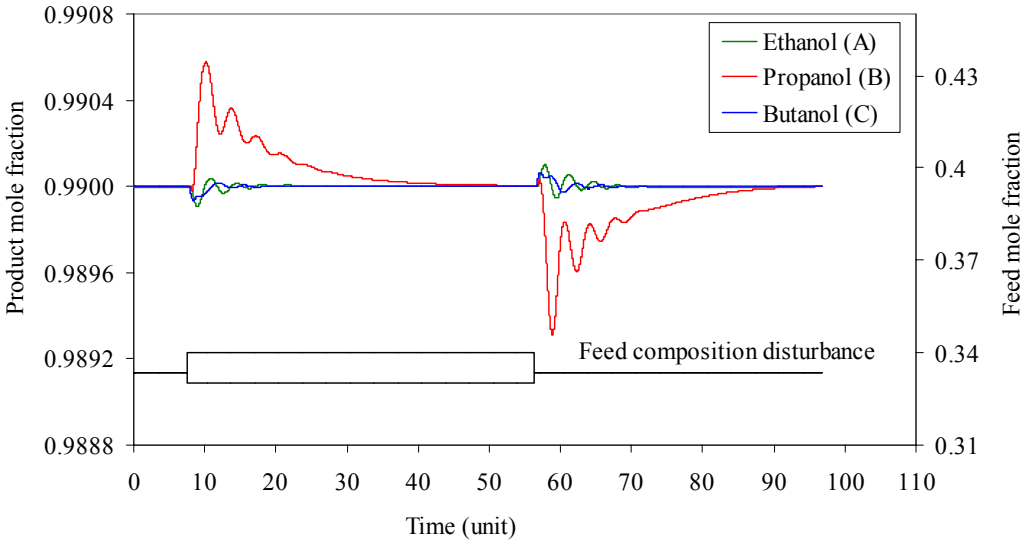

Figure 4.44: Closed-loop transient behavior of **SQB** scheme for feed composition disturbance using (L-S-B) manipulated variables

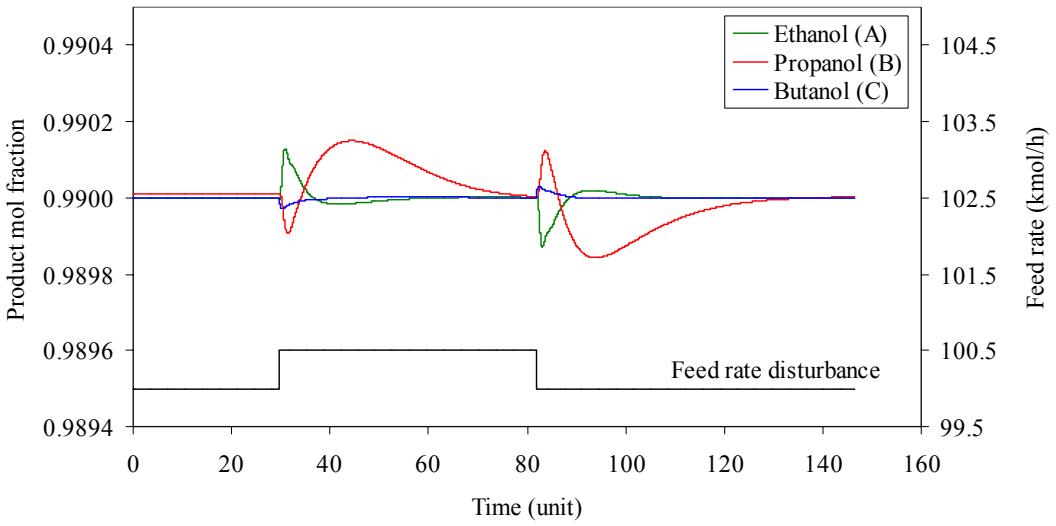

Figure 4.45: Closed-loop transient behavior of **SQB** scheme for feed rate disturbance using (D-S-Q) manipulated variables

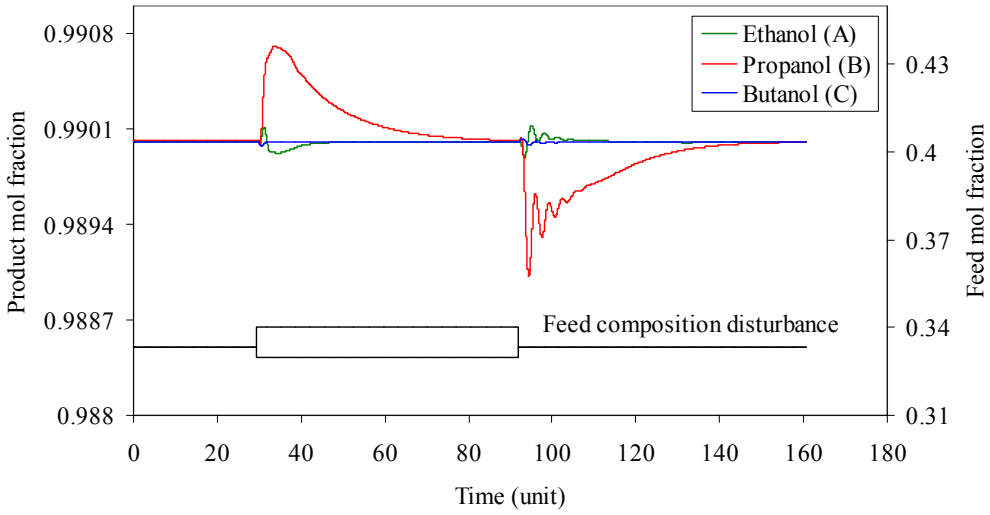

Figure 4.46: Closed-loop transient behavior of **SQB** scheme for feed composition disturbance using (D-S-Q) manipulated variables

4.2.11. Conclusions of the controllability case study

[1] The controllability study indicates that all the investigated schemes are controllable with decentralized controller structures.

[2] Open loop transient behavior of the studied schemes (conventional, conventional heat-integrated, Petlyuk column, and sloppy heat-integrated) show similar order of magnitude for the time constants (Tables 4.6-4.7) except for sloppy sequence with backward heat integration (**SQB**). **SQB** shows significantly slower dynamic behavior compared to the other schemes and its time constant is the highest.

[3] The conventional heat-integrated schemes doesn't deteriorate the controllability features significantly but the more complex arrangements (Petlyuk column, sloppy heat-integrated schemes), due to the serious internal interactions among the control loops, are more difficult to be controlled and they show worse controllability features than those of the conventional heat-integrated schemes.

[4] In case of energy integration those alternatives are easier to be controlled where the material flows and the energy flows in the same direction. This problem is, however, not serious in the case of the conventional heat-integrated schemes and this scheme can be generally recommended for the cases studied.

[5] The controllability features become critical in the case of the more complex sloppy heat integrated scheme. In case of the evaluation of the sloppy heat-integrated schemes the controllability features favor the arrangement where the material and energy flows in the same direction (e.g. **SQF)** and this makes the selection because the economic features of the **SQF** and **SQB** are similar. This result emphasizes again the necessity of the simultaneous consideration of the economic and controllability aspects during process design.

Chapter 5: Environmental consideration

Gaseous emissions from the process industries is one of the environmental problems in the industry and theses emissions can originate either from the process itself or the utility systems which service the process. In most cases combustion processes generate the largest volume of pollutants, which is associated with the utility systems. This study will deal with the flue gas emissions from the furnaces that are generated by the combustion processes of the utility systems.

Energy integration plays very important role not just in reducing the total cost of the chemical processes industries but also in reducing or minimizing the utility waste associated with the chemical process industries. In this chapter an estimation of the reduction of the flue gas emission by the various energy-integrated distillation schemes studied is presented.

5.1. Types of flue gas emissions

Gaseous pollutants can be divided into three categories:

1) the long-lived species (CO_2, CH_4, SO_2, N_2O) responsible for global warming,
2) the soluble acidic oxides (SOx, NOx) responsible for acid deposition,
3) the other species which contribute to smog and health hazards (particulates such as metal oxides, hydrocarbons, carbon monoxides, etc)

The main gaseous pollutants that are considered in this work are carbon dioxides, sulfur oxides, and nitrogen oxides.

5.2. Estimation of the flue gas emissions

Estimation of the flue gas emissions can be obtained by stoichiometric models (Smith and Delaby, 1991). For example, in the case of CO_2 where its emissions can be related to the amount of the fuel burnt by the following stiochiometric model:

$$C_nH_m + \left(n + \frac{m}{4}\right)O_2 \rightarrow nCO_2 + \frac{m}{2}H_2O \qquad [5\text{-}1]$$

It is assumed that all carbon in fuel is reacted to CO_2

$$CO_2 \ \ flow\ rate\left(\frac{kg}{h}\right) = \left(\frac{Q_{fuel}}{NHV}\right)\left(\frac{C\%}{100}\right)(\alpha_C) \qquad [5\text{-}2]$$

where

Q_{fuel} = heat duty from the fuel burnt (kJ/h)
NHV = fuel net heating value (kJ/h)
$C\ \%$ = mass percentage of carbon in fuel
$\propto_C$ = ratio of carbon dioxide and carbon molar masses (= 3.67)

The same type of stoichiometric model used for carbon dioxide can also be used for sulfur oxides:

$$C_nH_mS_p + \left(n + \frac{m}{4} + p\right)O_2 \rightarrow nCO_2 + \frac{m}{2}H_2O + pSO_2 \qquad [5\text{-}3]$$

however, sulfur in fuel is also reacted to SO_3:

$$SO_2 + \frac{1}{2}O_2 \leftrightarrow SO_3 \qquad [5\text{-}4]$$

The amount of SO_3 in flue gas varies but is usually around 10 % of the total SO_x. It is not necessary for the present purposes to distinguish between SO_2 and SO_3. It is therefore assumed that all sulfur is reacted to SO_2.

$$SO_2 \ \ flow\ rate\left(\frac{kg}{h}\right) = \left(\frac{Q_{fuel}}{NHV}\right)\left(\frac{S\%}{100}\right)(\alpha_S) \qquad [5\text{-}5]$$

where

Q_{fuel} = heat duty from the fuel burnt (kJ/h)

NHV = fuel net heating value (kJ/h)

$S\ \%$ = mass percentage of sulfur in fuel

$\propto_S$ = ratio of sulfur dioxide and sulfur molar masses (= 2)

There are two main reaction paths for NO_x formation:

(a) Thermal NO_x

$$N_2 + O_2 \leftrightarrow 2NO \quad [5\text{-}6]$$

$$NO + \frac{1}{2}O_2 \leftrightarrow NO_2 \quad [5\text{-}7]$$

Thermal NO_x is formed particularly at high temperatures.

(b) Fuel bound NO_x

$$[Fuel\ N] + \frac{1}{2}O_2 \leftrightarrow NO \quad [5\text{-}8]$$

$$NO + \frac{1}{2}O_2 \leftrightarrow NO_2 \quad [5\text{-}9]$$

It is virtually difficult to calculate a precise value of for the NO_x emitted by a real device. Therefore we have used estimates based on observed values found for different combustion technology (Smith and Delaby, 1991).

Table 5.1: Emission factors of steam boiler per unit of heat delivered to the process

	CO_2 (kg/ MW .hr)		SO_x (kg /MW.hr)		NO_x (kg /MW.hr)	
	Natural gas	Petroleum oil	Natural gas	Petroleum oil	Natural gas	Petroleum oil
LP-steam	188	264	0.14	0.65	0.03	0.12
MP-steam	204	286	0.15	0.71	0.05	0.14

Two different types of fuel, natural gas and petroleum oil are estimated its flue gas emissions factors for producing low-pressure steam level (LP-steam) and medium-pressure steam level (MP-steam) as shown in Table 5.1.

5.3 Flue gas emission by various energy-integrated schemes

Table 5.2: The flue gas emissions of Case 1

Schemes	**D**		**DQB**		**SP**		**SQF**		**SQB**	
Heating rate (MW)	5.5		3.7		3.5		3.4		3.5	
Fuel type	Natural gas	P.oil	Natural gas	P.oil	Natural gas	P.oil	Natural gas	P.oil	Natural gas	P.oil
CO_2 emissions (kg/hr)	1030	1447	691	971	659	926	689	968	716	1006
SO_x emissions (kg/hr)	0.75	3.57	0.50	2.39	0.48	2.28	0.50	2.39	0.52	2.48
NO_x emissions (kg/hr)	0.16	0.66	0.11	0.44	0.11	0.42	0.17	0.47	0.18	0.49
Total emissions (kg/hr)	1031	1451	692	974	660	928	689	971	717	1009
Emissions saving %	0		33		36		33		31	

Table 5.3: The flue gas emissions of Case 2

Schemes	**D**		**DQB**		**SP**		**SQF**		**SQB**	
Heating rate (MW)	6.7		3.7		4.5		3.2		3.2	
Fuel type	Natural gas	P.oil	Natural gas	P.oil	Natural gas	P.oil	Natural gas	P.oil	Natural gas	P.oil
CO_2 emissions (kg/hr)	1255	1762	691	970	837	1176	646	908	661	928
SO_x emissions (kg/hr)	0.91	4.34	0.50	2.39	0.61	2.90	0.47	2.24	0.48	2.29
NO_x emissions (kg/hr)	0.20	0.80	0.11	0.44	0.13	0.54	0.16	0.44	0.16	0.45
Total emissions	1256	1768	691	973	838	1180	647	911	661	931
Emissions saving %	0		45		33		48		47	

Table 5.4: The flue gas emissions of Case 3

Schemes	**D**		**DQB**		**SP**		**SQF**		**SQB**	
Heating rate (MW)	8.3		7.2		5.7		3.8		3.6	
Fuel type	Natural gas	P.oil	Natural gas	P.oil	Natural gas	P.oil	Natural gas	P.oil	Natural gas	P.oil
CO_2 emissions (kg/hr)	1567	2201	1360	1911	1068	1500	714	1003	678	952
SO_x emissions (kg/hr)	1.13	5.42	0.99	4.71	0.77	3.70	0.52	2.47	0.49	2.35
NO_x emissions (kg/hr)	0.25	1.00	0.22	0.87	0.17	0.68	0.11	0.46	0.11	0.43
Total emissions	1568	2207	1361	1916	1069	1505	715	1006	679	955
Emissions saving %	0		13		32		54		57	

5.4. Conclusions of the estimated flue gas emissions

(a) Case 1: in this case **SP** scheme shows the best scheme in gas emission savings with 36 % comparing to the base case (**D**). Although heating rate consumption of **SP** scheme is equal to that of **SQB** scheme and higher than SQF scheme, this means the operating pressure makes the difference and its clear that SP scheme operates at atmospheric pressure and LP-steam is used, consequently lower flue gas emissions are expected. In case of sloppy schemes (**SQF** and **SQB**) which is usually operated at higher pressures and MP-steam is used, the emissions are higher due to the use of MP-steam.

(b) Case2: in this case sloppy schemes are the best in gas emissions saving with 48-47 %, and this result is due to the lower heating rate of these schemes comparing to the other investigated schemes.

(c) Case 3: in this case also sloppy schemes are showing the highest emissions savings with 57 % and 54 % for **SQB** and **SQF** respectively, and its again due to lower heating demands for these schemes compares to the other energy-integrated schemes.

(d) As a general conclusion, the heating demands of the schemes is making the decision about the gas emissions savings, and if the difference between heating demands is close, steam level will make the decision. Fortunately this trend is found in the economic study of the energy-integrated schemes for TAC savings.

Chapter 6: Conclusions and major new results

Various energy-integrated schemes are investigated rigorously for the sake of lowering the high-energy consumption of distillation unit, which is the baseline in chemical process industries. Design, simulation, operation, and control aspects are analyzed, having the conventional distillation scheme as comparison basis. This study covers conventional schemes, conventional heat-integrated schemes, fully thermal coupled system (Petlyuk column), and sloppy heat-integrated schemes.

6.1. Conclusions of the economic study

A general rule governing the ranks of the studied schemes according to total annual costs (TAC) is the increasing heat duty requirement with increasing concentration of component B in the feed. The schemes with energy integration are sensitive for the heat duty while the Petlyuk column without energy integration (but thermal coupling) is not. The savings in TAC of Petlyuk columns are uniformly about 30 % to 33 % in all the three cases.

CASE 1: Here the Petlyuk column (**SP**) is the winner with 28 and 33 % savings in U.S. utility price and European utility price respectively. There is no qualitative ranking difference considering the two price structures. The second ranked direct sequence with backward heat integration (**DQB**) with 24 and 30 % savings that cannot be more because of low heat duty. It is back just with 3%. The forward heat integrated sloppy scheme (**SQF**, 21 % savings) is just the 4th ranked in case of U.S. utility prices, probably because there is an **AB→C** energy integration that involves a pressure shift and use of high pressure steam.

CASE 2, U.S. utility prices: Here the Petlyuk column is not amongst the best schemes. Direct sequence with backward heat integration (**DQB**) with 35% savings is at the 3rd place backed just with 1 % by both forward heat integrated sloppy scheme (**SQF**) and backward heat integrated sloppy scheme (**SQB**) by their 36% savings.

CASE 2, European utility prices: Here the direct sequence with backward integration (**DQB**) is the winner with 41% savings. Both the 2nd ranked forward integrated sloppy schemes (**SQF**, 36% savings) and the 3rd ranked backward integrated sloppy scheme (**SQB**, 30% savings) involve unpreferable integration **AB→C** or the even wider boiling point gap **A→C** comparing to the **B→BC** integration in the winner scheme.

CASE 3: This is the case where the heat integrated sloppy schemes, namely the 1st ranked backward heat integrated sloppy scheme (**SQB**, 53 % savings) and the 2nd ranked forward integrated sloppy scheme (**SQF**, 51 % savings) come to play since the heat duty is really high. The Petlyuk column (**SP**) with its 30 % savings is just 4th behind the 3rd ranked direct sequence with backward integration (**DQB**, 32 % savings).

Comparing the optimization results of rigorous simulations to the corollaries of the short-cut analysis, the domain where the thermally coupled system wins is even much lower, and is constrained to a small area near the **AC** edge of the composition triangle at balanced relative volatility ratio. At balanced relative volatility ratio and equimolar feed composition, as well as near the node of pure **B**, the Petlyuk column takes only the fourth place behind the heat-integrated schemes at European and U.S. price structures (Case 2 and Case 3). Yet, the Petlyuk column wins over the heat-integrated schemes at 10 % middle component in the feed. Its advantage, in total annual costs, over the second best (heat-integrated) scheme is no more than 5-6 %.

Considering all the energy, cost, operability and flexibility viewpoints, the advantageous application of the thermally coupled systems, if it exists indeed, is constrained to a very small range of relative volatility ratio, feed composition, and price structure. This small range is situated somewhere around balanced relative volatility ratio **A/B** to **B/C**, small amount of the middle component **B** (e.g. Case 1), balanced presence of the two swing components **A** and **C** in the feed or a little bit shifted to the direction of **C**.

On the other hand, the integrated sloppy schemes win, in a great TAC percent, at high **B** ratio in the feed, while the conventional heat integrated schemes, **DQB** in our particular case, is the best choice at equimolar feed.

In this economic study the optimized schemes are classified according to the ranking in TAC savings. Since the difference in TAC savings between the optimized schemes is a few percentages, a further aspect will be taken into consideration. Controllability features become critical in these cases and Chapter 4 will focus on the controllability aspects.

6.2. Conclusions of the optimal fractional recovery of the middle component

Theoretical fractional recovery β^* can be used as initial design parameter for Petlyuk column (**SP**) to determine the optimum solution of the recycle streams and theses results are in agreement with the previous study of Annakou and Mizsey (1996). This design parameter is found to be valid also for sloppy separation sequences (**SQF** and **SQB** schemes). In case of **SQF** scheme, due to the high pressure of the prefractionator a slight deviation is found in the optimal fractional recovery β_o from the theoretical values β^* especially in Case 1 and Case 2. In general TAC is not affected and the overall ranking of the schemes still the same. These results indicate that using of β^* as initial estimate is recommended in order to save effort and time on calculations.

6.3. Conclusions of the controllability study

6.3.1. Steady-state control indices study

Steady-state control analysis is carried out for the optimum schemes by investigating their control indices (Niederlniski index (NI), Morari resiliency (MRI), and RGA). The results show the following:

- The schemes are controllable with decentralized controller structures.
- Petlyuk column and sloppy heat integrated schemes shows poor indices and strong interactions in feed composition 1.
- Feed compositions 2 and 3 show good controllability indices than the same schemes of feed composition 1.
- Direct sequence with backward heat integration (**DQB**) is always the best from steady-state control analysis point of view.

6.3.2. Dynamic simulations case study

1. The controllability study indicates that all the investigated schemes are controllable with decentralized controller structures.

2. Open loop transient behavior of the studied schemes (conventional, conventional heat-integrated, Petlyuk column, and sloppy heat-integrated) show similar order of magnitude for the time constants (Tables 4.6-4.7) except for sloppy sequence with backward heat integration (**SQB**). **SQB** shows significantly slower dynamic behavior compared to the other schemes and its time constant is the highest.

3. Closed-loop dynamic simulations of the studied schemes (conventional, conventional heat-integrated, Petlyuk column, and sloppy heat-integrated) show the following:

(a) The conventional heat-integrated schemes doesn't deteriorate the controllability features significantly but the more complex arrangements (Petlyuk column, sloppy heat-integrated schemes), due to the serious internal interactions among the control loops, are more difficult to be controlled and they show worse controllability features than those of the conventional heat-integrated schemes.

(b) In case of energy integration those alternatives are easier to be controlled where the material flows and the energy flows in the same direction. This problem is, however, not serious in the case of the conventional heat-integrated schemes and this scheme can be generally recommended for the cases studied.

(c) The controllability features become critical in the case of the more complex sloppy heat integrated scheme. In case of the evaluation of the sloppy heat-integrated schemes the controllability features favor the arrangement where the material and energy flows in the same direction (e.g. **SQF)** and this makes the selection because the economic features of the **SQF** and **SQB** are similar. This result emphasizes again the necessity of the simultaneous consideration of the economic and controllability aspects during process design.

6.4. Conclusions of the estimated flue gas emissions

(i) Case 1: in this case **SP** scheme shows the best scheme in gas emission savings with 36 % comparing to the base case (**D**). Although heating rate consumption of **SP** scheme is equal to that of **SQB** scheme and higher than SQF scheme, this means the operating pressure makes the difference and its clear that SP scheme operates at atmospheric pressure and LP-steam is used, consequently lower flue gas emissions are expected. In case of sloppy schemes (**SQF** and **SQB**) which is usually operated at higher pressures and MP-steam is used, the emissions are higher due to the use of MP-steam.

(ii) Case2: in this case sloppy schemes are the best in gas emissions saving with 48-47 %, and this result is due to the lower heating rate of these schemes comparing to the other investigated schemes.

(iii) Case 3: in this case also sloppy schemes are showing the highest emissions savings with 57 % and 54 % for **SQB** and **SQF** respectively, and its again due to lower heating demands for these schemes compares to the other energy-integrated schemes.

(iv) As a general conclusion, the heating demands of the schemes is making the decision about the gas emissions savings, and if the difference between heating demands is close, steam level will make the decision. Fortunately this trend is found in the economic study of the energy-integrated schemes for TAC savings.

6.5. Major new results

Thesis 1. For the studied ternary mixture, heat-integrated conventional-schemes show the best economic features in case of equimolar feed (0.33/0.33/0.33) and very competitive to Petlyuk column at lower concentration of middle component B in the feed (0.45/0.1/0.45).

Thesis 2. The economic applications of the Petlyuk arrangement are constrained to a very small range of feed composition and relative volatility ratio. Since it is situated around balanced ratio of relative volatility **A/B** to **B/C**, small amount of the middle component **B**, and balanced presence of the two swing components **A** and **C** in the feed.

Thesis 3. Sloppy heat-integrated schemes (complex arrangements) have the highest TAC savings only at high concentration of middle component B (0.1/0.8/0.1).

Thesis 4. The optimum fractional recovery (β_o) of the middle component in the prefractionator column is found close to the theoretical values (β^*) in most of the cases (Table 3.8). The selection of the theoretical fractional recovery (β^*) as an initial design parameter is very important in determining the internal recycle streams in the Petlyuk arrangement and its extended for sloppy separation sequence and found to be valid also. The TAC is very sensitive to the optimum fractional recovery parameter (β_o).

Thesis 5. A general rule governing the ranking of the optimized schemes is that the priority for heat-integrated schemes to achieve higher savings in energy and TAC increases with higher middle component **B** concentration in the feed. The reason of this effect is that the heat requirement for the separation increases drastically with increasing concentration of the intermediate boiling substance **B** in the feed.

Thesis 6. At the price structure valid for the time being, the utility costs proved to be dominating the economic scheme selection. This explains the superiority of the

conventional and sloppy heat integrated schemes in both price structures (European and U.S. utility prices).

Thesis 7. Open loop transient behavior of the studied schemes (conventional, conventional heat-integrated, Petlyuk column, and sloppy heat-integrated) show similar order of magnitude for the time constants except for sloppy sequence with backward heat integration (**SQB**) (Tables 4.6-4.7). **SQB** shows significantly slower dynamic behavior compared to the other schemes and its time constant is the highest.

Thesis 8. The results of closed-loop dynamic behavior studies (Tables 4.8-4.9) show that complex distillation schemes (Petlyuk column and sloppy heat-integrated schemes) have worse controllability features by showing longer settling time and higher overshoots compared to conventional heat-integrated schemes. These results indicate that the interactions due to the control of three-product column, and flow direction of materials and energy plays important role on the transient dynamic behavior of the schemes. The schemes which have material and energy going in the same direction always faster than that having materials and energy flows in opposite direction. This phenomena becomes much more significant in the case of sloppy sequence with backward heat integration (**SQB**), due to interactions inside the column and the opposite directions of materials and energy. The effect of these obstacles on the heat-integrated conventional schemes is not significant.

Thesis 9. Petlyuk arrangement shows slower dynamic behavior in closed-loop compared to the conventional heat-integrated schemes and shows longer settling time due to the interactions inside the main column.

Thesis 10. The savings in gas emissions are proportional to the savings in energy of the energy-integrated schemes (Tables 5.2, 5.3, and 5.3) and a reduction of the flue gas emissions can be achieved in the range of 36-57 % compared to the conventional distillation schemes. The percentage of savings increases in the direction of increasing middle component **B** in the feed.

References

Abdul Mutalib, M. I. and Smith, R. (1998). Operation and control of dividing wall columns. *Transactions of Institute of Chemical Engineering, 76* (part A), 308.

Agrawal, R. (1996). Synthesis of distillation column configurations for a multicomponent separation. *Industrial Engineering and Chemistry Research,35,* 1059.

Agrawal, R. and Fidkoweski, Z. (1998). Are thermally coupled distillation columns always thermodynamically more efficient for ternary distillation? *Industrial Engineering and Chemistry Research,37,* 3444.

Annakou, O. (1996). Rigorous comparative study of energy integrated distillation schemes. *PhD Thesis.* Technical University of Budapest, Hungary.

Annakou, O. and Mizsey, P. (1996). Rigorous comparative study of energy-integrated distillation schemes. *Industrial Engineering and Chemistry Research, 35,* 1877.

Becker, H., Godorr, S., Kreis, H., and Vaughan, J. (2001). Partition distillation columns-Why, When & How. *Chemical Engineering,* January, 68.

Benedict, M. (1974). *Chemical Engineering Progress., 43*, 41.

Berglund, R. L. and Lawson, C. T. (1991). Preventing pollution in the CPI. *Chemical Engineering,* September, 120.

Biegler, L. T., Grossmann, I. E. and Westerberg, A. W. (1997). Systematic Methods for Chemical Process Design, Prentice-Hall, NJ.

Bildea, C. S., and Dimian, A. C. (1999). Interaction between design and control of a heat-integrated distillation system with prefractionator. *Trans IchemE.*, *77,* 597.

Douglas, J. M. (1985). A hierarchical design procedure for process synthesis. *American Institute of Chemical Engineers Journal*, 31, 353.

Douglas, J. M. (1988). Conceptual Design of Chemical Process. McGraw-Hill Inc., New York.

Douglas, J. M. (1992). Process synthesis for waste minimisation, *Industrial Engineering and Chemistry Research, 31,* 238.

Dunnebier, G. and Pantelides, C. C. (1999). Optimal design of thermally coupled distillation columns. *Industrial Engineering and Chemistry Research, 38,* 162.
Emtir, M., Mizsey, P., Rev, E. and Fonyo, Z. (2002). Economic Optimization and Control of Energy-Integrated Distillation Schemes. Paper submitted to *Chemical and Biochemical Engineering Quarterly*.

Emtir, M., Rev, E. and Fonyo, Z. (2001). Rigorous simulation of energy integrated and thermally coupled distillation schemes for ternary mixture. *Applied Thermal Engineering*, Pergamon. 21, 1299-1317.

Fidkowski, Z. and Krolikowski, L. (1986). Thermally coupled system of distillation columns: optimization procedure. *American Institute of Chemical Engineers Journal*, 32, 537.

Fisher, W. R., Doherty, M. F. and Douglas, J. M. (1988). The interface between design and control. *Industrial Engineering and Chemistry Research, 27,* 597.

Fonyo, Z and Benko, N. (1998). Comparison of various heat pump assisted distillation configurations. *Transactions of Institute of Chemical Engineering, 76* (part A), 348.

Fonyo, Z. (1974). Thermodynamic analysis of rectification I. reversible mode of rectification. *International Chemical Engineering, 14*, 18.

Fonyo, Z. and Benko, N. (1996). Enhancement of process integration by heat pumping. *Computers and Chemical Engineering, 20,* 85.

Fonyo, Z., Szabo, J. and Foldes, P. (1974). Study of thermally coupled distillation system. *Acta Chimica Academia Scientiarum Hungaricae, 82,* 235.

Glinos, K., Malone, M. F. (1988). Optimality regions for complex column alternatives in distillation systems*. Chemical Engineering Research Design*, *66*, 229.

Grossmann, I. E. and Morari, M. (1984). Operability, resiliency, and flexibility-process design objectives for a changing world, *Proc. Of the 2nd Int. Conf. On Foundation of Computer Design,* Austin, Texas, pp. 931.

Halvorsen, I. J. and Skogestad, S. (1997). Opimizing control of Petlyuk distillation: Understanding the steady-state behavior, *Computers and Chemical Engineering*, 21, 249.

Hernandez, S. and Jimenez, A. (1999). Controllability analysis of thermally coupled distillation systems. *Industrial Engineering and Chemistry Research, 38,* 3957.

Huckins, H. A. (1978). Conserving energy in chemical plants. *Chemical Engineering Progress*, May, 85.

Humphrey, J. L. (1995). Separation process: playing a critical role. Chemical Engineering Progress, October 1995.

Humphrey, J. L. and Seibert, A. F. (1992). Separation Technologies: An opportunity for energy savings, *Chemical Engineering Progress*, March, 32.

HYSYS Reference volume 1 and 2, Hyprotech Ltd., 1996.

Jimenez, A., Hernandez, S., Montoy, F. A., and Zavala-Garcia, M. (2001). Analysis of control properties of conventional and non-conventional distillation sequence. *Industrial Engineering and Chemistry Research, 40,* 3757.

Kaibel, G. (1987). Distillation columns with vertical partition. *Chemical Engineering Technology, 10,* 92.

King, C. J. (1980). Separation processes 2nd Ed., McGraw-Hill Inc., New York.

Luyben, W. L. (1990). Process modeling, Simulation and control for chemical Engineering. McGraw-Hill Inc., New York.

Luyben, W. L., Tyreus, B. D. and Luyben, M. L. (1999). Plantwide process control. McGraw-Hill Inc., New York.

MATLAB, The MathWorks, Inc. Version 5.1.0.421. (1997).

Meszaros, I. and Fonyo, Z. (1986). Design strategy for heat pump assisted distillation system. *Heat Recovery Systems*, *6,* 469.

Meszaros, I. and Fonyo, Z. (1988). A simple heuristic method to select heat-integrated distillation schemes. *Chemical Engineering Science*, *43,* 3109.

Mix, T. J., Dweck, J. S., Weinberg, M. and Armstrong, R. C. (1978). Energy conservation in distillation. *Chemical Engineering Progress*, April, 49.

Mizsey, P. (1991). A global approach to the synthesis of entire chemical process. *Ph.D theises,* ETH-Zurich.

Mizsey, P. (1994). Waste reduction in the chemical industry. *Journal of Hazardous Material, 37,* 1.

Mizsey, P., Fonyo, Z. (1990). Towards a more realistic process synthesis-The combined approach. *Computers and Chemical Engineering, 14,* 1303.

Mizsey, P., Hau, N. T., Benko, N., Kalmar, I. and Fonyo, Z. (1998). Process control for energy integrated distillation schemes. *Computers and Chemical Engineering, 22,* 427.

Morari, M. (1983). Design of resilience processing plants-III. A general framework for the assessment of dynamic resilience. *Chemical Engineering Science,* 38, 1881.

Nishida, N. G., Stephanopoulos, G. and Westerberg, A. W. (1981). A review of process synthesis, *American Institute of Chemical Engineers Journal*, 321.

Papastathopoulou, H. and Luyben, W. L. (1991). *Industrial Engineering and Chemistry Research, 30,* 705.

Peter, M. S., and Timmerhaus, K. D. (1988). Plant Design and Economic for Chemical Engineer. 3d ed., McGraw-Hill Inc., New York.

Petlyuk, F. B., Platonov, V. M. and Slavinskii, D. M. (1965). Thermodynamically optimal method for separating multicomponent mixtures. *International Chemical Engineering, 5,* 561.

Rathore, R. N. S., Van wormer, K. N., and Powers, G. J. (1974 b). Synthesis of distillation systems with energy integration. *American Institute of Chemical Engineers Journal, 20,* 940.

Rev, E. (1990). The constant heat transport model and design of distillation columns with one single distributing component, *Industrial Engineering and Chemistry Research, 29,* 1935.

Rev, E., Emtir, M., Szitkai, Z., Mizsey, P., and Fonyo, Z. (2001). Energy savings of integrated and coupled distillation systemes. *Computers and Chemical Engineering*, Elsevier. 25, 119-140.

Richard, T., Richard, C. B., Wallace, B. W. and Joseph, A. S. (1998). Analysis, Synthesis, and Design of Chemical Processes, Prentice-Hall, NJ.

Rosenbrock, H. H. (1970). State-space and multivariable control, Nelson, London.

Schultz, M. A., Stewart, D. G., Harris, J. M., Rosenblum, S. P., Shakur, M. S., and O'brien, D. E. (2002). Reduce costs with dividing-wall columns, *Chemical Engineering Progress*, May, 64.

Serra, M., Espuna, A., and Puigjaner, L. (1999). Control and optimization of the dividing wall column, *Chemical Engineering and Processing*, *38,* 549.

Serra, M., Perrier, M., Espuna, A., and Puigjaner, L. (2001). Analysis of different control possibilities for the dividing wall column: feedback diagonal and dynamic matrix control, *Computers and Chemical Engineering*, *25,* 859.

Skogestad, S. (1997). Dynamic and control of distillation columns – A critical survey. *Modeling, Identification and Control*, 18, 177-217.

Smith, R. (1995). Chemical Process design. McGraw-Hill Inc., New York.

Smith, R. and Delaby, O. (1991). Targeting flue gas emissions, *Trans. IChemE*, *69*, 492.

Smith, R., and Linnhoff, B. (1988). The design of separators in the context of overall process. *Trans. IchemE.,* 66, 195.

Stichlmair, J. and Stemmer, A. (1989). Reduction of energy requirement in distillation. *Chemical Engineering Technology, 12,* 163.

Stupin, W. J. and Lockhart, F. J. (1972). Thermally coupled distillation–A case history, *Chemical Engineering Progress*, *68,* 71.

Tedder, W. D. and Rudd, D. F. (1978). Parametric Studies in Industrial Distillation. *American Institute of Chemical Engineers Journal, 24,* 303.

Treybal, R. E. (1986). Mass transfer operation 2nd Ed., McGraw-Hill Inc., New York.

Triantafyllou, C., and Smith, R. (1992). The design and optimisation of fully thermally coupled distillation columns. *Trans IchemE., 70,* 118.

Wolff, E. A. and Skogestad, S. (1995). Operation of integrated three-product (Petlyuk) distillation columns. *Industrial Engineering and Chemistry Research*, 34, 2094.

Wright, R. O. (1949). Fractionation apparatus, *US Patent No. 2, 471,* 134.

Yu, C. and Luyben, W. L. (1987). Control of multicomponent distillation columns using rigorous composition estimators. *I. Chem. E. Symposium Ser.* No. 104, 29.

Publications

(I) Contributions in scientific journals

1. M. Emtir, E. Rev, P. Mizsey, and Z. Fonyo (**1999**)
   "Comparison of integrated and coupled distillation schemes using different utility prices", *Computers and Chemical Engineering,* Pergamon. Vol. 23, S799-S802.

2. Z. Fonyo, E. Rev, Z. Szitkai, M. Emtir, and P. Mizsey (**1999**) "Energy savings of integrated and coupled distillation systemes", *Computers and Chemical Engineering,* Pergamon. Vol. 23, S89-S92.

3. M. Emtir, E. Rev, and Z. Fonyo (**2000**)
   "Rigorous simulation of energy integrated and thermally coupled distillation schemes for ternary mixture", *Journal of Saharian Studies*, Volume No. 2, Issue 5, Murzuk-Libya.

4. M. Emtir, E. Rev, and Z. Fonyo (**2001**)
   "Rigorous simulation of energy integrated and thermally coupled distillation schemes for ternary mixture", *Applied Thermal Engineering*, Pergamon. 21, 1299-1317.

5. E. Rev, M. Emtir, Z. Szitkai, P. Mizsey, and Z. Fonyo (**2001**)
   "Energy savings of integrated and coupled distillation systemes",
   Computers and Chemical Engineering, Elsevier. 25, 119-140.

6. M. Emtir, P. Mizsey, E. Rev and Z. Fonyo (**2002**)
   "Economic Optimization and Control of Energy-Integrated Distillation Schemes", Paper submitted to *Chemical and Biochemical Engineering Quarterly*.

(II) Contributions in local and international conferences

1) P. Mizsey, M. Emtir, and Z. Fonyo "Rigorous evaluation of energy integrated distillation schemes", *13th International Congress of Chemical and Process Engineering, (CHISA 98)* Praha-Czech Republic, 23-28 August (**1998**).

2) M. Emtir, E. Rev, and Z. Fonyo
"Economic and controllability evaluation of energy integrated distillation schemes", *Workshop on Chemical Engineering* (Muszaki Kemiai Napok), Veszprem, April (**2000**).

3) M. Emtir, E. Rev, and Z. Fonyo
"Rigorous simulation of energy integrated and thermally coupled distillation schemes for ternary mixture", *ISCAPE 2000*, Cartagena de indias, Colombia (**2000**).

4) M. Emtir, E. Rev, P. Mizsey, and Z. Fonyo
"Economic and controllability evaluation of energy integrated distillation schemes", *AIChE annual meeting*, Los Angles, November (**2000**).

5) M. Emtir, E. Rev, and Z. Fonyo
"Rigorous simulation of energy integrated and thermally coupled distillation schemes for ternary mixture", *(CHISA 2000)* Praha-Czech Republic, 27-31 August (**2000**).

6) M. Emtir, P. Mizsey, E. Rev, and Z. Fonyo
"Economic optimization and control of energy integrated distillation schemes". *15th International conference on efficiency, costs, optimization, simulation and environmental impact of energy systems* (volume II), pp. 1095, Berlin, July 3-5, (**2002**).

Nomenclature

A	heat transfer area
A	light component
B	bottom product rate of the main column (kmol/h)
B	middle component
B_2	bottom product rate of the column 2 (kmol/h)
BLT	biggest log-modulus tuning
BR	boil up ratio = V/B
C	heavy component
CN	condition number
Col.1	column 1
Col.2	column 2
C_P	specific heat of water
d	column diameter (m)
D	conventional direct sequence
D	distillate rate of the main column (kmol/h)
D	flow rate of the overhead product of the prefractionator (kmol/h)
D_1	distillate rate of column 1 (kmol/h)
D_2	distillate rate of column 2 (kmol/h)
Det	determinant of a matrix
DQB	direct sequence with backward heat integration
DQF	direct sequence with forward heat integration
DV_1	distillate to vapor ratio = D_1/V_1
DV	distillate to vapor ratio = D/V
EMAT	exchange minimum approach temperature
E_o	overall column efficiency
F	feed rate (kmol/h)
F_{BLT}	detuning factor
G	Gibbs free energy
HX	heat-exchanger
H	column height (m)
h	tray stack height (m)
h	tray stack height (m)

h_l	liquid height above valve opening (m)
I	conventional indirect sequence
IQB	indirect sequence with backward heat integration
IQF	indirect sequence with forward heat integration
ISE	integral square error
K_C	Controller gain
K_U	Ultimate gain
K_p	matrix of stedy-state gain
K_{pu}	diagonal elements in steady-state gain matrix
L	reflux rate of the main column (kmol/h)
L_1	reflux rate of column 1 (kmol/h)
L_{12}	liquid flow from the prefractionator to the main column (kmol/h)
L_2	reflux rate of column 2 (kmol/h)
L_{21}	liquid flow from the main column to the prefractionator (kmol/h)
L_m	molar liquid flow rate (kmol/h)
LMTD	logarithmic mean temperature difference
LP	low-pressure steam
LV_1	reflux to vapor ratio = L_1/V_1
M&S	Marshall and Swift index
MIMO	multiple input-multiple output variables
m_i	manipulated variable
$\dot{m}_{CW}$	water mass flow rate (kg/s)
MP	middle-pressure steam
N	number of theoretical plates
NI	Niederlinski index
OS	overshoot (%)
P	column design pressure (kpa)
PFD	process flow diagram
PSO	product of settling time and overshoot
P_U	Ultimate frequency
Q	heat duty (KJ/hr)
Q	heat duty of main column (KJ/hr)
Q_2	heat duty of column 2 (KJ/hr)

Q_H	heat supplied to the system (energy/time)
Q_L	heat leaves to the system (energy/time)
R	gas constant
R	reflux ratio = L/D
RGA	relative gain array
S	side product rate of the main column (kmol/h)
SI	separation index
SISO	single input-single output variable
SP	thermally coupled sloppy sequence (Petlyuk column)
SQB	sloppy sequence with backward heat integration
SQF	sloppy sequence with forward heat integration
SR	sidestream reflux flow rate (Kmol/h)
ST	settling time (time unit)
T	absolute temperature (K)
TAC	total annual costs
T_H	temperature at which heat is supplied (K)
T_L	temperature at which heat is removed (K)
T_o	ambient temperature (K)
U	overall heat transfer coefficient
V	vapor rate of the main column (kmol/h)
V_1	vapor rate of column1 (kmol/h)
V_2	vapor rate of column2 (kmol/h)
V_{12}	vapor flow from the prefractionator to the main column (kmol/h)
V_{21}	vapor flow from the main column to the prefractionator (kmol/h)
V_b	boil-up vapor rate of the main column (kmol/h)
V_m	molar vapor flow rate (kmol/h)
W_{min}	minimum work consumption per mole of feed
W_n	net work consumption
$\mathbf{X_A}$	composition of component **A** (ethanol)
x_A	mole fraction of component A in liquid phase
x_B	mole fraction of component B in liquid phase
$\mathbf{X_B}$	composition of component **B** (n-propanol)
$\mathbf{X_C}$	composition of component **C** (n-butanol)
$x_{D,B}$	composition of the middle component (**B**) in the product stream

$x_{F,B}$	composition of the middle component (**B**) in the feed
x_{i1}	mole fraction of component i in product 1
x_{i2}	mole fraction of component i in product 2
x_{j1}	mole fraction of component j in product 1
x_{j2}	mole fraction of component j in product 2
x_{jF}	mole fraction of component j in the feed

Greek letters

α_{ij}^{s}	separation factor between componen i and j
β	fractional recovery of the middle component (**B**)
β^{*}	theoretical fractional recovery of the middle component (**B**)
β_o	optimal fractional recovery obtained by the optimization study
α_A	relative volatility of component A
α_B	relative volatility of component B
α_C	relative volatility of component C
σ	singular value of a matrix
η	thermodynamic efficiency
μ_{avg}	average viscosity of feed (cP)
τ_C	Controller reset time
ΔG	change in Gibbs free energy
ΔH	enthalpy of products minus enthalpy of feed
λ	average latent heat of steam
λ_{ij}	diagonal elements of RGA
γ_{jf}	activity coefficient of component j in the feed
ΔS	change in entropy (energy/mass/temperature)
ΔT	temperature difference

Appendix A: Activity model interaction parameters

A1. NRTL thermodynamic property package

Table A1.1: A_{ij} Coefficient matrix for NRTL

	Ethanol	1-Propanol	1-Butanol
Ethanol	-------	56.239	-32.941
1-Propanol	-2.559	-------	45.899
1-Butanol	38.072	-46.904	-------

Table A1.2: $(alpha)_{ij}$ Coefficient matrix for NRTL

	Ethanol	1-Propanol	1-Butanol
Ethanol	-------	0.301	0.304
1-Propanol	0.301	-------	0.305
1-Butanol	0.304	0.305	-------

A2. UNIQUAC thermodynamic property package

Table A2.1: A_{ij} Coefficient matrix for UNIQUAC

	Ethanol	1-Propanol	1-Butanol
Ethanol	-------	71.759	-38.707
1-Propanol	-35.282	-------	-338.670
1-Butanol	75.355	499.094	-------

Appendix B: Sizing and costing of distillation columns and heat exchangers

B.1. Sizing distillation columns

For a given number of theoretical trays, HYSYS simulator calculates column diameter after converging for selected valve tray distillation column with 50.8 mm weir height. Valve trays of Glitsch type are considered. In order to estimate the actual number of trays, overall column efficiency is calculated using simplified equation (Peter, and Timmerhaus, 1988):

$$\log E_0 = 1.67 - 0.25 \log(\mu_{avg} \cdot \alpha_{avg}) + 0.30 \log(\frac{L}{V}) + 0.30 h_1 , \quad [B\text{-}1]$$

where μ_{avg} is the average viscosity of the liquid flow on each tray in the column:

$$\mu_{avg} = \frac{1}{N} \sum_{i=1}^{N} \mu_i \quad [B\text{-}2]$$

N is the theoretical numbers of trays in the column and μ_i is the viscosity on the ith tray.

α_{avg} is the average relative volatility of the key components over the whole column section:

$$\alpha_{avg} = \frac{1}{N_F} \sum_{i=1}^{N_F} \alpha_{iS} + \frac{1}{N - N_F} \sum_{i=N_F+1}^{N} \alpha_{iR} , \quad [B\text{-}3]$$

where N_F is the location of the feed tray. α_{iS} and α_{iR} refers to the relative volatility of the key components in the stripping and rectifying section of the column respectively:

$$\alpha_i = \frac{\frac{V_L}{V_H}}{\frac{L_L}{L_H}} \qquad [B\text{-}4]$$

V_L and L_L refer to the vapor and liquid flow of the low-key component and V_H and L_H refer to the vapor and liquid flow of the high-key component.

h_l in formula [B-1] is the liquid level above weir height (calculated by HYSYS using France's formula), and L and V is the total molar flow of liquid and vapor respectively:

$$\frac{L}{V} = \frac{L_{ref} + L_{reb}}{V_{cond} + V_{boil}}, \qquad [B\text{-}5]$$

where L_{ref} is the reflux rate, L_{reb} is the liquid molar flow rate to the reboiler, V_{cond} is the vapor molar flow rate to the condenser, and V_{boil} is the boil up rate.

The actual number of trays, N_{actual}, is estimated by dividing the theoretical number of trays, N, in the column section by the efficiency, E_0:

$$N_{actual} = \frac{N}{E_0} \qquad [B\text{-}6]$$

The height of the column H, is estimated from the number of actual trays, N_{actual}:

$$H = (N_{actual} - 1)(0.6) + 6.0 \qquad [B\text{-}7]$$

B.2. Capital cost of distillation columns

The installed cost of distillation columns is estimated applying an installation factor to the purchased cost. The purchase cost consists of shell and tray costs. For carbon steel construction distillation column with valve tray internals, the following cost equations that are updated from mid 1968 to 1997 using the ratio of Marshall & Swift index (1056.8/280) are used:

$$\text{Installed cost of column shell} = \left(\frac{M\&S}{280}\right)(937.61)(d^{1.066})(H^{0.802})(3.18) \qquad [B\text{-}8]$$

If the design pressure was more than 345 kPa, a correction factor of [1+0.000145(P-345)] is applied, where P is the column pressure. M&S is the Marshall and Swift index equal to 1056.8, d is the diameter of the column, and H is the height of the column.

$$\text{Installed costs of column trays} = \left(\frac{M\&S}{280}\right)(97.24)(d^{1.55})(h), \qquad [B\text{-}9]$$

where h is the tray stack height:

$$h = (N_{actual} - 1)(0.6) \qquad [B\text{-}10]$$

The column cost is the sum of the installed costs of the shell and trays:

Column cost = Installed cost of column shell + Installed cost of column trays [B-11]

B.3. Sizing heat transfer equipment

The heat transfer area *A*, of the condensers, reboilers and heat exchangers are calculated assuming the overall heat transfer coefficients, *U*, given in Table B.1.

Table B.1 Overall heat transfer coefficients

Heat transfer equipment	Overall heat transfer coefficient, *U*, [kJ / m^2 h °C]
Condenser	2800
Reboiler	3400
Heat exchanger	2100

and are calculated according to the following equation:

$$A = \frac{Q}{U \cdot LMTD} \quad , \qquad \text{[B-12]}$$

where *Q* is the heat duty, and *LMTD* is the logarithmic mean temperature difference:

$$LMTD = \frac{\Delta T_2 - \Delta T_1}{\ln \frac{\Delta T_2}{\Delta T_1}} \qquad \text{[B-13]}$$

ΔT_2 is the temperature difference between the inlet streams, and ΔT_1 is the temperature difference between the outlet streams of the heat transfer equipment.

B.4. Capital cost of heat transfer equipment

The cost of heat transfer equipment can be correlated as a function of surface area. Assuming shell and tube, floating head, and carbon steel construction, the following cost equation is used:

$$\text{Installed cost of heat exchanger} = \left(\frac{\text{M \& S}}{280}\right)(474.67)(\text{A}^{0.65})(3.29), \quad \text{[B-14]}$$

where M&S is the Marshall and Swift index and A is the heat transfer area.

B.5. Operating costs

The operating costs are assumed to be only steam and cooling water costs. The operating hours per year is set to be 8000.

The flow of cooling water, $\dot{m}_{CW}$, is calculated after the following equation:

$$\dot{m}_{CW} = \frac{Q}{C_P \cdot \Delta T}, \quad \text{[B-15]}$$

where the specific heat capacity of water, C_P, equals 4.181 J/K·g and ΔT equals 15 K.

The flow of steam, $\dot{m}_{STM}$, is calculated after the following equation:

$$\dot{m}_{STM} = \frac{Q}{\lambda}, \quad \text{[B-16]}$$

where λ is the latent heat of steam, equal to 2083 kJ/kg for low-pressure steam and 2000 kJ/kg for medium-pressure steam.

B.6. Annual capital costs

The capital, purchase, and installation costs are annualized over a period referred to as the plant lifetime, and assumed to be 10 years.

$$\text{Annual capital costs} = \frac{\text{capital costs}}{\text{plant life time}} \qquad \text{[B-17]}$$

The total annual costs is the sum of the annual operating and capital costs:

$$\text{Total annual cost} = \text{annual operating cost} + \text{annual capital cost} \qquad \text{[B-18]}$$

Appendix C: Optimization results of the rigorous cases

Table C.1: Optimal scheme results of Case 1 based on U.S. utility prices

Description	D		DQF		IQF		DQB		IQB		SP		SQF		SQB	
	Col.1	Col.2	Col.1	Col.2	Col.1	Col.2	Col.1	Col.2	Col.1	Col.2	Col. 1	Col.2	Col. 1	Col.2	Col. 1	Col.2
Pressure (kPa)	101.3	101.3	512.5	101.3	249	101.3	101.3	230.5	101.3	512	101.3	101.3	495	101.3	101.3	458
Diameter (m)	1.49	1.21	1.39	1.35	1.42	1.36	1.49	1.20	1.51	1.23	1.31	1.54	1.22	1.24	1.31	1.28
Reflux ratio	1.26	5.46	1.50	7.73	0.92	1.30	1.26	6.36	0.85	1.62	0.64	1.32	0.74	0.94	0.63	1.06
Actual plates	80	75	83	47	71	53	78	50	71	52	61	126	52	114	53	105
Total actual plates	155		130		124		128		123		187		166		158	
Heating rate (kJ/hr)	1.98E+07		1.53E+07		1.37E+07		1.33E+07		1.38E+07		1.27E+07		1.22E+07		1.27E+07	
Cooling rate (kJ/hr)	1.93E+07		1.36E+07		1.21E+07		1.19E+07		1.19E+07		1.22E+07		1.17E+07		9.21E+06	
Main HX duty (kJ/hr)	------		8.04E+06		1.14E+07		8.01E+06		1.22E+07		------		7.15E+06		9.66E+06	
Steam cost ($/yr)	5.04E+05		4.47E+05		3.49E+05		3.39E+05		3.51E+05		3.23E+05		3.57E+05		3.70E+05	
C.W cost ($/yr)	1.65E+04		1.17E+04		1.03E+04		1.01E+04		1.02E+04		1.04E+04		9.98E+03		7.88E+03	
Operating cost ($/yr)	5.21E+05		4.58E+05		3.59E+05		3.49E+05		3.61E+05		3.33E+05		3.67E+05		3.78E+05	
Capital cost ($/yr)	1.19E+05		1.38E+05		1.45E+05		1.35E+05		1.50E+05		1.25E+05		1.37E+05		1.43E+05	
TAC ($/yr)	6.40E+05		5.97E+05		5.04E+05		4.84E+05		5.11E+05		4.58E+05		5.04E+05		5.21E+05	
Capital savings (%)	0		-16		-22		-13		-26		-5		-15		-20	
Op. cost savings (%)	0		12		31		33		31		36		30		27	
TAC savings (%)	**0**		**7**		**21**		**24**		**20**		**28**		**21**		**19**	

Table C.2: Optimal scheme results of Case 1 based on European utility prices

Description	D		DQF		IQF		DQB		IQB		SP		SQF		SQB	
	Col.1	Col.2	Col.1	Col.2	Col.1	Col.2	Col.1	Col.2	Col.1	Col.2	Col. 1	Col.2	Col. 1	Col.2	Col. 1	Col.2
Pressure (kPa)	101.3	101.3	512.5	101.3	249.5	101.3	101.3	230.5	101.3	512	101.3	101.3	495	101.3	101.3	457
Diameter (m)	1.49	1.20	1.37	1.35	1.41	1.36	1.48	1.20	1.51	1.23	1.30	1.53	1.21	1.24	1.31	1.28
Reflux ratio	1.26	5.39	1.49	7.73	0.90	1.30	1.24	6.36	0.82	1.62	0.63	1.31	0.73	0.93	0.63	1.06
Actual plates	80	86	96	47	84	53	86	50	83	52	67	128	56	116	55	105
Total actual plates	166		143		137		136		135		195		172		160	
Heating rate (kJ/hr)	1.97E+07		1.52E+07		1.36E+07		1.32E+07		1.37E+07		1.26E+07		1.22E+07		1.27E+07	
Cooling rate (kJ/hr)	1.92E+07		1.36E+07		1.21E+07		1.18E+07		1.17E+07		1.21E+07		1.16E+07		9.20E+06	
Main HX duty (kJ/hr)	------		8.04E+06		1.14E+07		8.01E+06		1.22E+07		------		7.09E+06		9.64E+06	
Steam cost ($/yr)	1.34E+06		1.32E+06		9.24E+05		9.01E+05		9.30E+05		8.59E+05		1.06E+06		1.10E+06	
C.W cost ($/yr)	6.67E+04		4.70E+04		4.19E+04		4.09E+04		4.07E+04		4.20E+04		4.04E+04		3.19E+04	
Operating cost. ($/yr)	1.41E+06		1.37E+06		9.66E+05		9.42E+05		9.70E+05		9.01E+05		1.10E+06		1.13E+06	
Capital cost ($/yr)	1.22E+05		1.43E+05		1.50E+05		1.38E+05		1.55E+05		1.28E+05		1.39E+05		1.43E+05	
TAC ($/yr)	1.53E+06		1.51E+06		1.12E+06		1.08E+06		1.13E+06		1.03E+06		1.24E+06		1.28E+06	
Capital savings (%)	0		-16		-22		-12		-27		-4		-13		-17	
Op. cost savings (%)	0		3		31		33		31		36		22		19	
TAC savings (%)	**0**		**1**		**27**		**30**		**27**		**33**		**19**		**17**	

Table C.3: Optimal scheme results of Case 2 based on U.S. utility prices

Description	**D**		**DQF**		**IQF**		**DQB**		**IQB**		**SP**		**SQF**		**SQB**	
	Col.1	Col.2	Col.1	Col.2	Col.1	Col.2	Col.1	Col.2	Col.1	Col.2	Col. 1	Col.2	Col. 1	Col.2	Col. 1	Col.2
Pressure (kPa)	101.3	101.3	512.5	101.3	184.5	101.3	101.3	184.3	101.3	512.0	101.3	101.3	454.5	101.3	101.3	376.5
Diameter (m)	1.49	1.50	1.37	1.52	1.65	1.59	1.48	1.46	1.72	1.27	1.27	1.75	1.17	1.29	1.25	1.26
Reflux ratio	2.14	1.82	2.41	2.32	0.99	3.16	2.14	2.11	0.93	2.48	0.67	3.05	0.76	1.87	0.67	1.59
Actual plates	79	77	79	55	72	61	81	59	79	57	65	116	59	137	65	128
Total actual plates	156		134		133		140		136		181		196		193	
Heating rate (kJ/hr)	2.43E+07		1.52E+07		1.70E+07		1.32E+07		1.79E+07		1.61E+07		1.15E+07		1.17E+07	
Cooling rate (kJ/hr)	2.39E+07		1.39E+07		1.61E+07		1.23E+07		1.56E+07		1.57E+07		1.11E+07		8.85E+06	
Main HX duty (kJ/hr)	------		1.15E+07		7.80E+06		1.24E+07		1.19E+07		------		8.36E+06		9.11E+06	
Steam cost ($/yr)	6.17E+05		4.43E+05		4.31E+05		3.39E+05		4.54E+05		4.10E+05		3.37E+05		3.43E+05	
C.W cost ($/yr)	2.04E+04		1.19E+04		1.38E+04		1.04E+04		1.34E+04		1.34E+04		9.50E+03		7.57E+03	
Operating cost. ($/yr)	6.38E+05		4.55E+05		4.45E+05		3.49E+05		4.68E+05		4.23E+05		3.46E+05		3.51E+05	
Capital cost ($/yr)	1.33E+05		1.46E+05		1.45E+05		1.50E+05		1.69E+05		1.35E+05		1.44E+05		1.45E+05	
TAC ($/yr)	7.71E+05		6.01E+05		5.90E+05		4.99E+05		6.37E+05		5.58E+05		4.90E+05		4.95E+05	
Capital savings (%)	0		-10		-9		-13		-27		-1		-8		-8	
Op. cost savings (%)	0		29		30		45		27		34		46		45	
TAC savings (%)	**0**		**22**		**23**		**35**		**17**		**28**		**36**		**36**	

Table C.4: Optimal scheme results of Case 2 based on European utility prices

Description	D		DQF		IQF		DQB		IQB		SP		SQF		SQB	
	Col.1	Col.2	Col.1	Col.2	Col.1	Col.2	Col.1	Col.2	Col.1	Col.2	Col. 1	Col.2	Col. 1	Col.2	Col. 1	Col.2
Pressure (kPa)	101.3	101.3	512.5	101.3	202.5	101.3	101.3	184.3	101.3	512	101.3	101.3	455	101.3	101.3	377
Diameter (m)	1.48	1.49	1.36	1.52	1.61	1.39	1.48	1.46	1.71	1.26	1.26	1.73	1.16	1.29	1.25	1.25
Reflux ratio	2.12	1.79	2.39	2.32	0.99	2.13	2.12	2.11	0.91	2.47	0.65	2.99	0.76	1.84	0.65	1.57
Actual plates	88	90	91	55	88	60	90	59	92	60	75	132	61	151	65	137
Total actual plates	178		146		148		149		152		207		212		202	
Heating rate (kJ/hr)	2.41E+07		1.51E+07		1.69E+07		1.32E+07		1.78E+07		1.59E+07		1.14E+07		1.17E+07	
Cooling rate (kJ/hr)	2.36E+07		1.38E+07		1.60E+07		1.21E+07		1.55E+07		1.54E+07		1.10E+07		8.79E+06	
Main HX duty (kJ/hr)	------		1.15E+07		1.15E+07		1.24E+07		1.19E+07		------		8.27E+06		9.05E+06	
Steam cost ($/yr)	1.64E+06		1.31E+06		1.15E+06		9.00E+05		1.21E+06		1.08E+06		9.96E+05		1.02E+06	
C.W cost ($/yr)	8.20E+04		4.80E+04		5.56E+04		4.19E+04		5.38E+04		5.36E+04		3.82E+04		3.05E+04	
Operating cost. ($/yr)	1.72E+06		1.36E+06		1.21E+06		9.42E+05		1.26E+06		1.13E+06		1.03E+06		1.05E+06	
Capital cost ($/yr)	1.42E+05		1.50E+05		1.63E+05		1.54E+05		1.76E+05		1.45E+05		1.49E+05		1.47E+05	
TAC ($/yr)	1.86E+06		1.51E+06		1.37E+06		1.10E+06		1.44E+06		1.28E+06		1.18E+06		1.19E+06	
Capital savings (%)	0		-6		-15		-9		-24		-2		-5		-3	
Op. cost savings (%)	0		21		30		45		27		34		40		39	
TAC savings (%)	**0**		**19**		**26**		**41**		**23**		**31**		**36**		**36**	

Table C.5: Optimal scheme results of Case 3 based on European utility prices

	D		**I**		**DQB**		**SP**		**SQF**		SQB	
Description	Col.1	Col.2	Col.1	Col.2	Col.1	Col.2	Col. 1	Col.2	Col. 1	Col.2	Col. 1	Col.2
Pressure (kPa)	101.33	101.33	101.33	101.33	101.33	145.50	101.33	101.33	338.50	101.33	101.33	295.50
Diameter (m)	1.41	1.88	1.94	1.38	1.50	1.80	1.13	1.99	1.33	1.50	1.37	1.37
Reflux ratio	8.74	0.88	0.79	8.34	10.06	0.92	0.69	17.15	1.60	11.11	1.09	9.53
Actual plates	93	96	96	94	51	94	69	116	41	127	56	122
Total actual plates	189		190		145		185		168		178	
Heating rate (kJ/hr)	3.00E+07		3.09E+07		2.61E+07		2.05E+07		1.37E+07		1.30E+07	
Cooling rate (kJ/hr)	2.99E+07		3.08E+07		1.24E+07		2.03E+07		1.36E+07		1.09E+07	
Main HX duty (kJ/hr)	------		------		1.25E+07		------		1.14E+07		1.09E+07	
Steam cost ($/yr)	2.04E+06		2.10E+06		1.35E+06		1.39E+06		9.31E+05		8.84E+05	
C.W cost ($/yr)	1.04E+05		1.07E+05		4.30E+04		7.05E+04		4.80E+04		3.79E+04	
Operating cost. ($/yr)	2.15E+06		2.21E+06		1.40E+06		1.46E+06		9.79E+05		9.21E+05	
Capital cost ($/yr)	1.65E+05		1.68E+05		1.76E+05		1.49E+05		1.58E+05		1.69E+05	
TAC ($/yr)	2.31E+06		2.37E+06		1.57E+06		1.61E+06		1.14E+06		1.09E+06	
Capital savings (%)	0		-2		-7		10		4		-2	
Op. cost savings (%)	0		-3		35		32		54		57	
TAC savings (%)	**0**		**-3**		**32**		**30**		**51**		**53**	

Table C.6: Optimal scheme results of equimolar feed, based on European utility prices and UNIQUAC property package

Description	**D**		**I**		**DQF**		**DQB**		**SP**		**SQF**		**SQB**	
	Col.1	Col.2	Col.1	Col.2	Col.1	Col.2	Col.1	Col.2	Col. 1	Col.2	Col. 1	Col.2	Col. 1	Col.2
Pressure (kPa)	101.3	101.33	101.3	101.3	511	101.3	101.3	178.5	101.3	101.3	451	101.3	101.3	367
Diameter (m)	0.84	0.82	0.96	0.78	0.76	0.87	0.84	0.85	0.72	0.98	0.65	0.74	0.71	0.71
Reflux ratio	2.25	1.67	0.90	1.87	2.56	2.38	2.25	2.20	0.67	2.99	0.82	1.92	0.67	1.61
Actual plates	91	98	93	88	93	55	92	61	87	145	57	147	79	143
Total actual plates	189		181		148		153		232		204		223	
Heating rate (kJ/hr)	8.01E+06		8.99E+06		5.19E+06		4.56E+06		5.28E+06		3.91E+06		3.94E+06	
Cooling rate (kJ/hr)	7.88E+06		8.85E+06		4.78E+06		4.19E+06		5.15E+06		3.78E+06		3.00E+06	
Main HX duty (kJ/hr)	------		------		3.94E+06		4.26E+06		------		2.89E+06		3.07E+06	
Steam cost ($/yr)	5.45E+05		6.11E+05		4.52E+05		3.10E+05		3.59E+05		3.41E+05		3.43E+05	
C.W cost ($/yr)	2.73E+04		3.07E+04		1.66E+04		1.45E+04		1.79E+04		1.31E+04		1.04E+04	
Operating cost. ($/yr)	5.72E+05		6.41E+05		4.69E+05		3.25E+05		3.77E+05		3.54E+05		3.54E+05	
Capital cost ($/yr)	7.54E+04		7.85E+04		7.80E+04		8.14E+04		8.18E+04		7.62E+04		7.98E+04	
TAC ($/yr)	6.48E+05		7.20E+05		5.47E+05		4.06E+05		4.59E+05		4.30E+05		4.33E+05	
Capital savings (%)	0		-4		-3		-8		-8		-1		-6	
Op. cost savings (%)	0		-12		18		43		34		38		38	
TAC savings (%)	**0**		**-11**		**16**		**37**		**29**		**34**		**33**	

Appendix D: Simulation results of closed-loop dynamic behavior

Table D.1: Closed-loop performance for feed rate disturbance

Studied schemes	Ethanol ($\mathbf{X_A}$)		n-Propanol ($\mathbf{X_B}$)		n-Butanol ($\mathbf{X_C}$)		Σ ST	Σ OS	Σ PSO
	Settling time (time unit)	Overshoot (%)	Settling time (time unit)	Overshoot (%)	Settling time (time unit)	Overshoot (%)			
D (D_1-L_2-B_2)	0.960	0.000	7.460	0.010	2.160	0.000	10.580	0.010	0.075
D (L_1-D_2-B_2)	0.500	0.000	21.600	0.010	10.640	0.001	32.740	0.011	0.227
DQF (D_1-L_2-B_2)	0.820	0.000	8.540	0.006	2.260	0.000	11.620	0.006	0.051
DQF (L_1-D_2-Q_2)	0.500	0.000	14.800	0.012	4.800	0.000	20.100	0.012	0.178
DQF (L_1-D_2-B_2)	0.100	0.000	34.100	0.010	2.350	0.002	36.550	0.012	0.346
DQB (D_1-L_2-B_2)	5.800	0.001	13.230	0.023	4.300	0.000	23.330	0.024	0.310
DQB (L_1-D_2-Q_2)	2.650	0.000	22.750	0.033	1.350	0.000	26.750	0.033	0.751
DQB (L_1-D_2-B_2)	6.950	0.000	20.300	0.033	7.000	0.001	34.250	0.034	0.677
SP (L-S-B)	10.810	0.014	11.500	0.004	8.300	0.005	30.610	0.023	0.238
SP (D-S-Q)	13.720	0.006	12.860	0.006	12.860	0.008	39.440	0.020	0.262
SQF (L-S-B)	14.000	0.012	16.500	0.030	10.000	0.015	40.500	0.057	0.813
SQF (D-S-Q)	18.420	0.004	21.890	0.037	19.650	0.001	59.960	0.042	0.903
SQB (L-S-B)	31.520	0.013	31.520	0.011	7.110	0.006	70.150	0.030	0.799
SQB (D-S-Q)	49.000	0.013	52.000	0.015	49.000	0.003	150.000	0.031	1.564

Table D.2: Closed-loop performance for feed composition disturbance

Studied schemes	Ethanol ($\mathbf{X_A}$)		n-Propanol ($\mathbf{X_B}$)		n-Butanol ($\mathbf{X_C}$)		Σ ST	Σ OS	Σ PSO
	Settling time (time unit)	Overshoot (%)	Settling time (time unit)	Overshoot (%)	Settling time (time unit)	Overshoot (%)			
D (D_1-L_2-B_2)	3.460	0.001	8.160	0.005	2.580	0.000	14.200	0.006	0.044
D (L_1-D_2-B_2)	0.500	0.000	12.800	0.020	7.900	0.001	21.200	0.021	0.264
DQF (D_1-L_2-B_2)	2.320	0.000	8.320	0.003	2.520	0.000	13.160	0.003	0.025
DQF (L_1-D_2-Q_2)	1.140	0.000	15.400	0.041	6.800	0.000	23.340	0.041	0.631
DQF (L_1-D_2-B_2)	1.150	0.000	24.300	0.080	6.500	0.001	31.950	0.081	1.951
DQB (D_1-L_2-B_2)	6.040	0.003	7.190	0.016	3.300	0.000	16.530	0.019	0.133
DQB (L_1-D_2-Q_2)	6.550	0.000	29.150	0.130	2.150	0.000	37.850	0.130	3.790
DQB (L_1-D_2-B_2)	8.400	0.001	27.300	0.128	9.140	0.001	44.840	0.130	3.512
SP (L-S-B)	10.300	0.025	10.490	0.016	7.600	0.002	28.390	0.043	0.441
SP (D-S-Q)	14.680	0.016	14.000	0.038	14.000	0.010	42.680	0.064	0.907
SQF (L-S-B)	13.600	0.003	17.000	0.011	11.000	0.003	41.600	0.017	0.261
SQF (D-S-Q)	23.320	0.003	26.970	0.026	18.000	0.001	68.290	0.030	0.789
SQB (L-S-B)	34.200	0.010	48.750	0.060	21.900	0.006	104.850	0.076	3.398
SQB (D-S-Q)	22.500	0.010	62.310	0.070	22.500	0.003	107.310	0.083	4.654